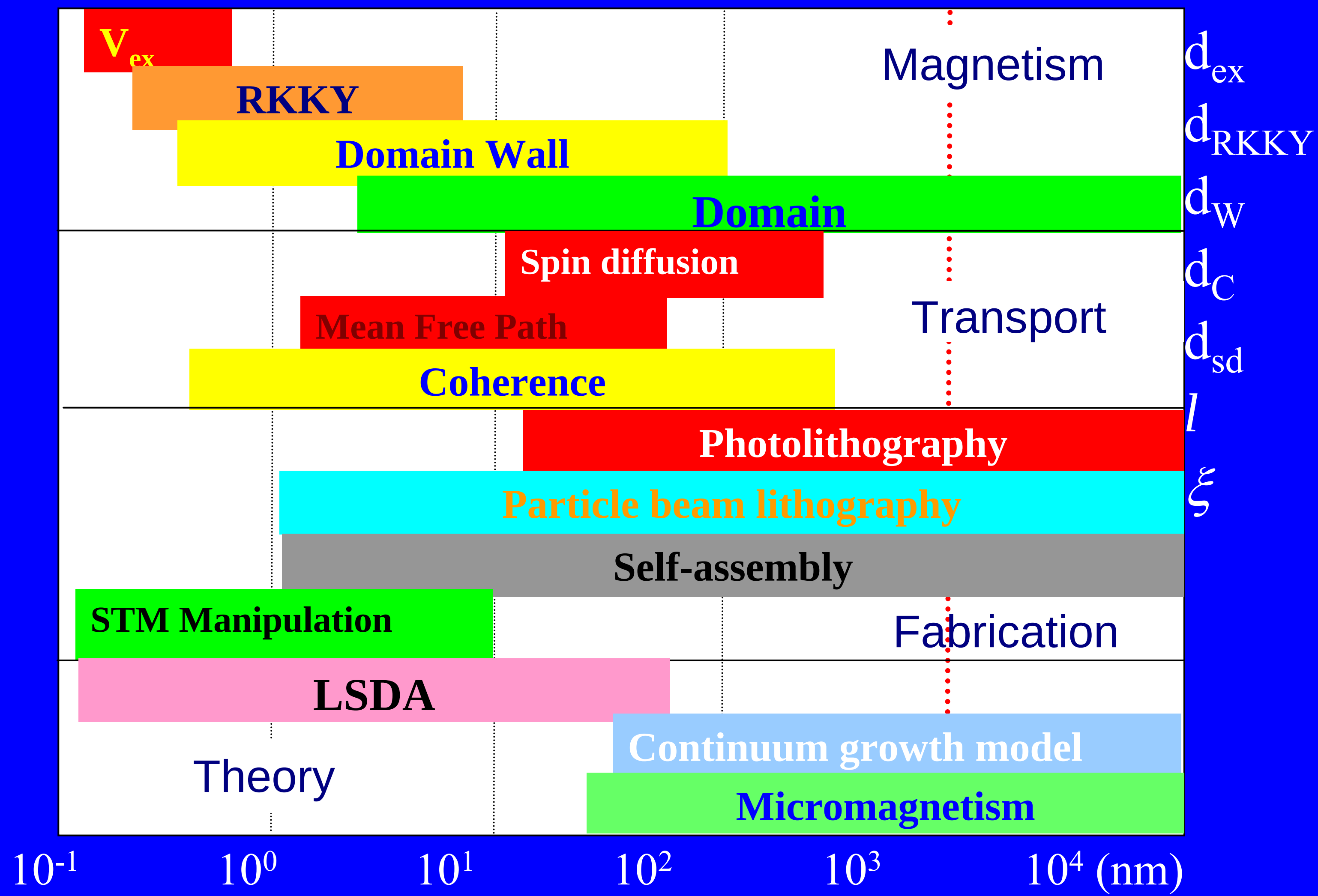

V_{ex}
RKKY
Domain Wall
Domain
Magnetism
Spin diffusion
Mean Free Path
Coherence
Transport
Photolithography
Particle beam lithography
Self-assembly
STM Manipulation
Fabrication
LSDA
Continuum growth model
Micromagnetism
Theory
d_{ex}
d_{RKKY}
d_W
d_C
d_{sd}
l
ξ
10^{-1} 10^{0} 10^{1} 10^{2} 10^{3} 10^{4} (nm)

Exchange-spring magnets

20 nm   30 nm

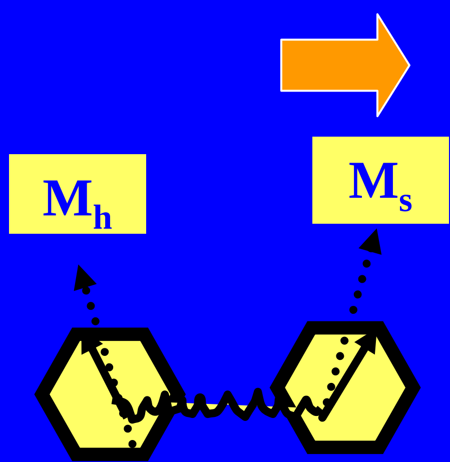

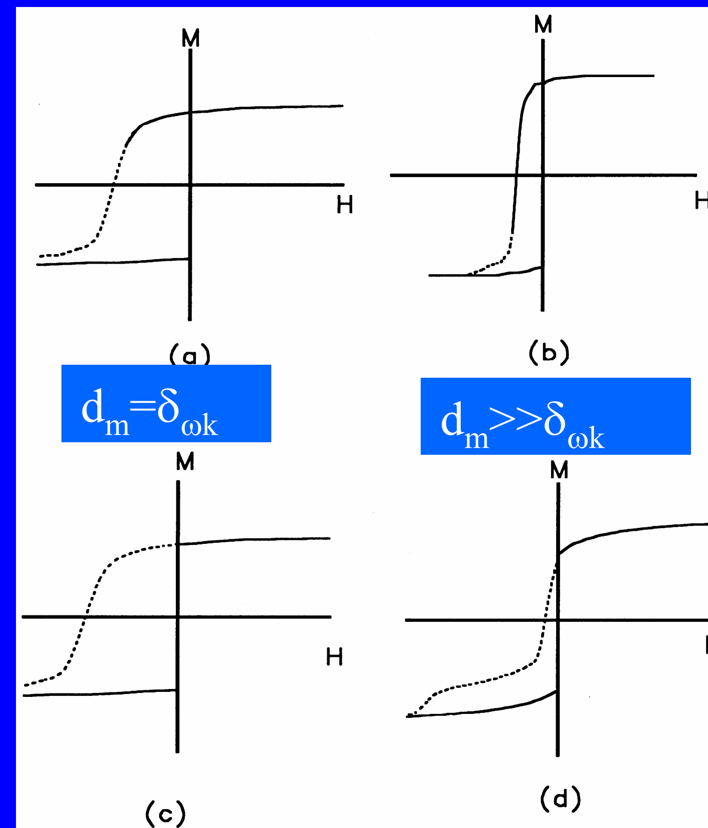

Single-phase

Without coupling

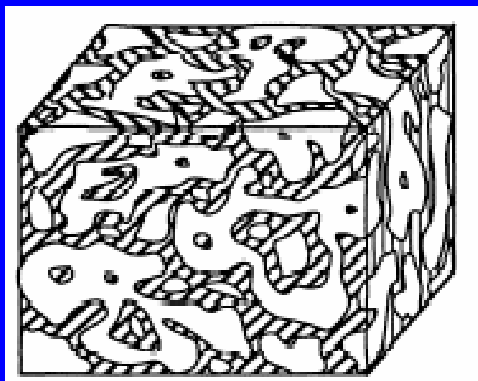

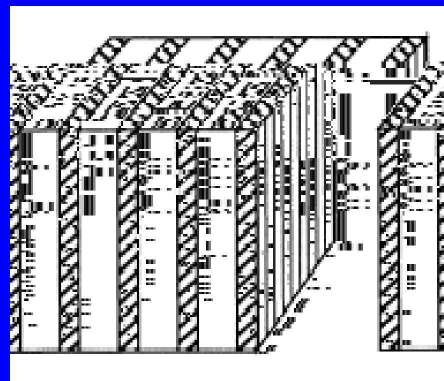

$$M_r = f_h M_h + f_s M_s$$

$$H_n = 2\frac{f_s K_s + f_h K_H}{\mu_0 (f_s M_s + f_h M_h)}$$

$$(BH)_{\max} = \frac{1}{4}\mu_0 M_s^2 [1 - \frac{\mu_0 (M_s - M_h) M_s}{2K_h}]$$

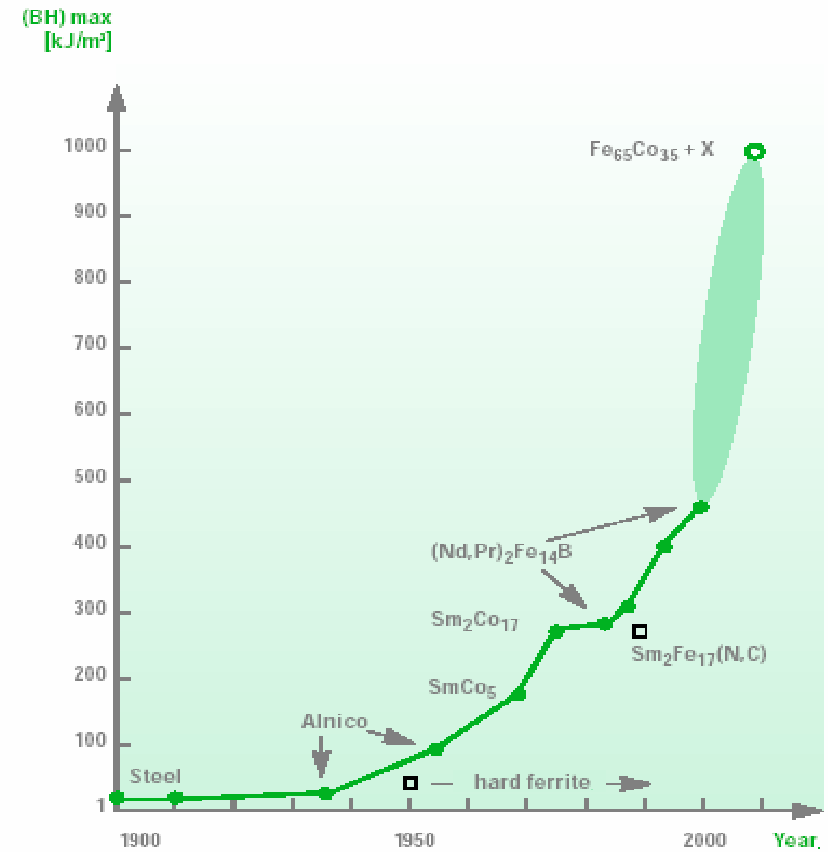

Fig. 2.15. Progress in improving $(BH)_{max}$ over the last century. The shaded region covers hypothetical FeCo-based alloys, which are magnetically hardened by additives X.

Self-assembly (particles)

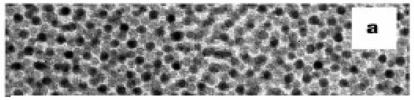

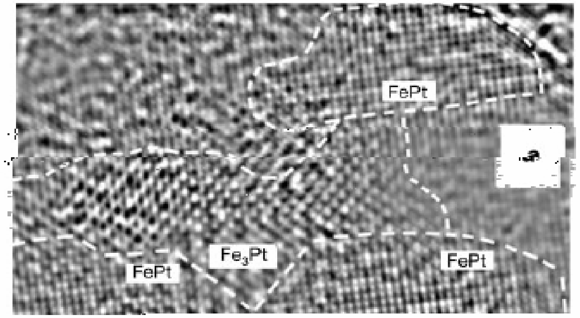

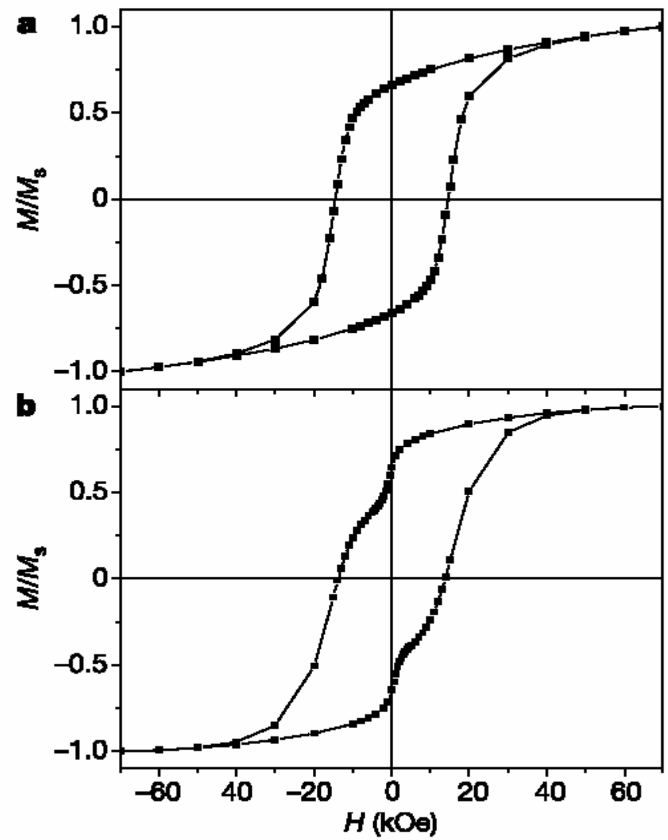

(BH)max=20.1MG Oe

H. Zeng et al., Nature 420(2002)395

IOP PUBLISHING JOURNAL OF PHYSICS D: APPLIED PHYSICS
J. Phys. D: Appl. Phys. 41 (2008) 093001 (20pp) doi:10.1088/0022-3727/41/9/093001

TOPICAL REVIEW

The discovery, development and future of GMR: The Nobel Prize 2007

Sarah M Thompson

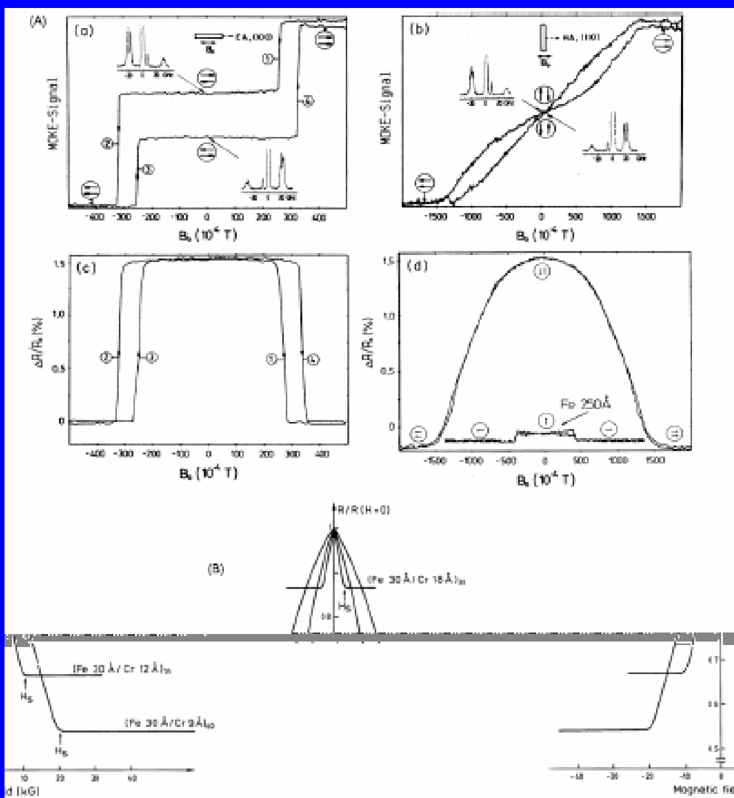

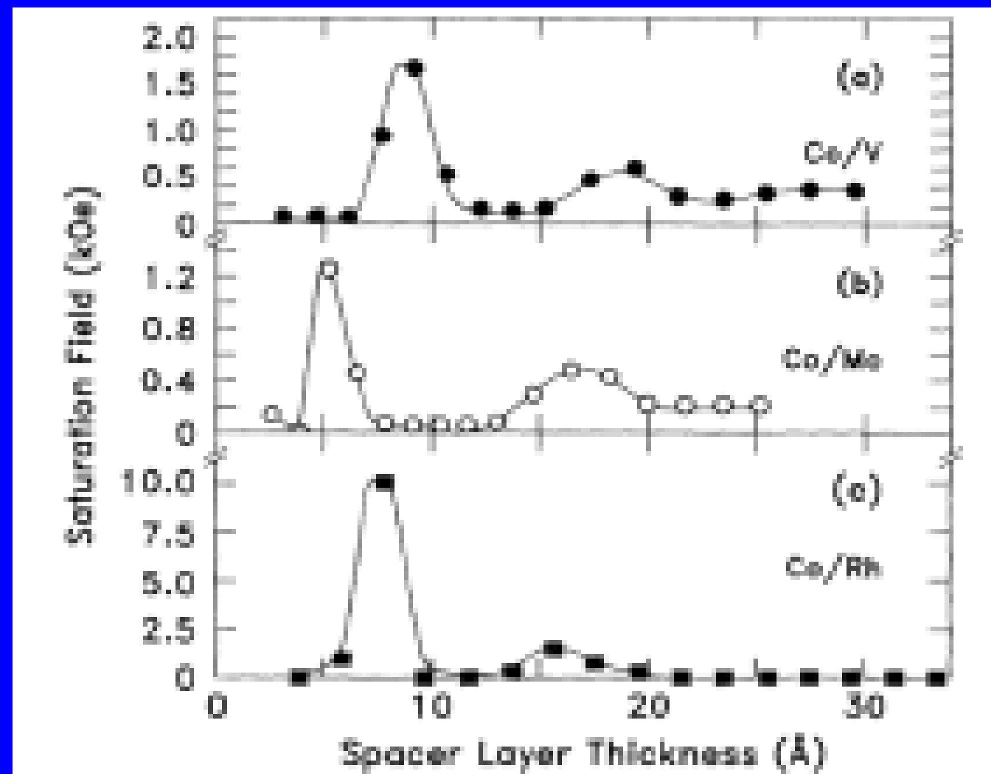

State Key Lab. of Magnetism, IPCAS; http://maglab.iphy.ac.cn

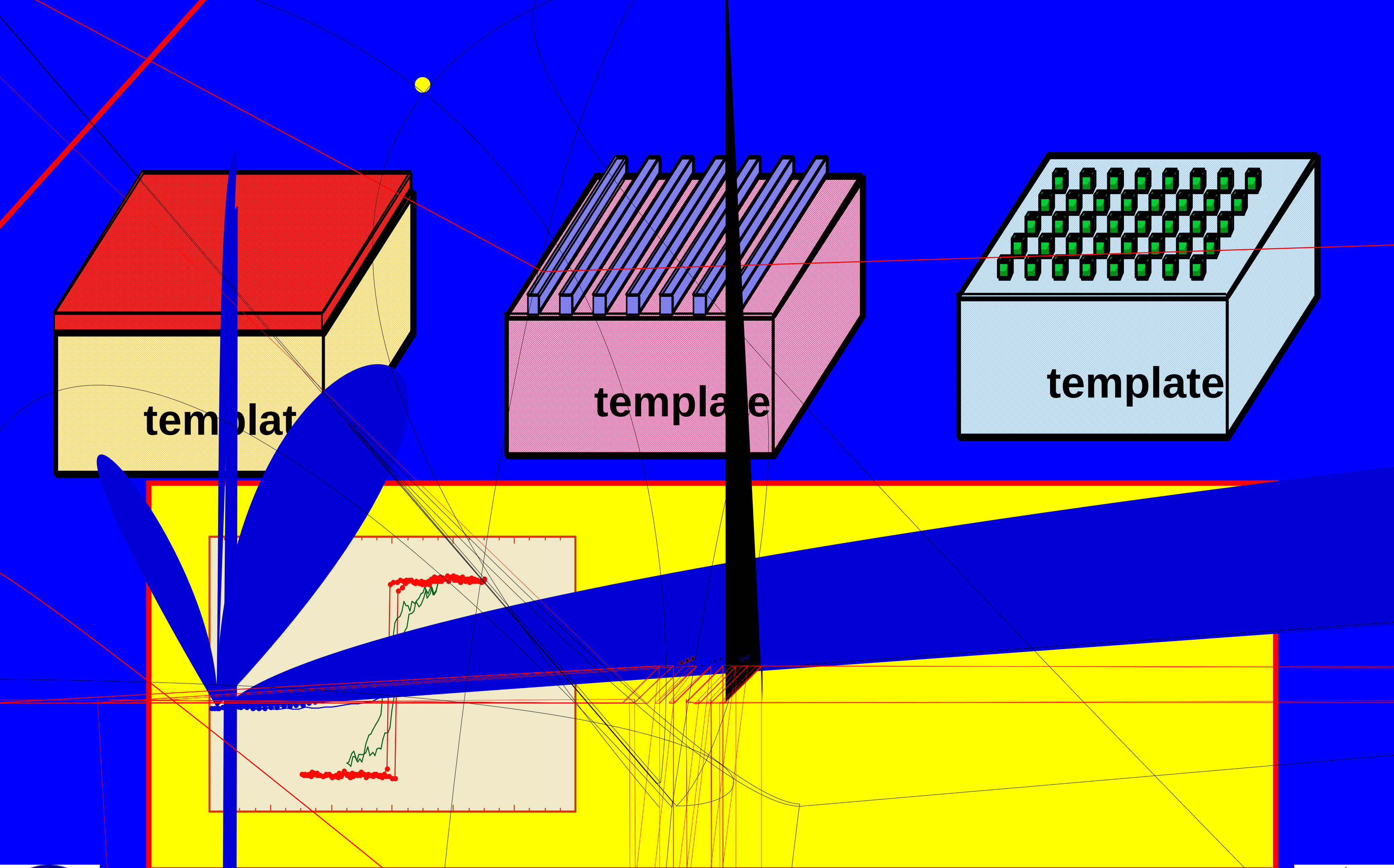
template

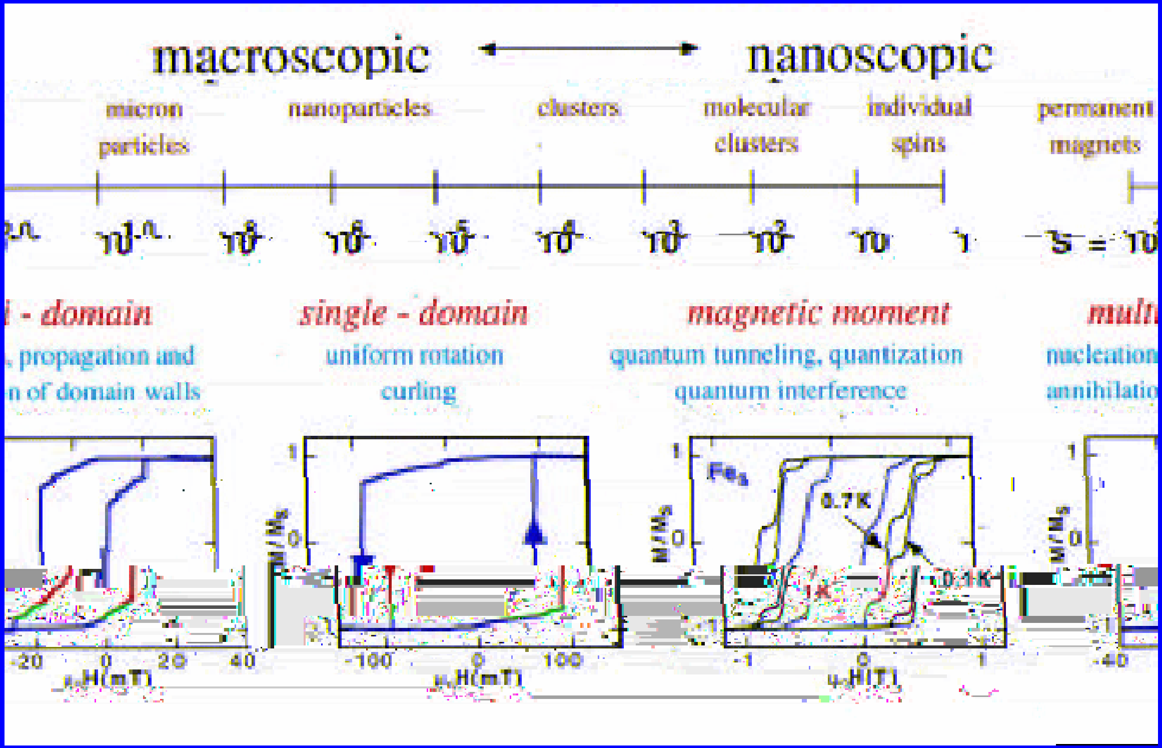
macroscopic
nanoscopic
micron particles
nanoparticles
clusters
molecular clusters
individual spins
permanent magnets
single - domain
magnetic moment
uniform rotation
curling
quantum tunneling, quantization
quantum interference

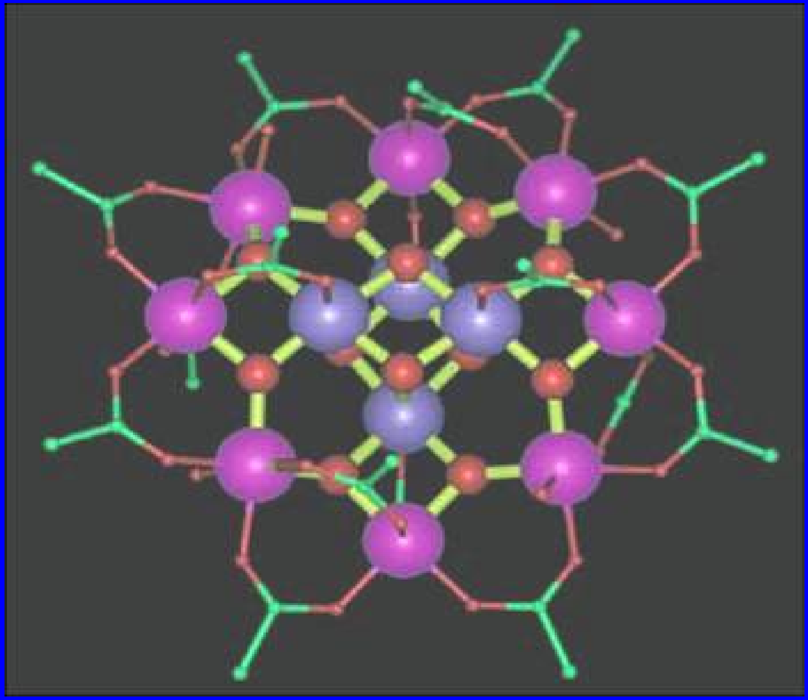

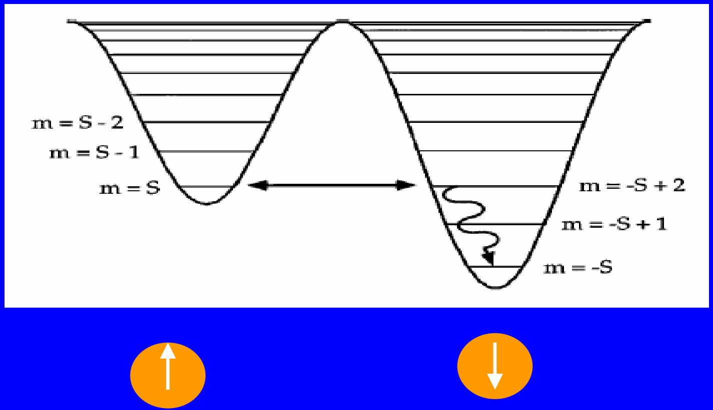
m = S - 2
m = S - 1
m = S
m = -S + 2
m = -S + 1
m = -S

quantum bit

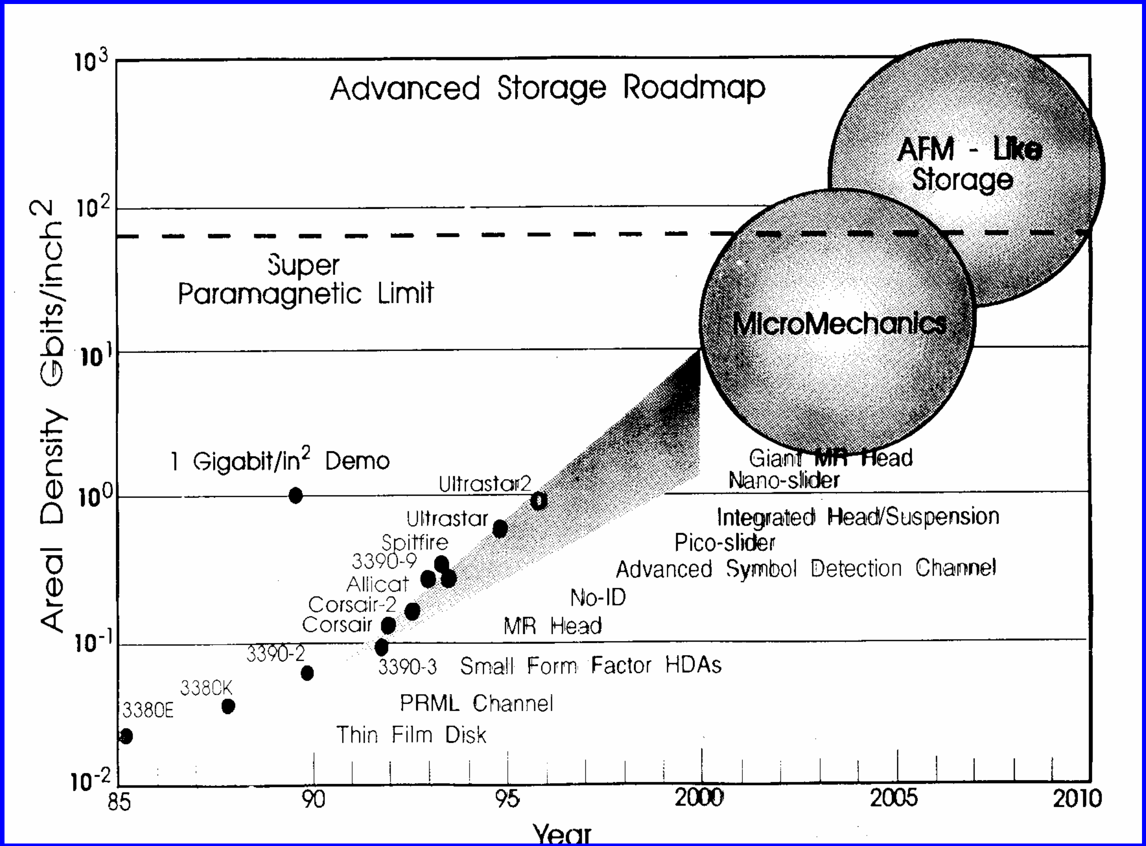

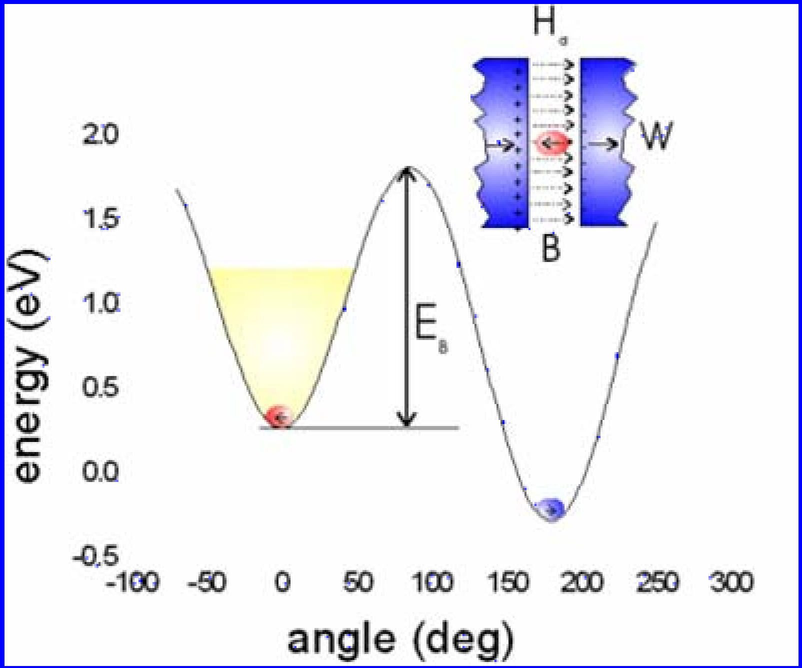

$$t = 10 \quad \text{year}$$

$$\frac{KV}{k_B T} > 40$$

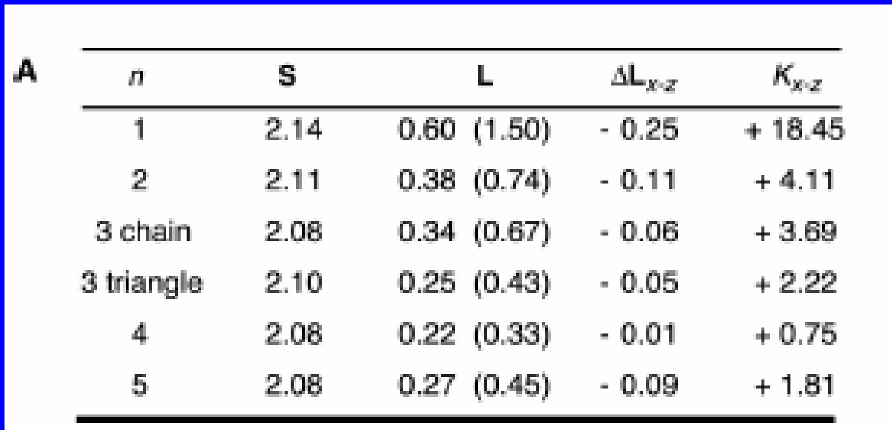

A n	S	L	ΔL_{x-z}	K_{x-z}
1	2.14	0.60 (1.50)	- 0.25	+ 18.45
2	2.11	0.38 (0.74)	- 0.11	+ 4.11
3 chain	2.08	0.34 (0.67)	- 0.06	+ 3.69
3 triangle	2.10	0.25 (0.43)	- 0.05	+ 2.22
4	2.08	0.22 (0.33)	- 0.01	+ 0.75
5	2.08	0.27 (0.45)	- 0.09	+ 1.81

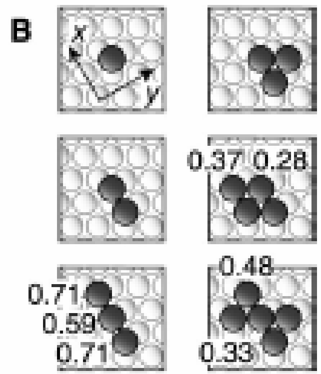

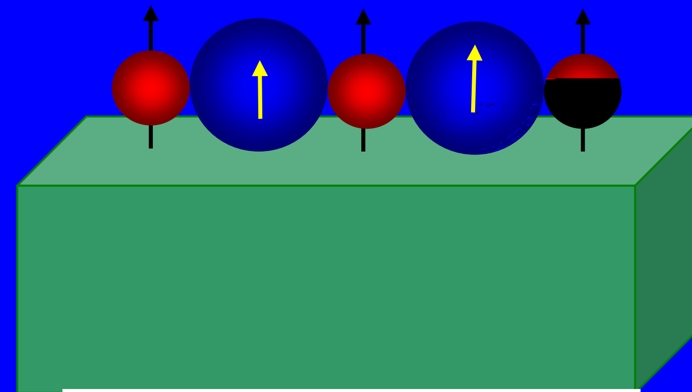

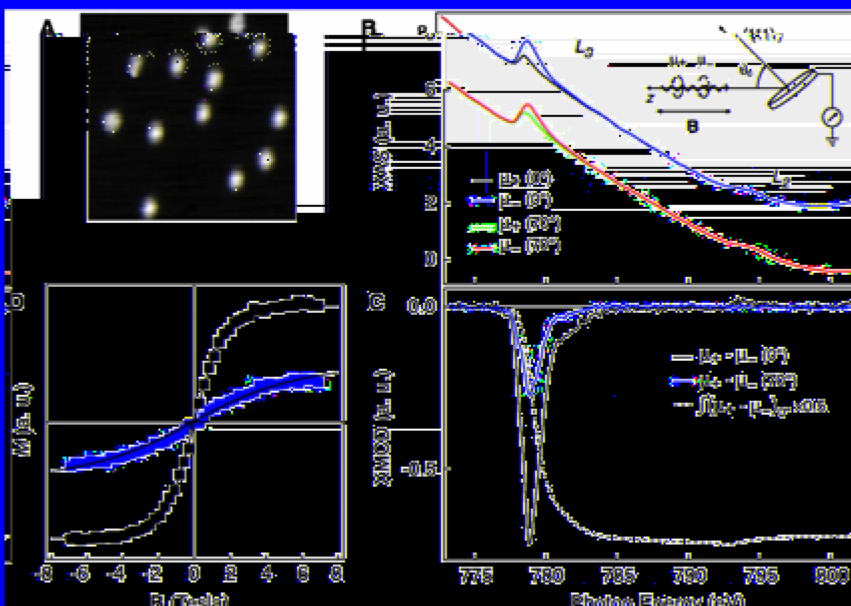

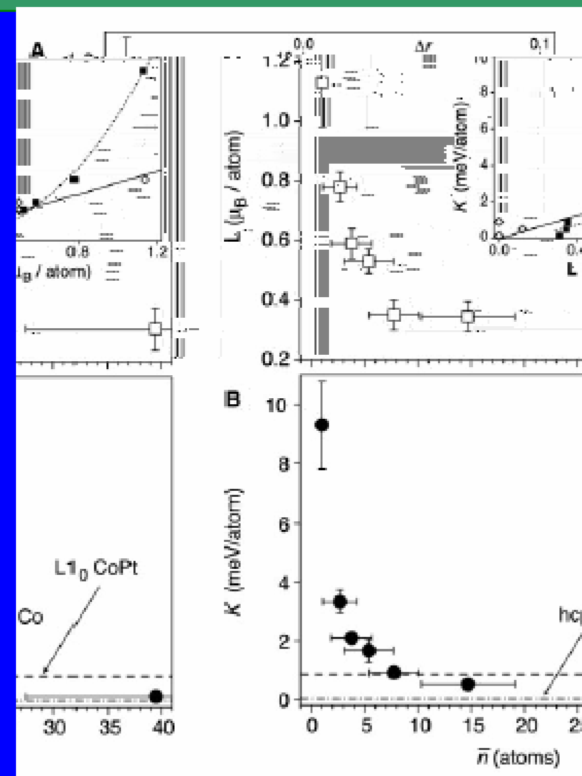

P. Gambardella et al., Science, 300,1130(2003)

Large Magnetic Anisotropy of a Single Atomic Spin Embedded in a Surface Molecular Network

Cyrus F. Hirjibehedin,[1] Chiung-Yuan Lin,[1,2] Alexander F. Otte,[1,3] Markus Ternes,[1,4] Christopher P. Lutz,[1] Barbara A. Jones,[1] Andreas J. Heinrich[1]

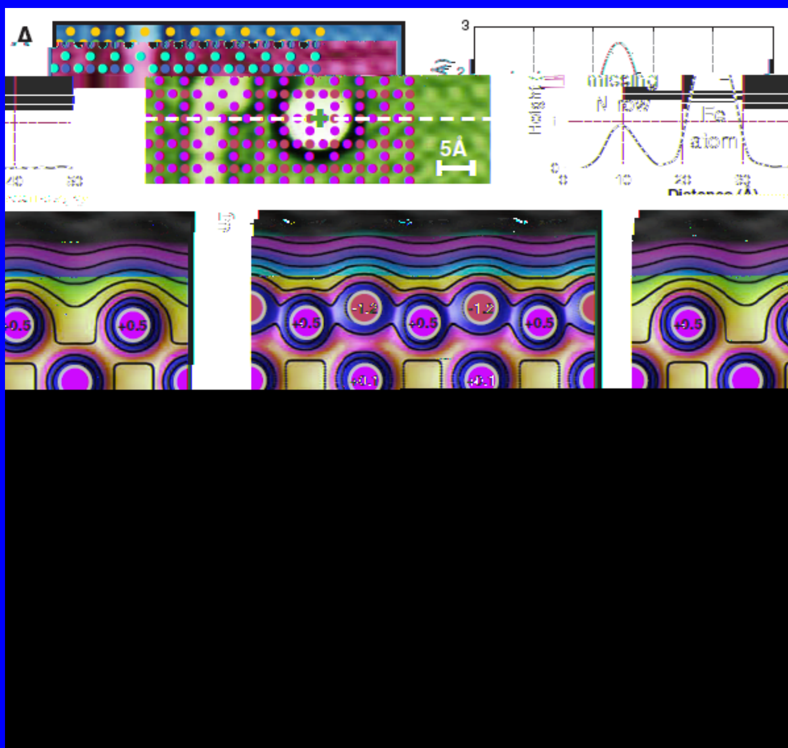

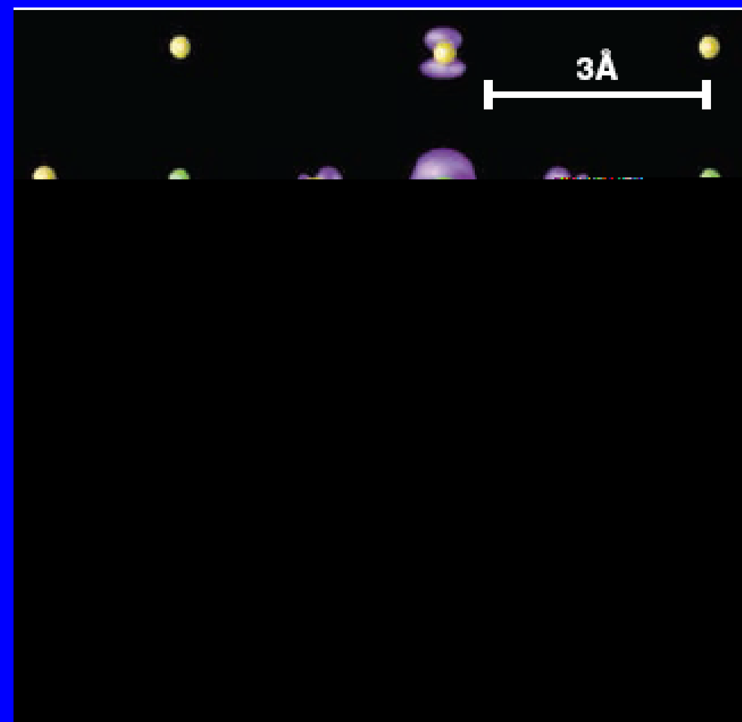

2003)

2002)

(2006)

•

•

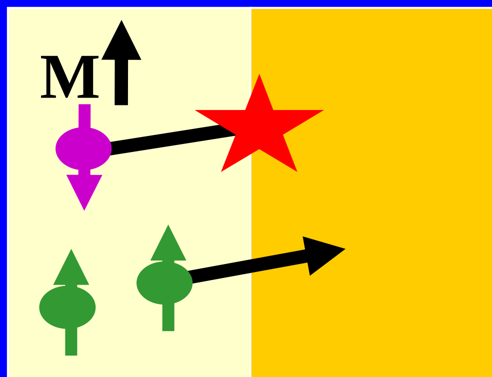

M

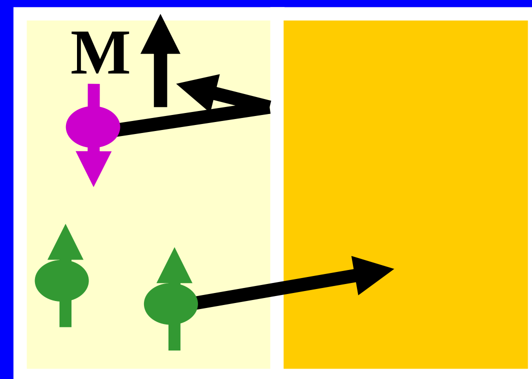

M

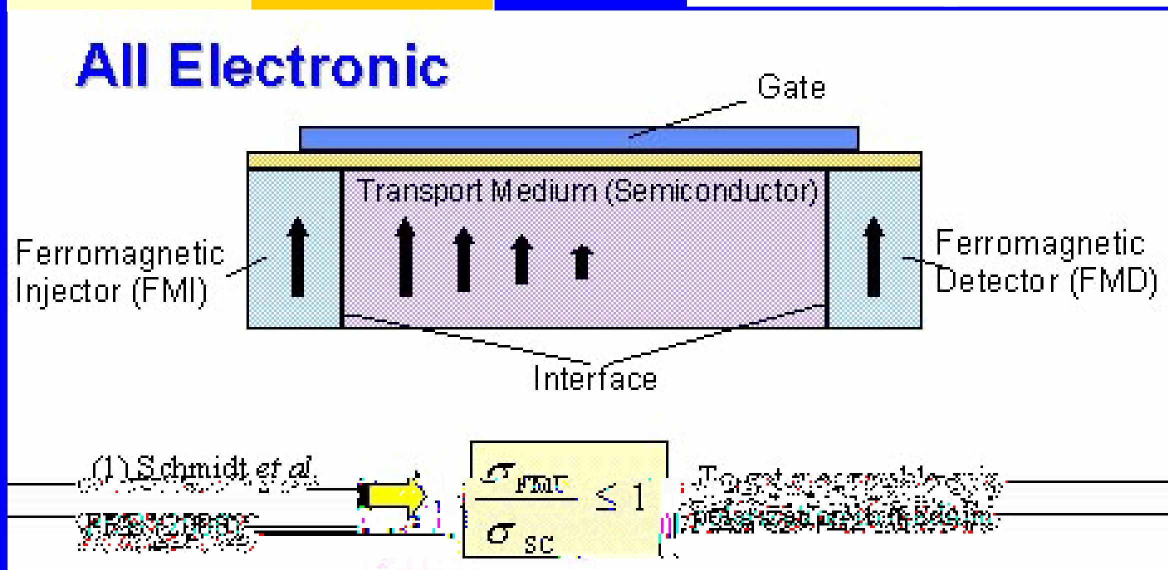

All Electronic
Gate
Transport Medium (Semiconductor)
Ferromagnetic Injector (FMI)
Ferromagnetic Detector (FMD)
Interface
(1) Schmidt et al.

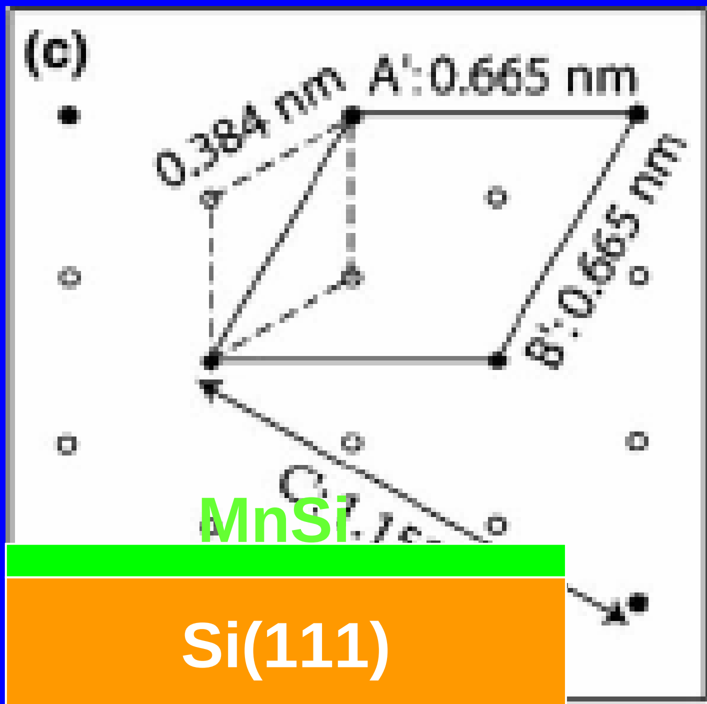

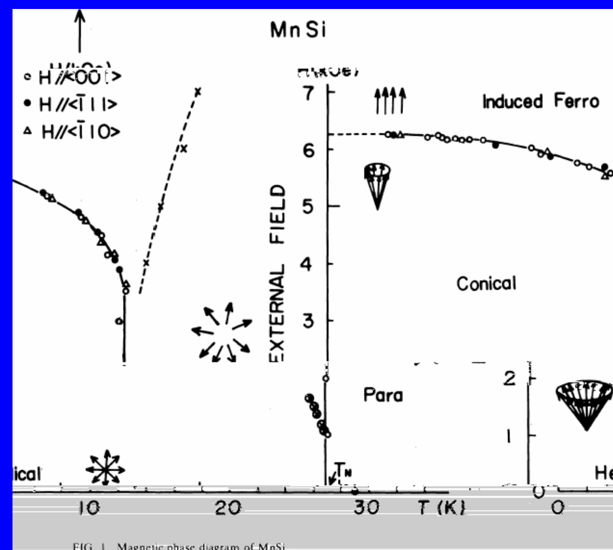

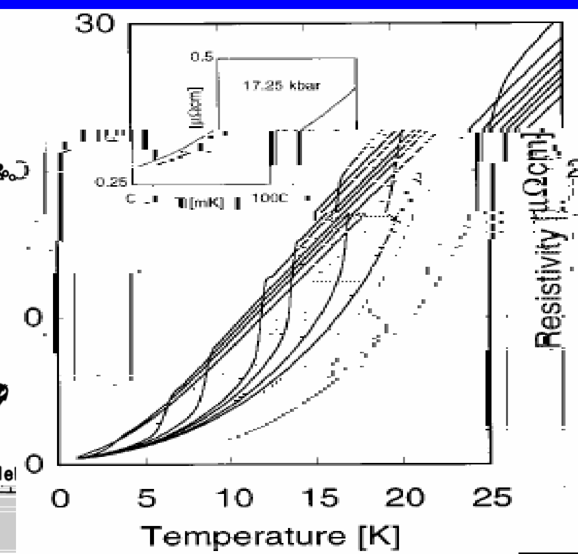

C. Pfleider, PRB,55,8330(1997)

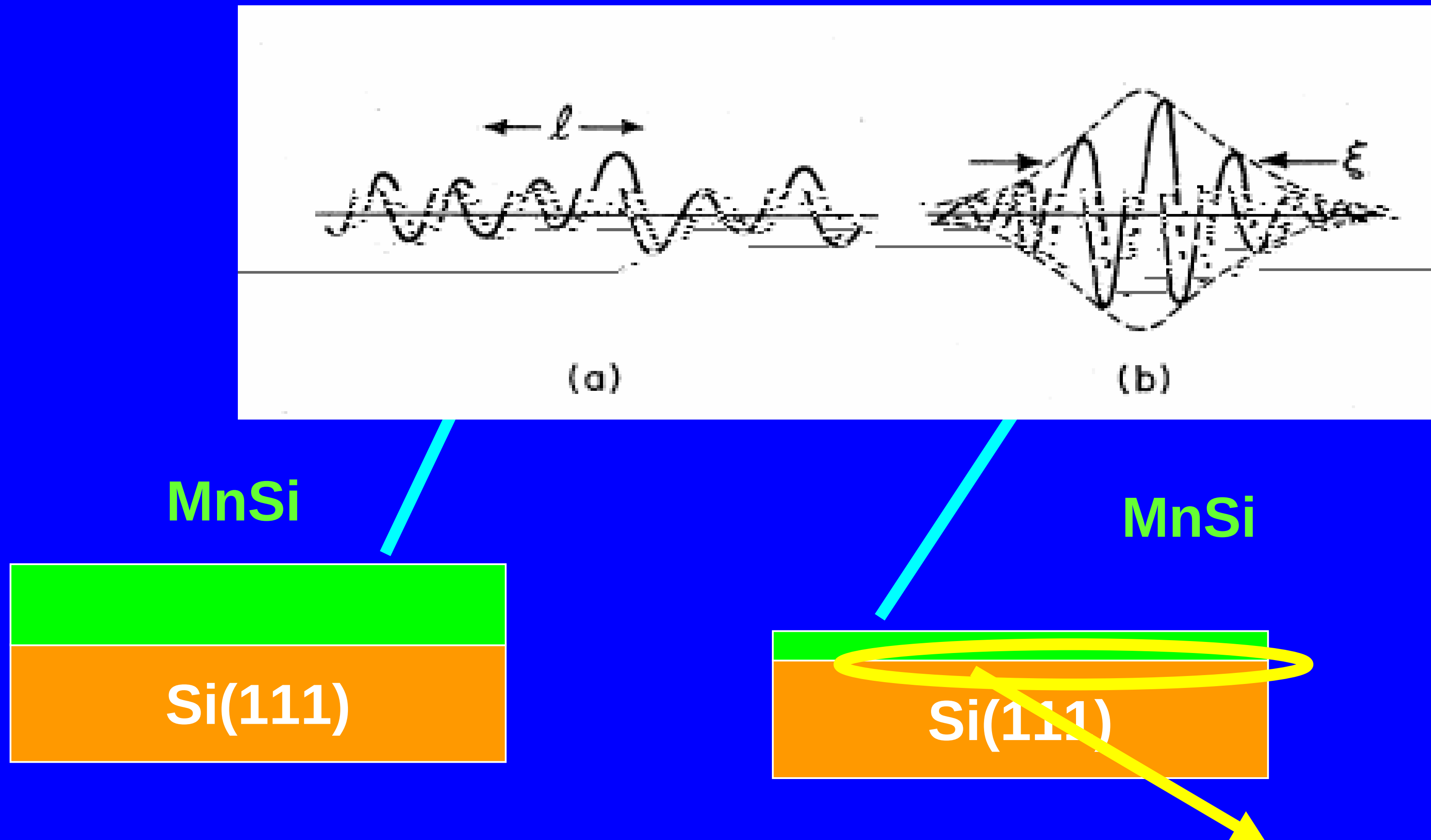
ℓ
ξ
(a)
(b)
MnSi
Si(111)
MnSi
Si(111)

Epitaxial Growth of metal or metal Silicides on Si

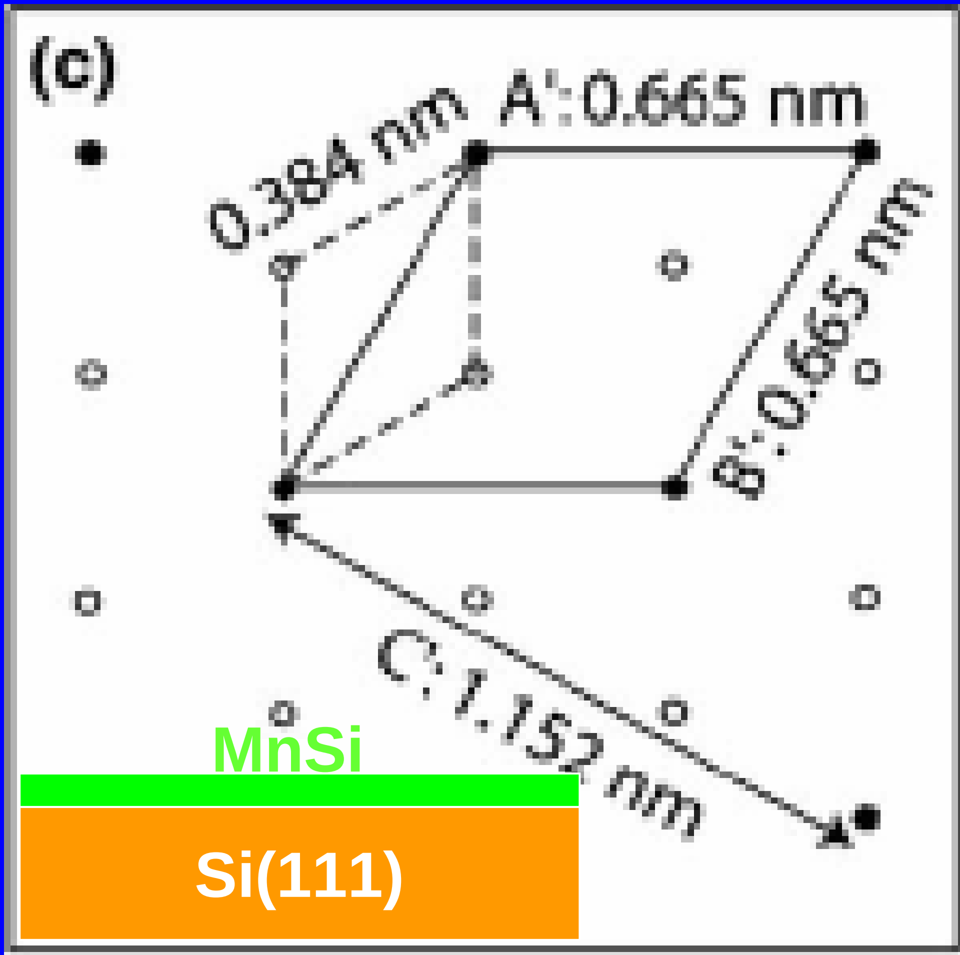

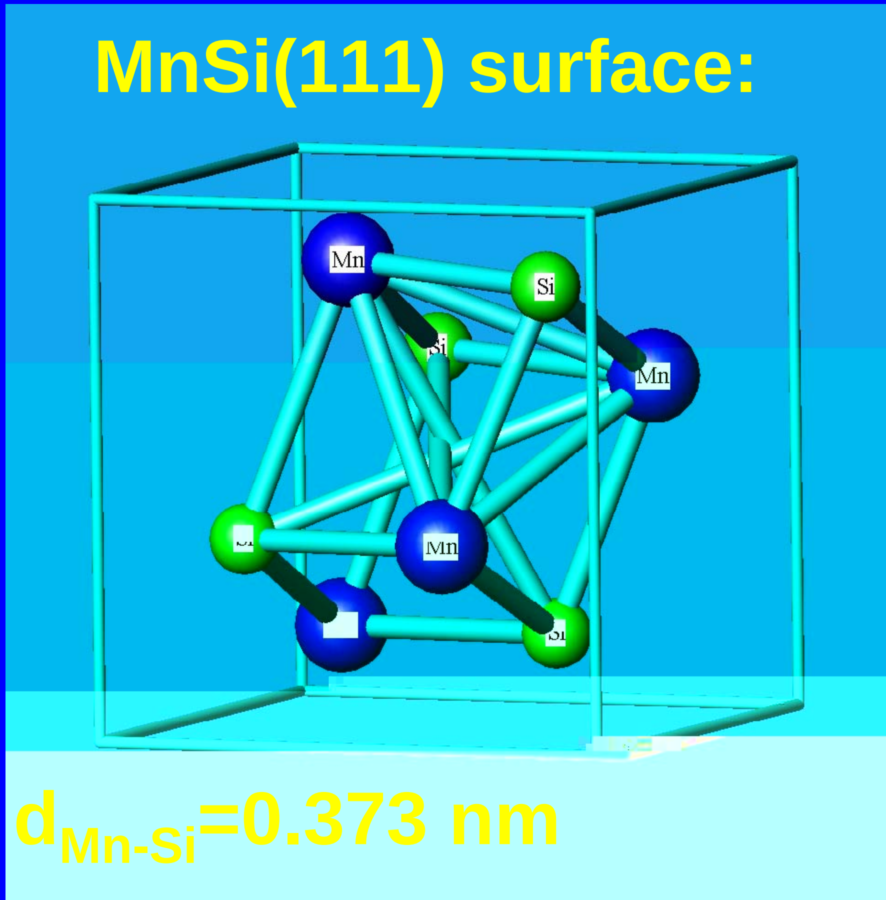

MnSi(111) surface:A=B=0.645nm,C=1.17nm

Ferromagnetic and Metallic Properties of MnSi bulk intermetallic Compounds

FeSi, CoSi, NiSi   weak, or non-magnetic

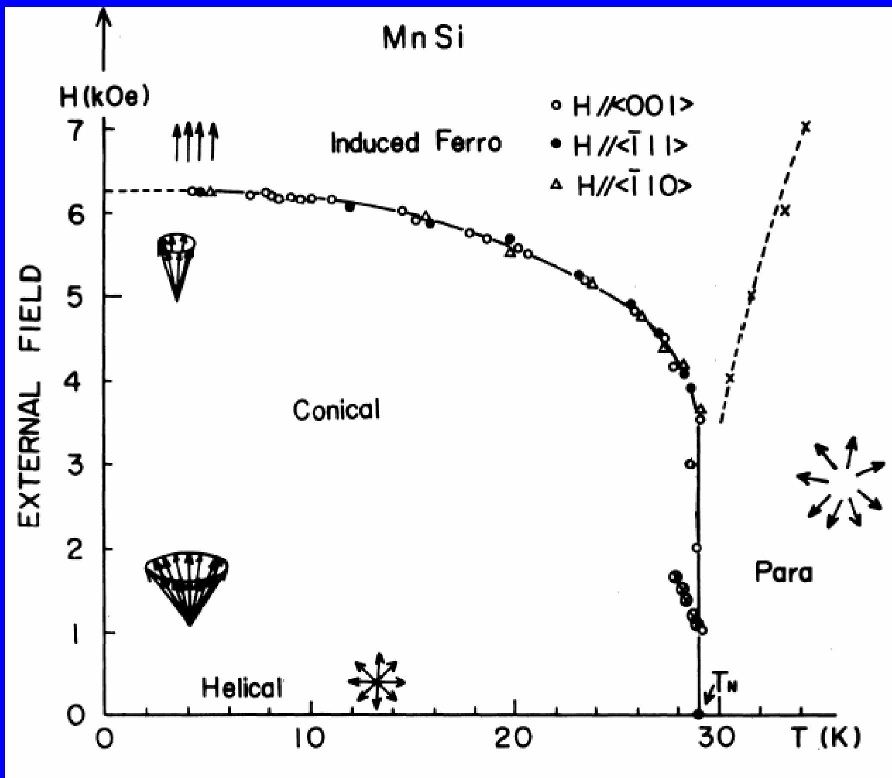

FIG. 1. Magnetic phase diagram of MnSi.

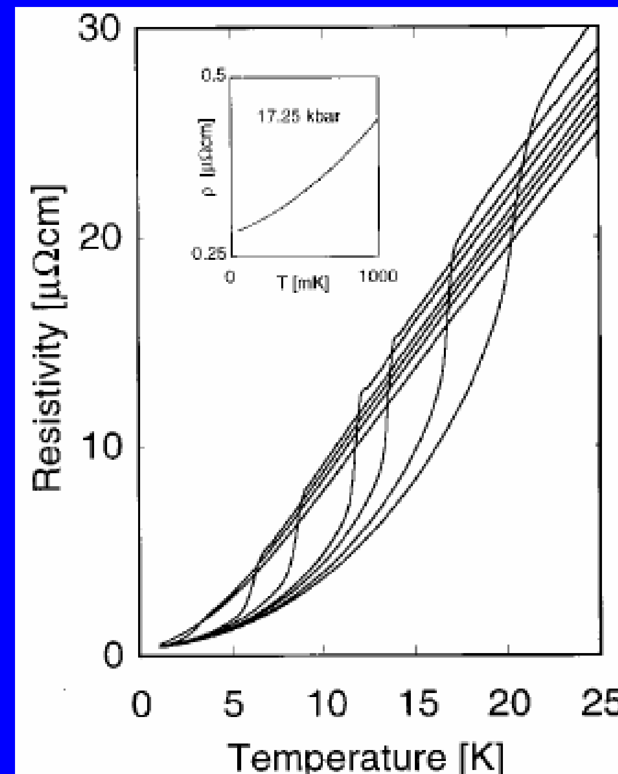

C. Pfleider, PRB,55,8330(1997)

Scaling Theory of Localization

$$g = G/(e^2/\hbar)$$

$$\beta(g) = \frac{d\ln g}{d\ln L} = \frac{L}{g}\frac{dg}{dL}$$

$$\beta(g) = 1$$ Ohm's-law

$$\beta(g) > 0$$ Extended state

$$\beta(g) < 0$$ Localized state

D.J. Thouless, PRL,39,1167(1977)

P.W. Anderson, PRL,43,718(1979)

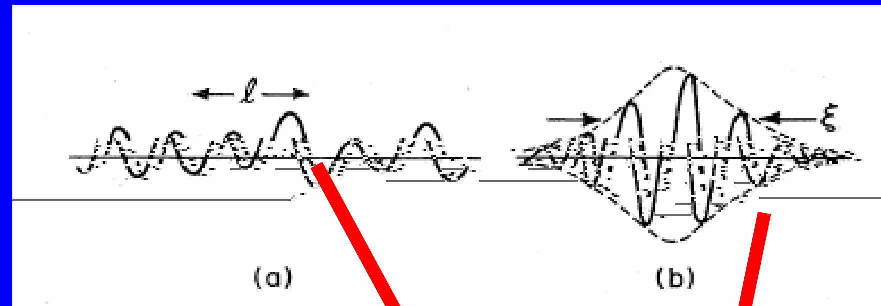

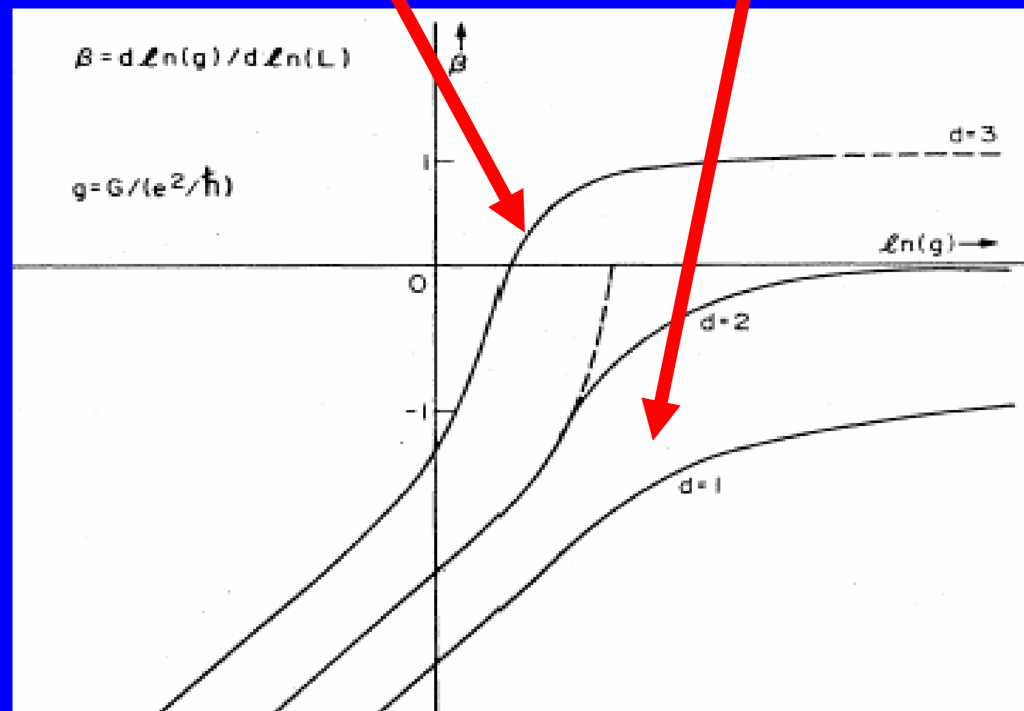

Experimental Studies of Localization

Cu on glass 11.9nm

Ag/Si(111)-7 × 7

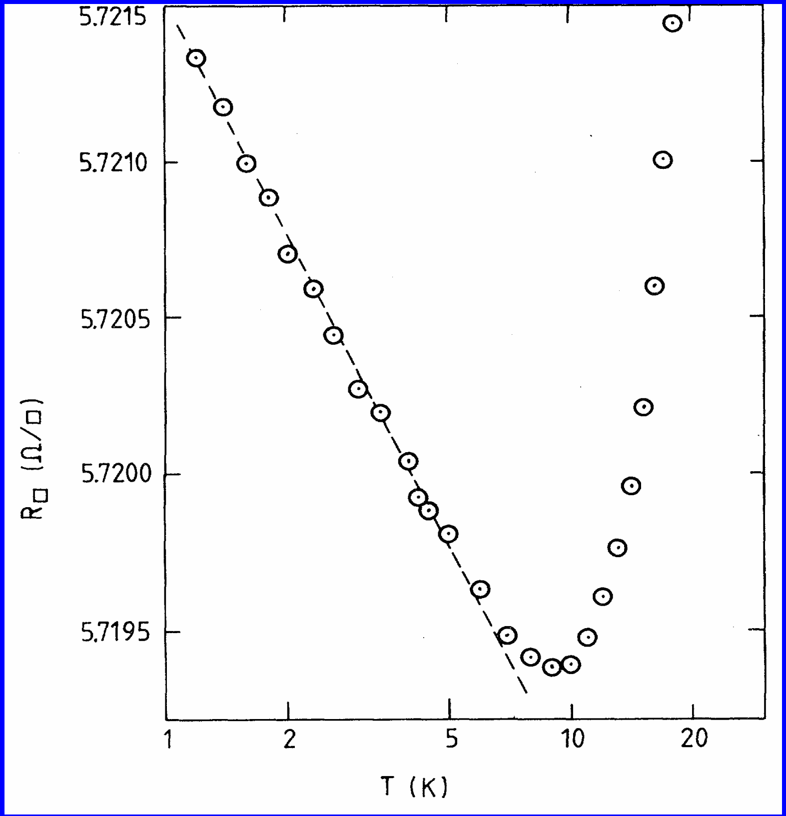

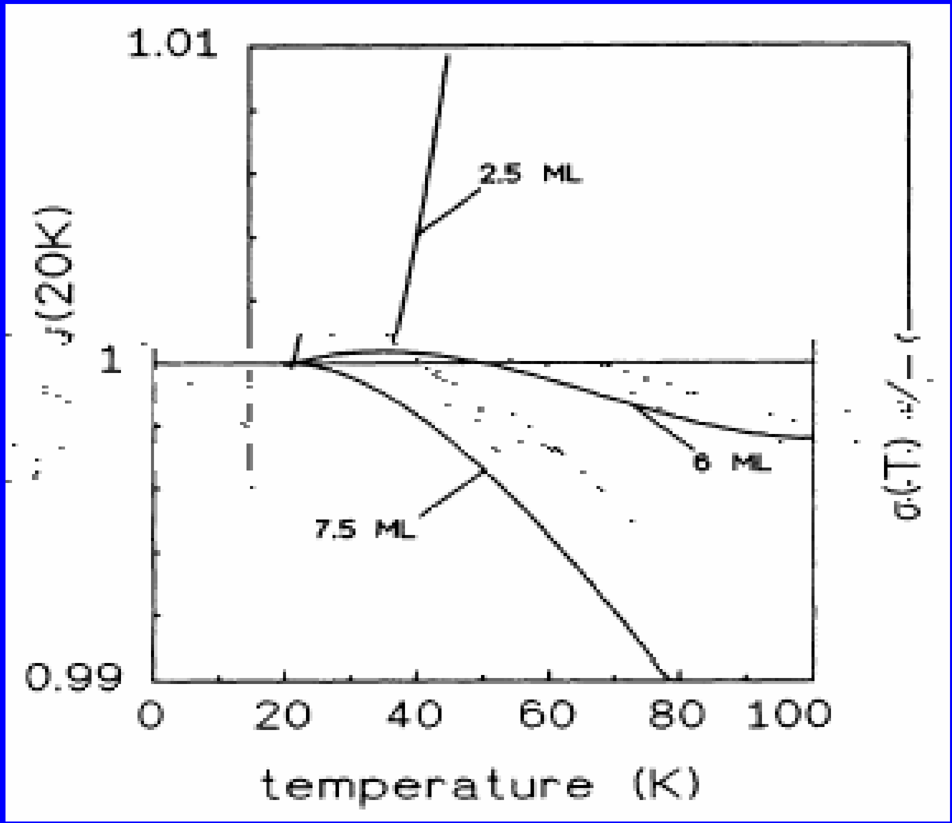

L. Van de dries, PRL 46, 565(1981)

PRB 45 11430

Uniform Mn nanodots on Si(111)

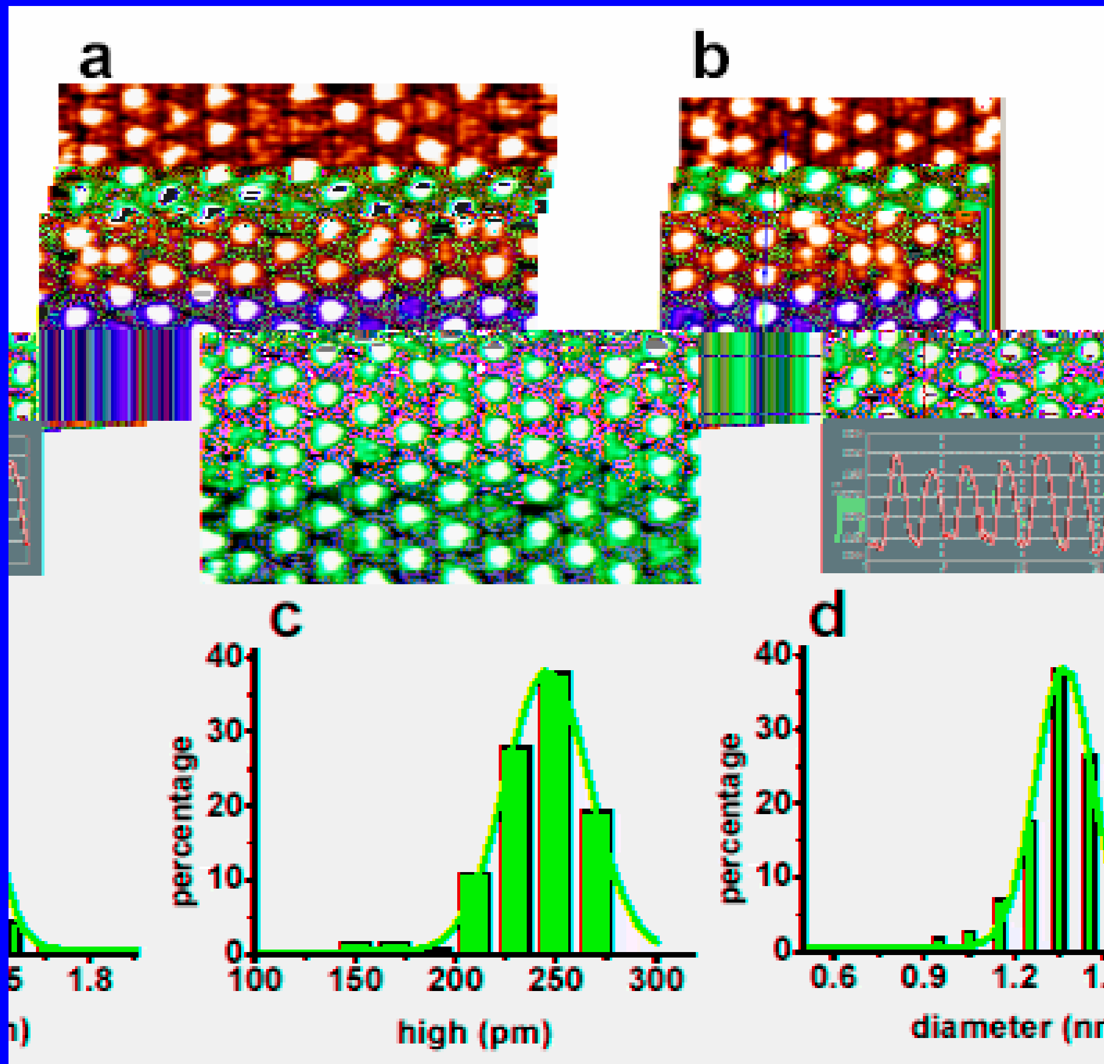

II. Preferential arrangement and Controllable Growth of Mn Nanodots

Triangular structure

Honeycomb structure

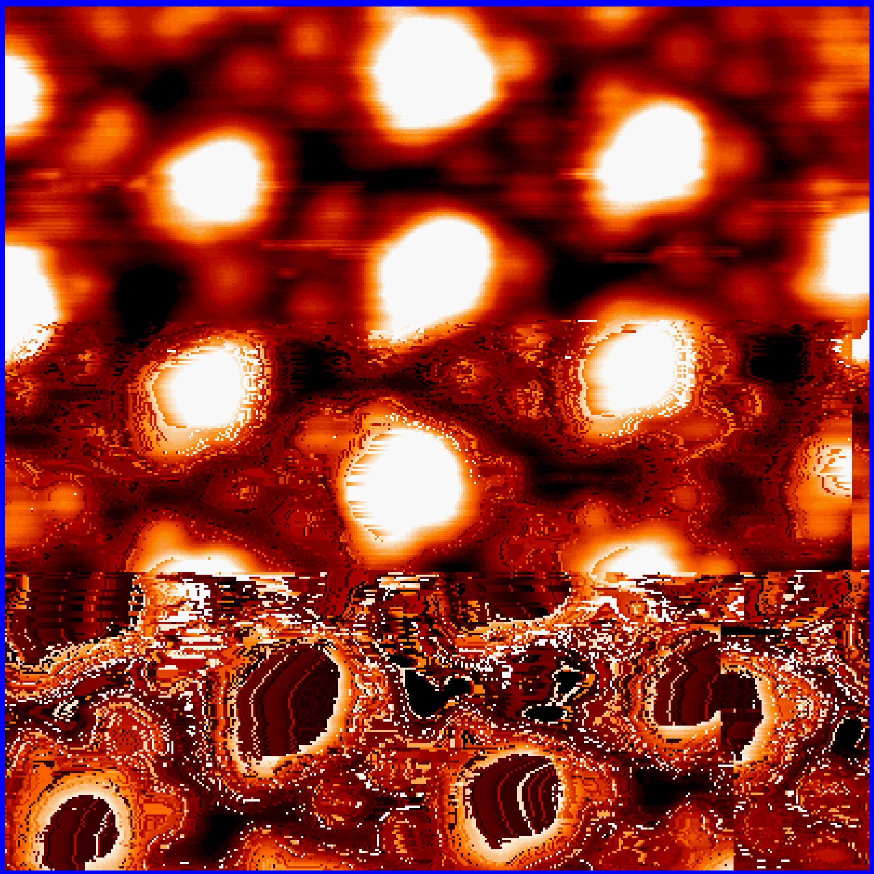

Deposition Rate

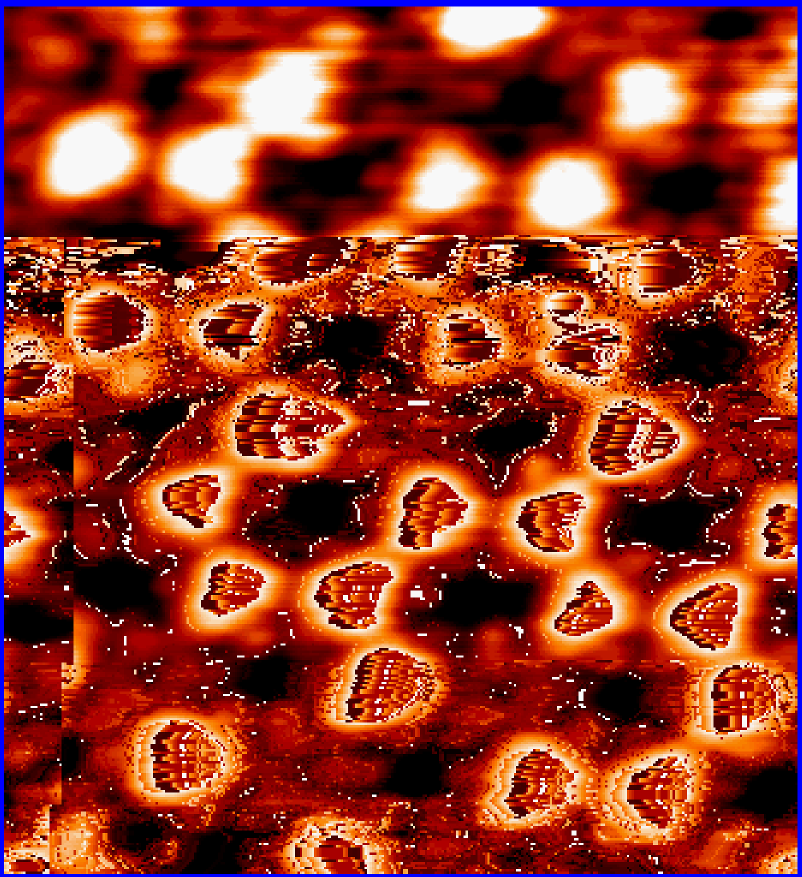

Kinetic Monte Carlo Simulation

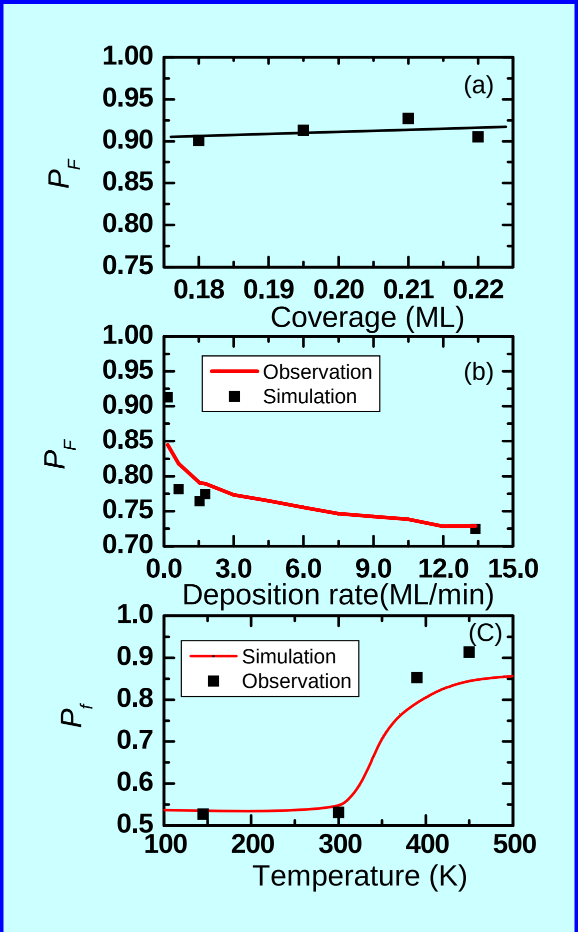

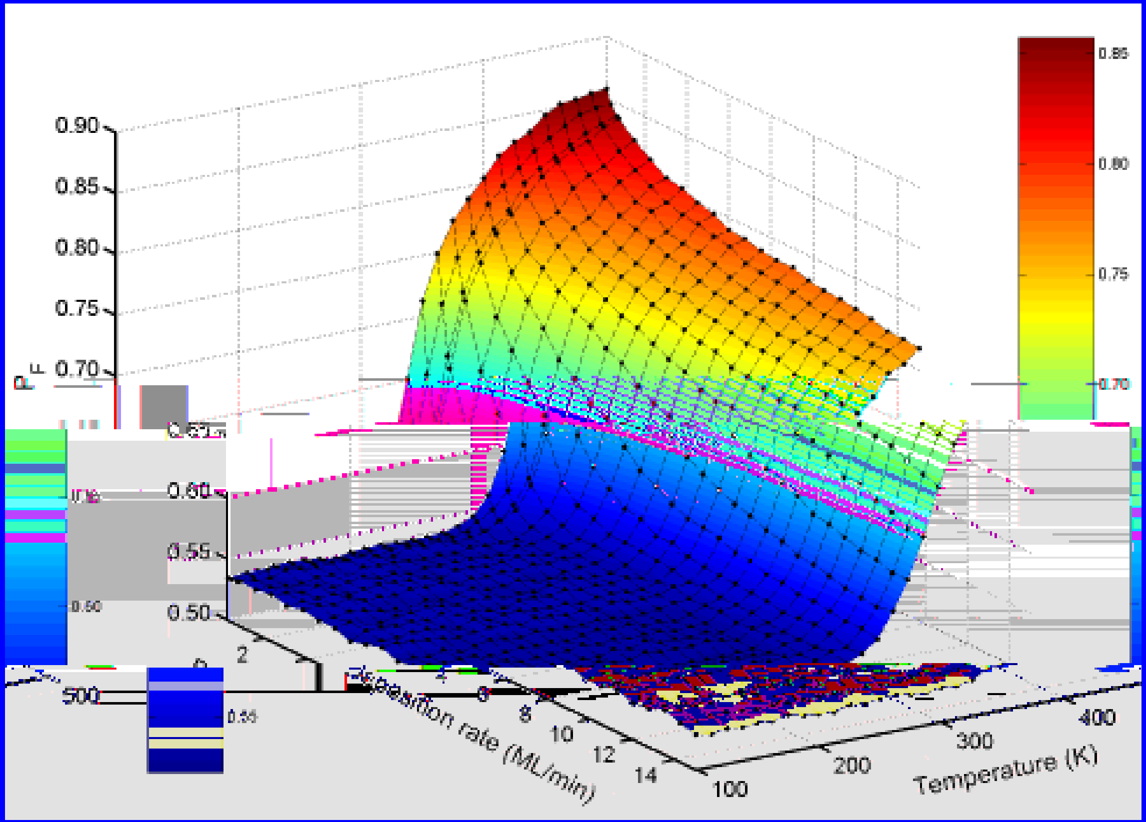

III. Fabrication of MnSi ultrathin film on Si(111)

0.02ML

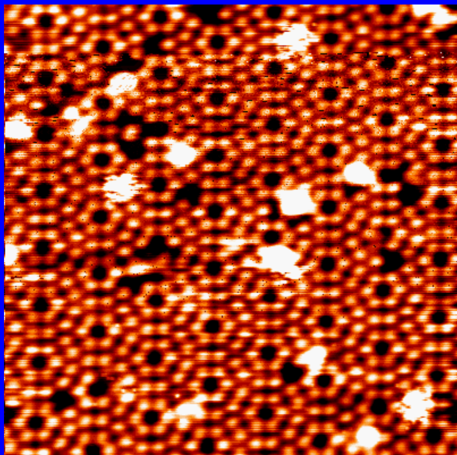

250 × 250nm²

1.6ML

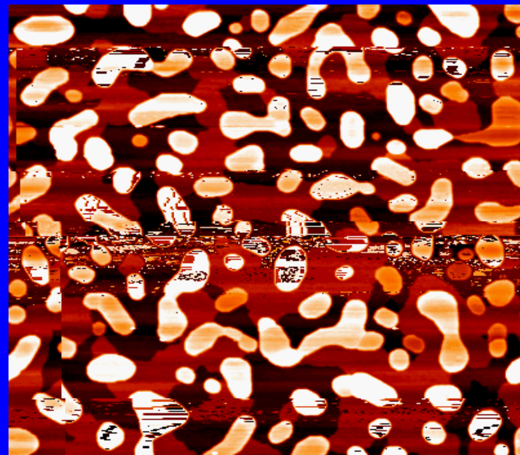

250 × 250nm²

2.4ML

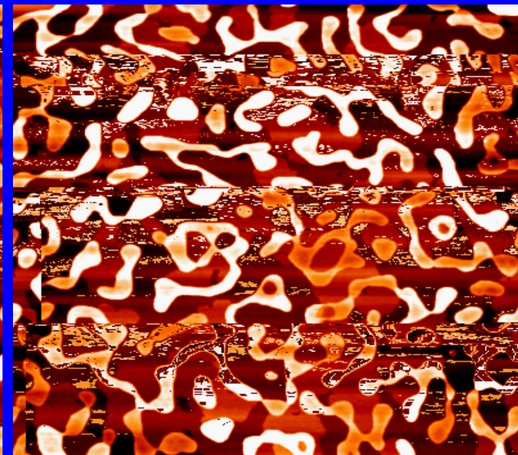

1000 × 1000nm²

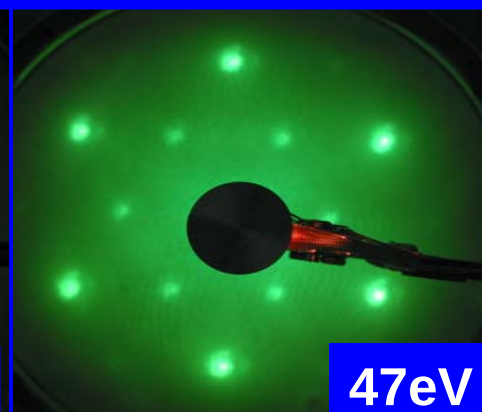

6ML

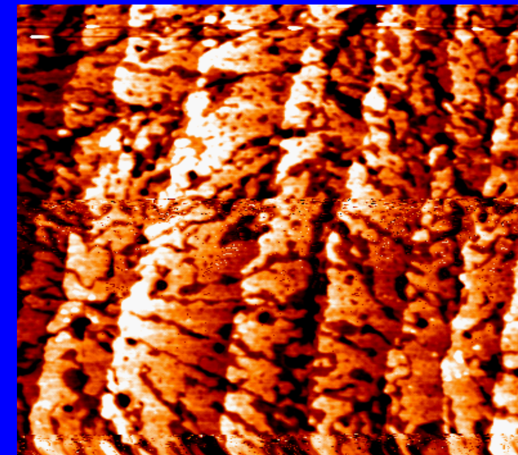

1000 × 1000nm²

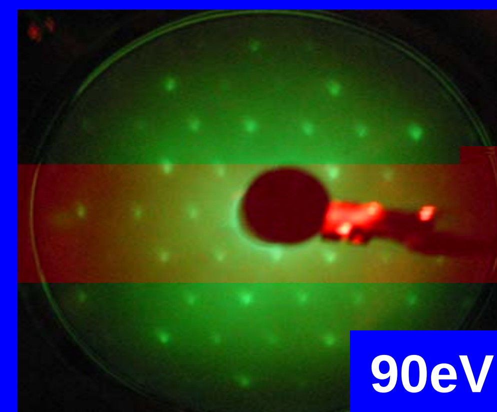

III. Fabrication of MnSi ultrathin film on Si(111)

XRD

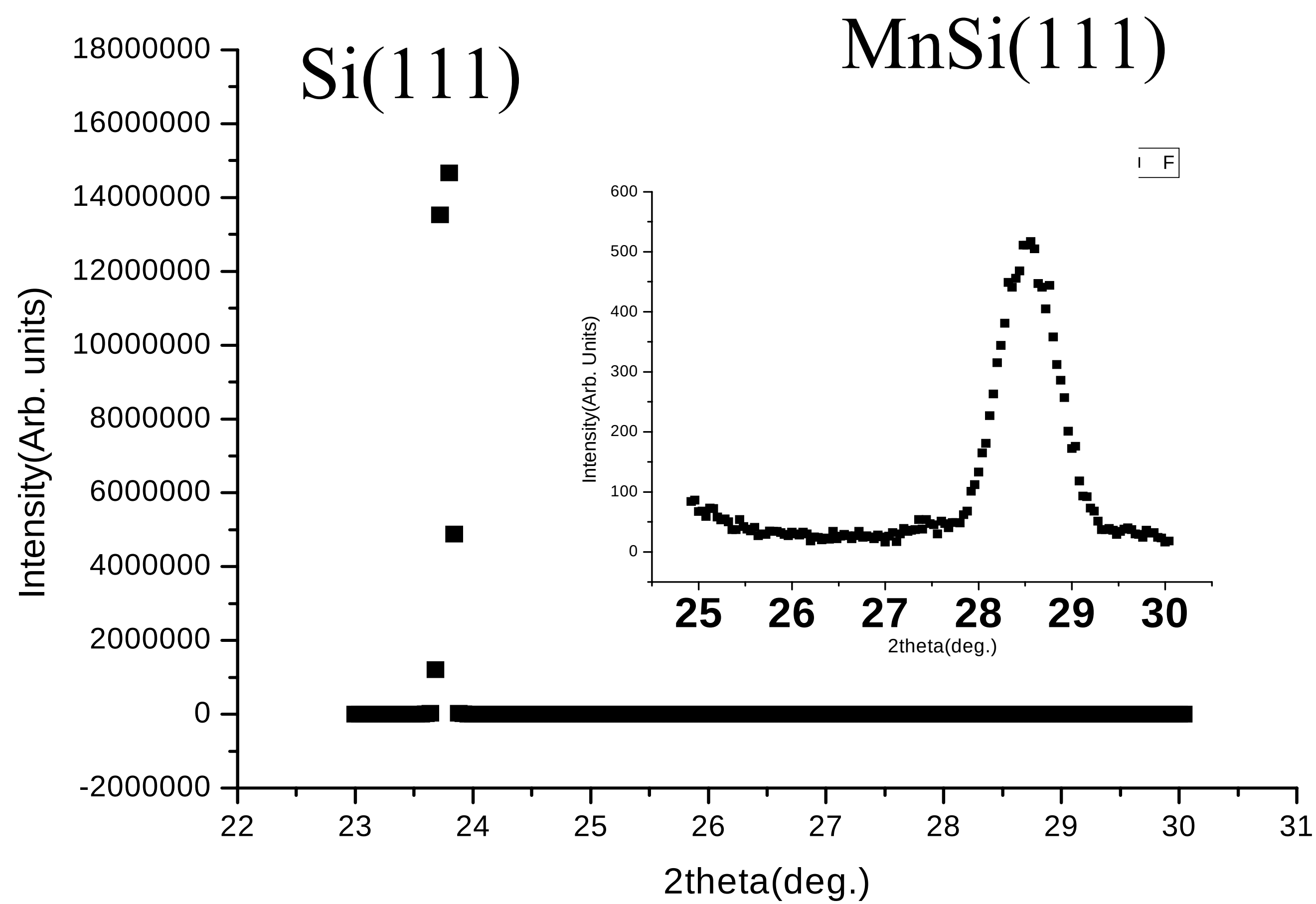

Growth model of MnSi

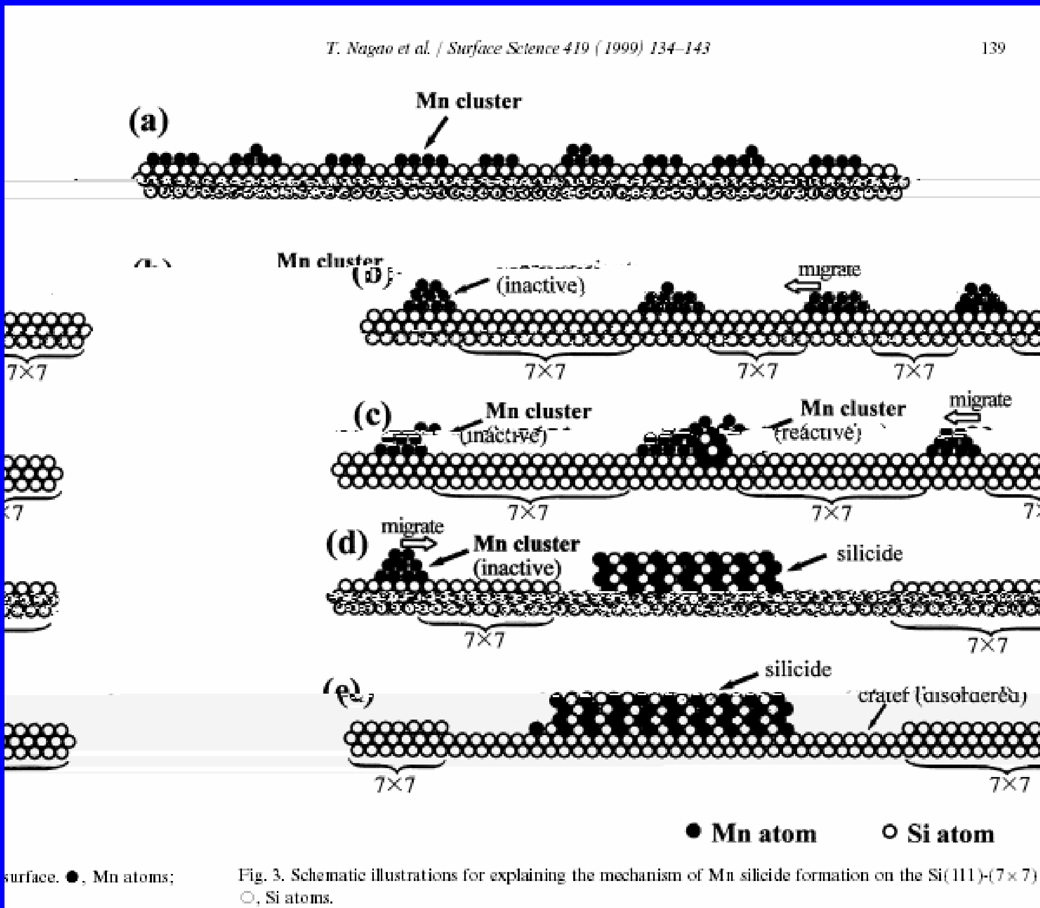

T. Nagao et al., Surf. Sci. 419(1999), 134

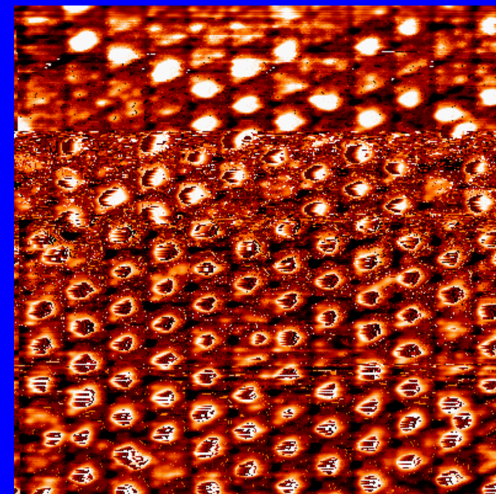

As-deposited

$30 \times 30 nm^2$

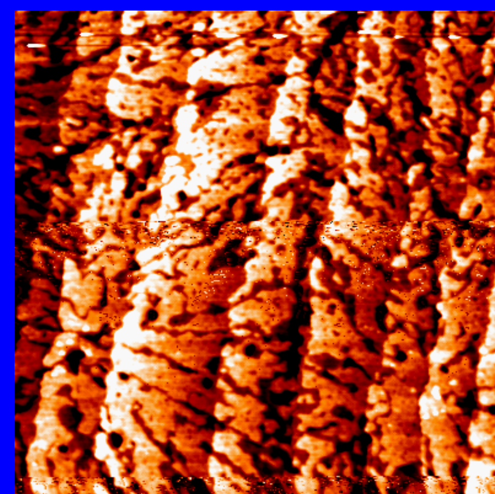

Post-annealed

$1000 \times 1000 nm^2$

24ML 6ML 4ML

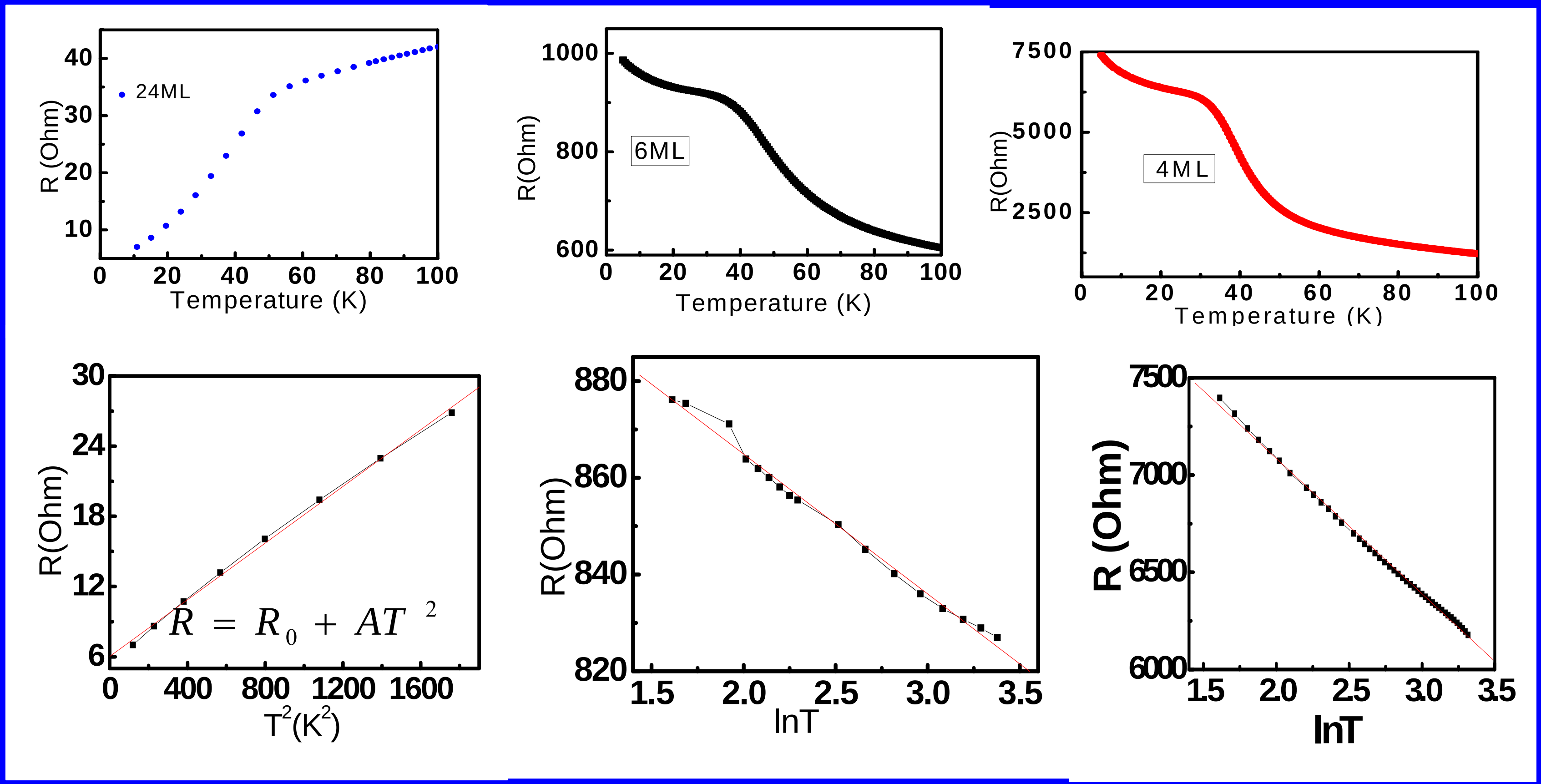

24ML
R (Ohm)
Temperature (K)
6ML
R(Ohm)
Temperature (K)
4ML
R(Ohm)
Temperature (K)
R(Ohm)
$R = R_0 + AT^2$
$T^2(K^2)$
R(Ohm)
lnT
R (Ohm)
lnT

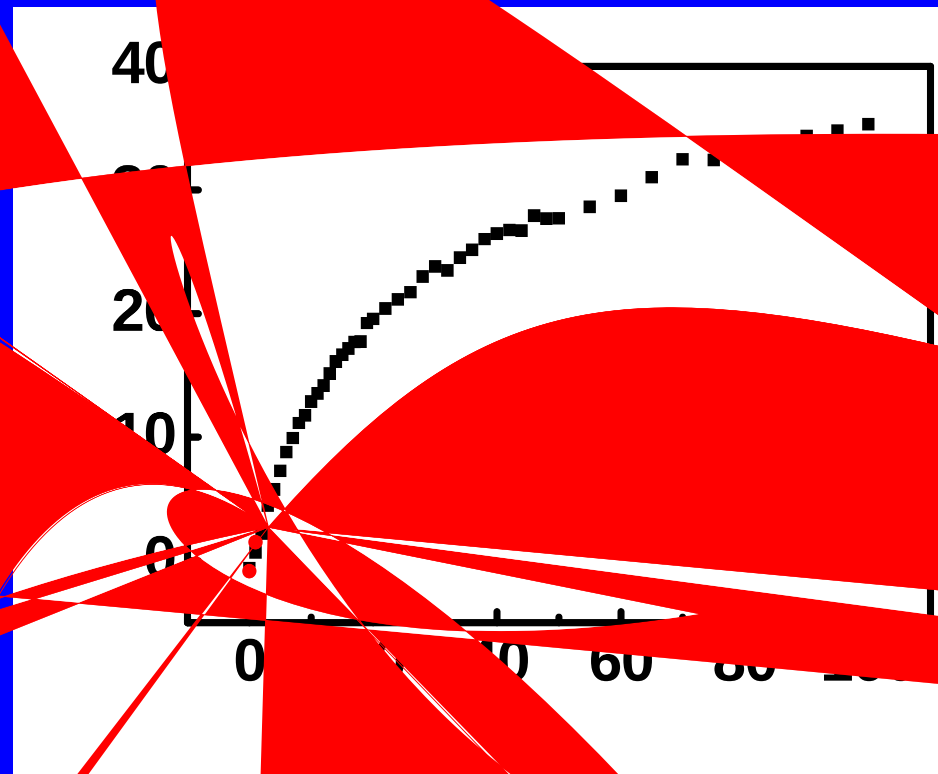
40
20
10
0
0
60
80

IV. Magnetic and Magnetotransport Properties of MnSi Ultrathin films

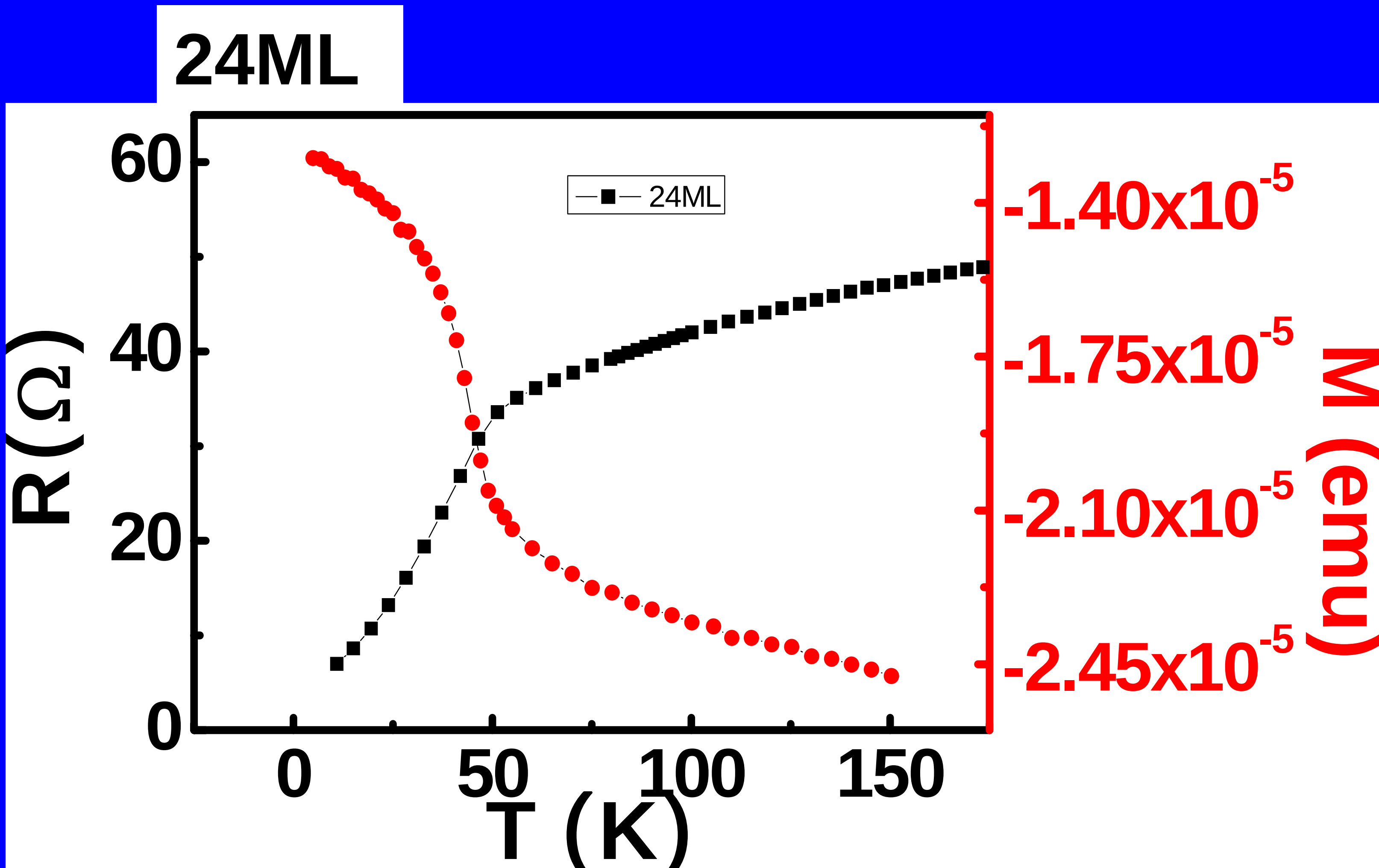

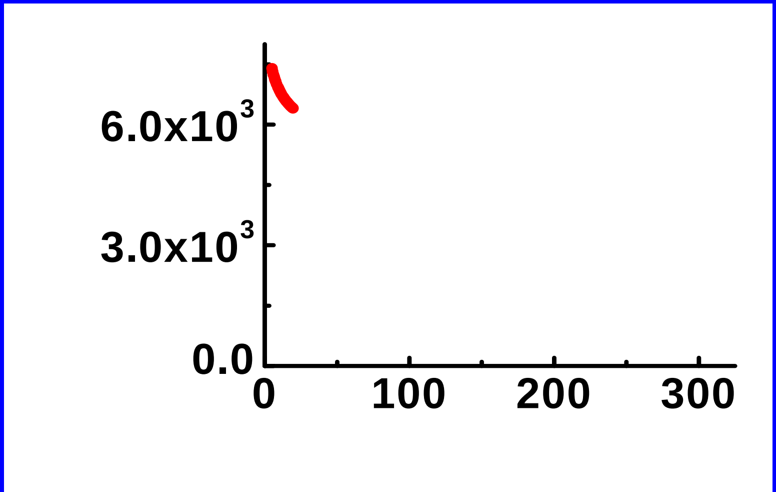
6.0x10^3
3.0x10^3
0.0
0
100
200
300

MnSi(111) surface:

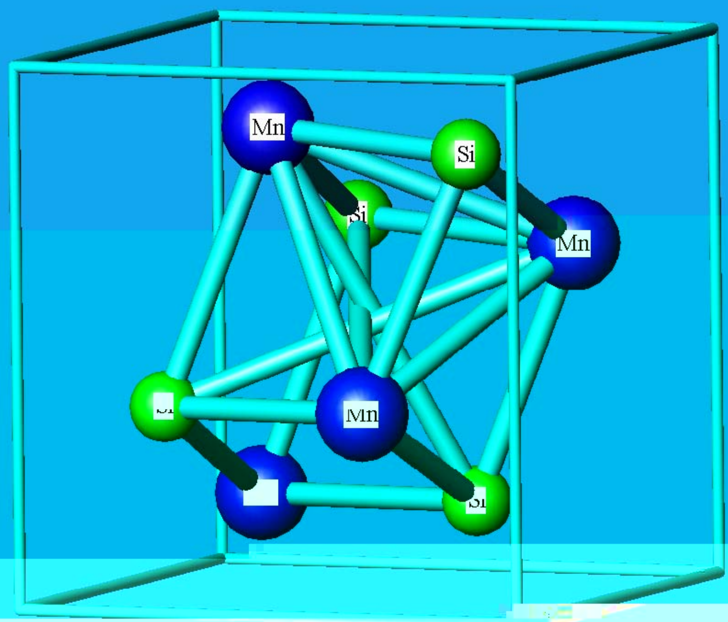

$d_{Mn\text{-}Si}$=0.373 nm

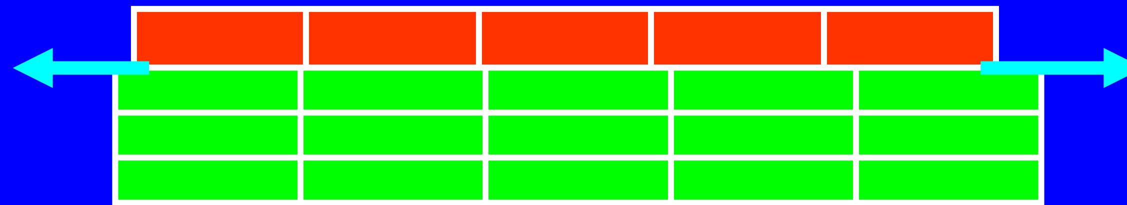

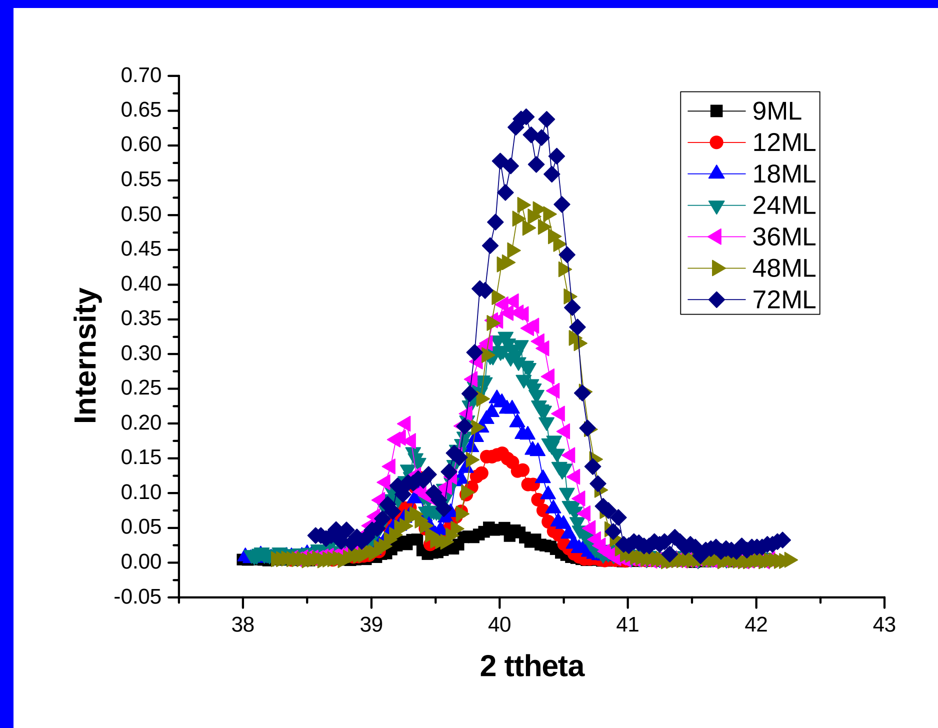

Si(111) dSi-Si=0.384 nm

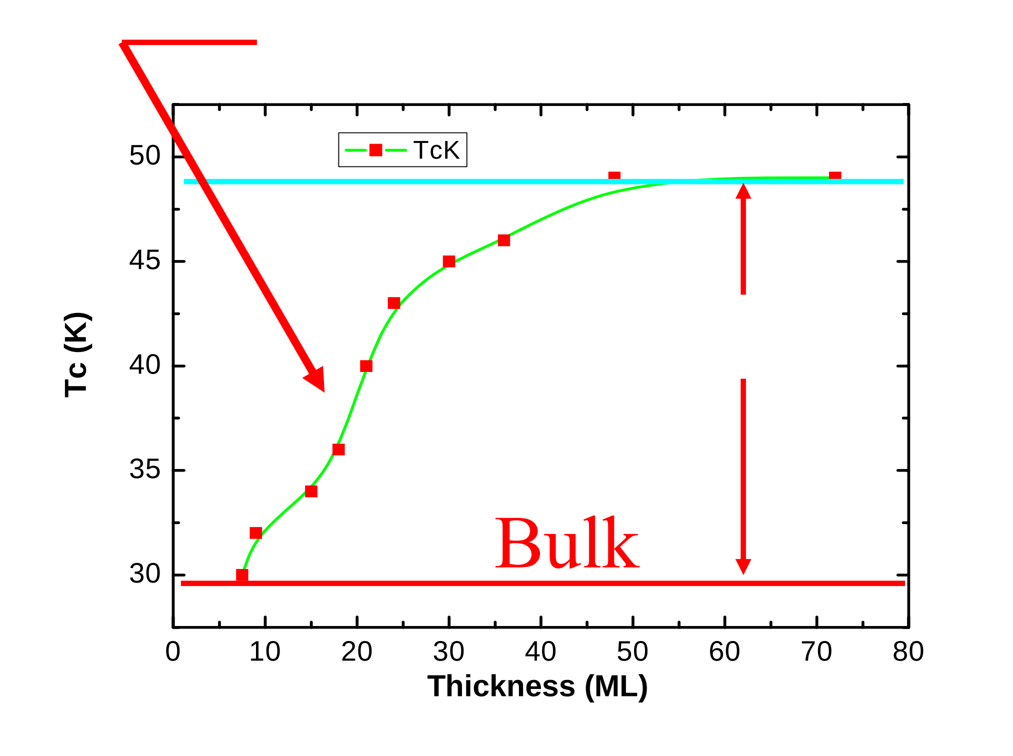

Strain relaxation

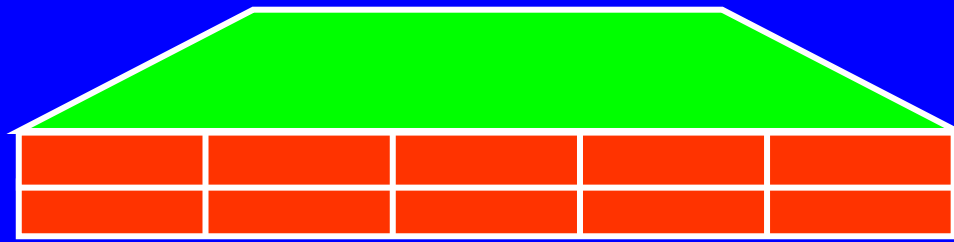

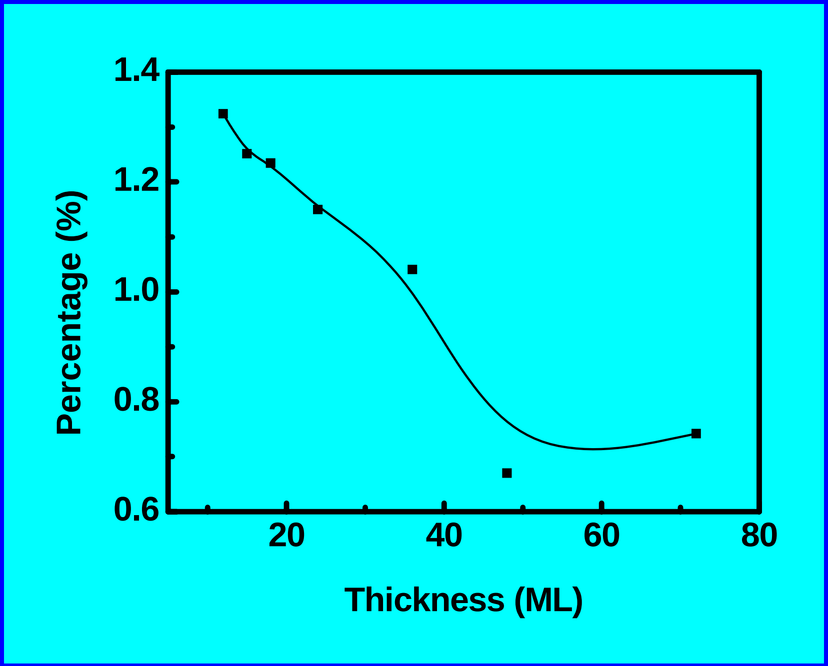

- Thickness

$$[T_c(\infty) - T_c(d)]/T_c(\infty) = (c/d)^{\lambda},$$

- Strain

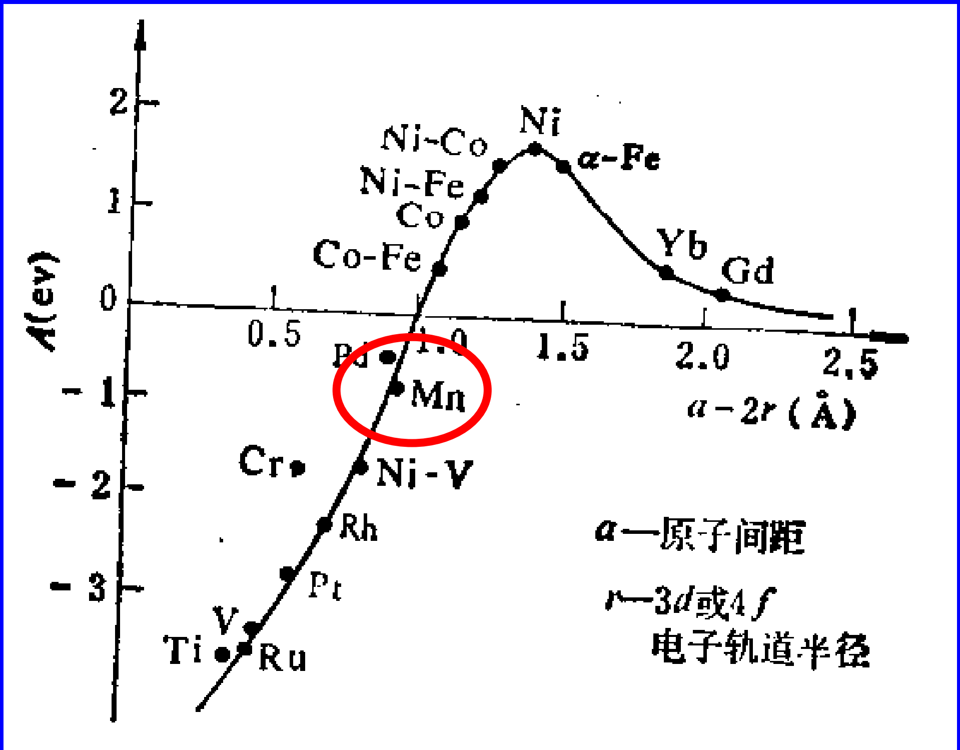

图 3.3　奈耳给出的交换能与(a − 2r)的关系曲线。

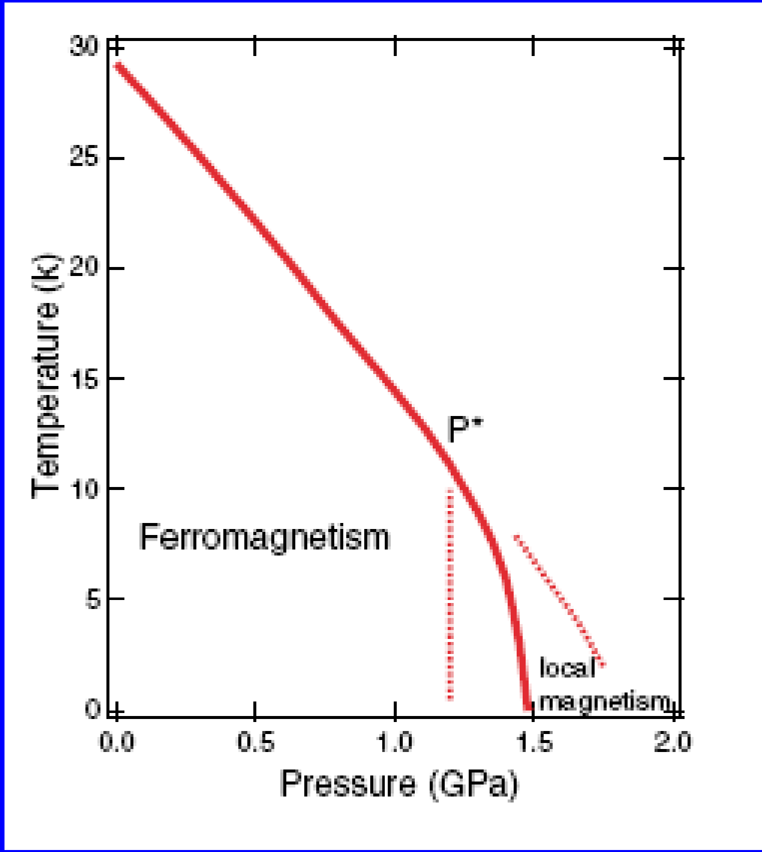

W. Yu et al., PRL, 92,086403(2004)

1. MnSi

2. MnSi

3. MnSi

4.

1.

2.

-
-
-
- ……………

Long Range Magnetic Order low-dimensional System

Mermin-Wagner Theorem

An infinite *d* dimensional lattice of localized spins cannot have LRO at any finite temperature for *d*<3 if the effective exchange interactions among spins are isotropic in spin space and of finite range

T=0 K, **FM LRO, No AFM LRO**

FM LRMO at T>0 if

- **Anisotropy (exchange,dipolar or single-ion anisotropy)**

- **Dipolar or RKKY interactions**

Mermin and Wagner, PRL 17(1966),1133; M. Bander and D.L. Mills, Phys. Rev. B. 38(1988)

Importance of Magnetic anisotropy

- Origin of Long range Magnetic order in low dimensional system

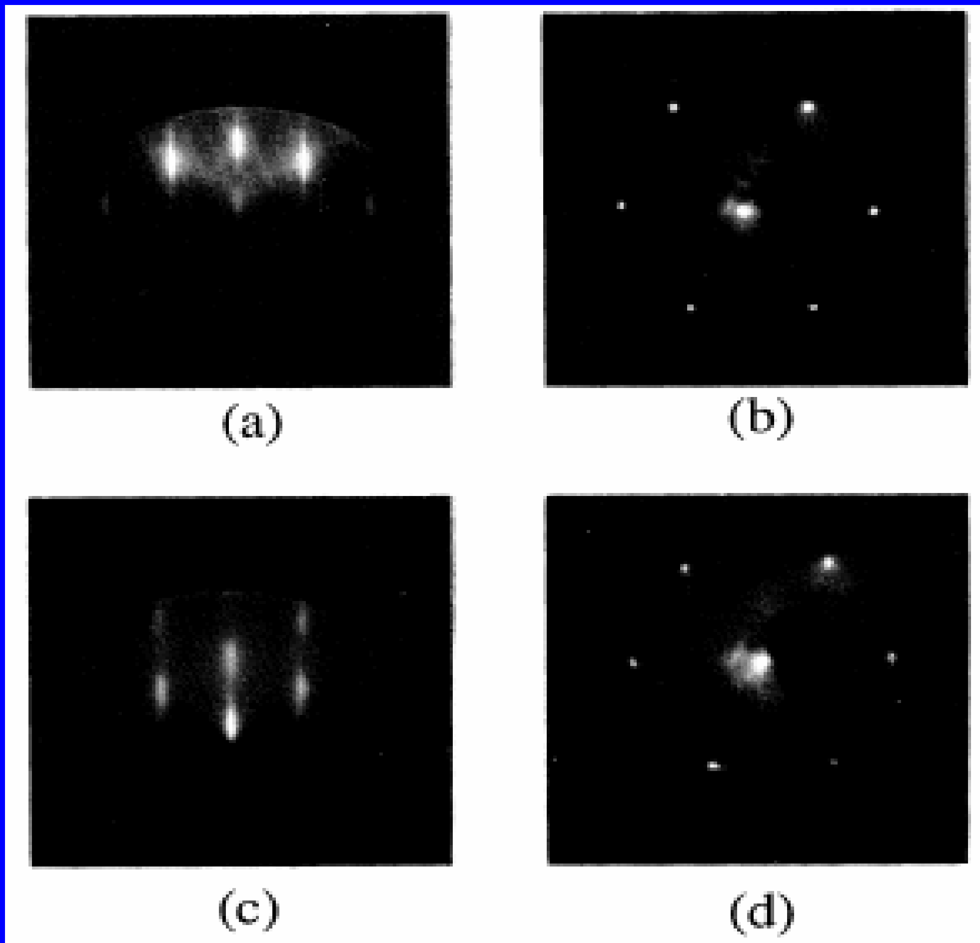

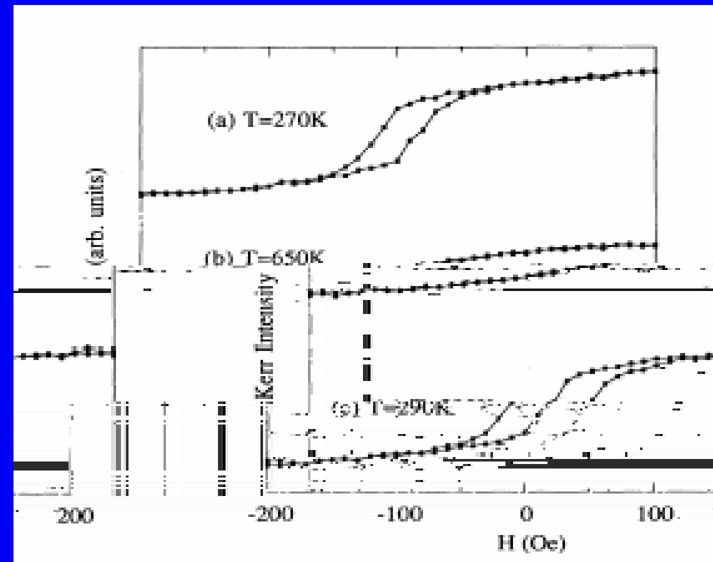

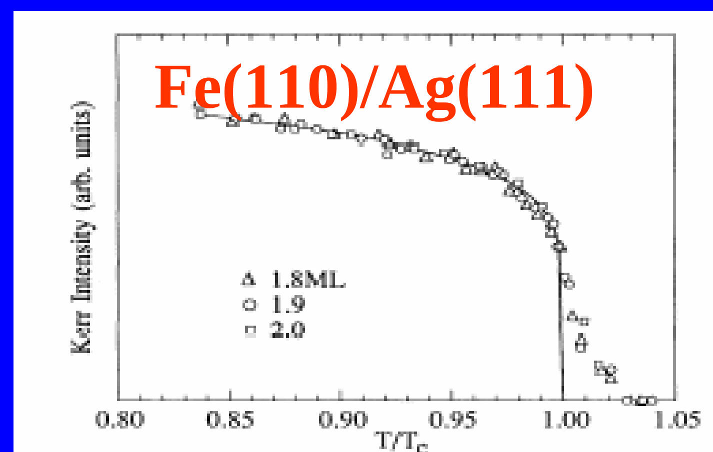

Z.Q. Qiu et al., PRL 67(1991),1133

Importance of Magnetic anisotropy

•Strong permanent magnet

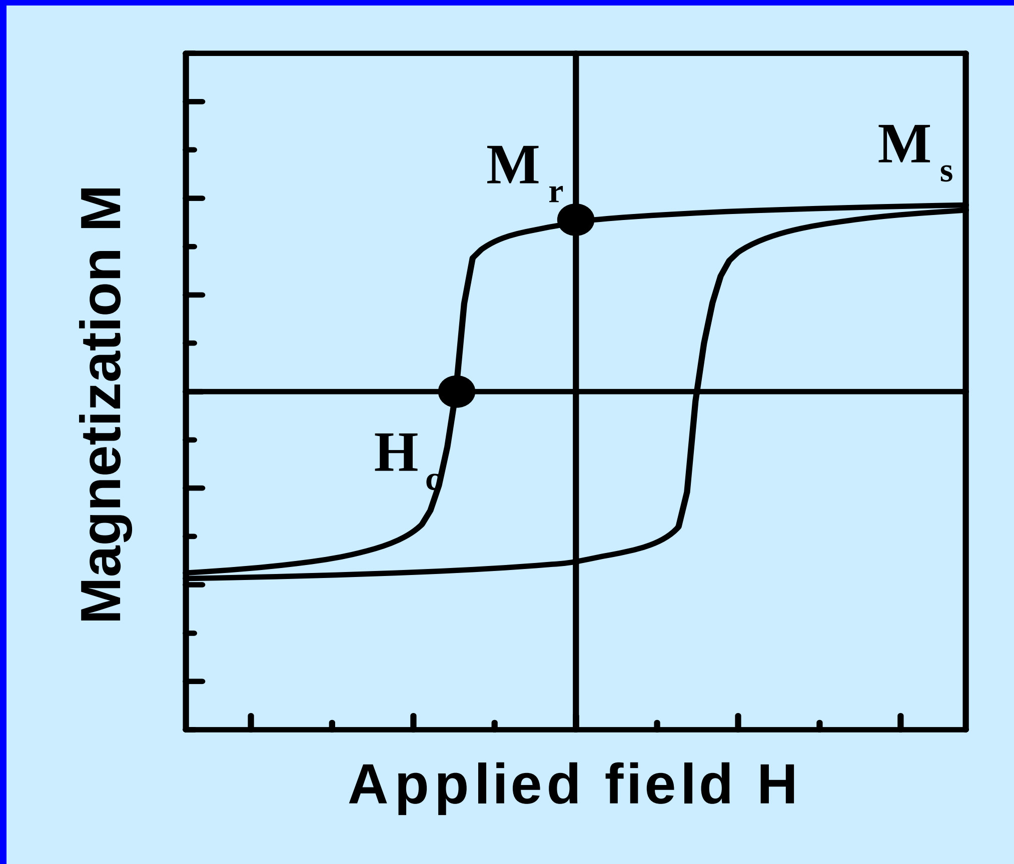

$$H_0 = \alpha \cdot \frac{2 \cdot K_u}{M_S} - N_{eff} \cdot M_S$$

Importance of Magnetic anisotropy

- Ultrahigh density of magnetic media and superparamagnetism limit

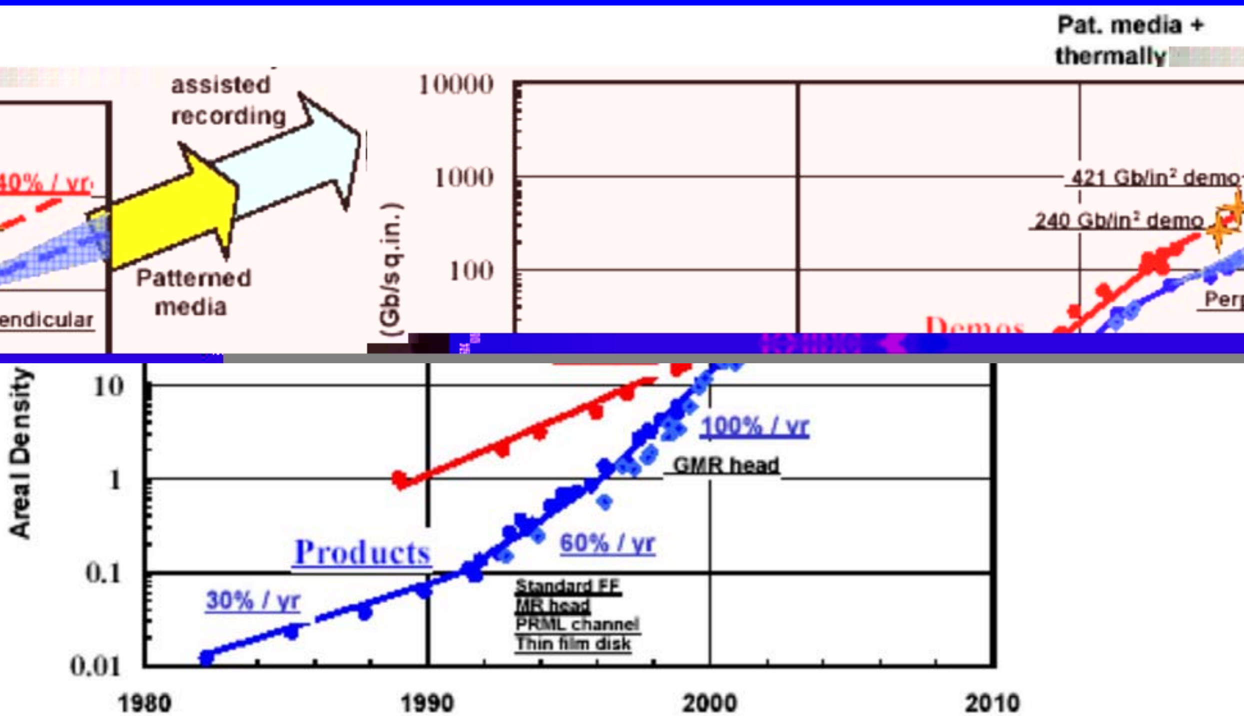

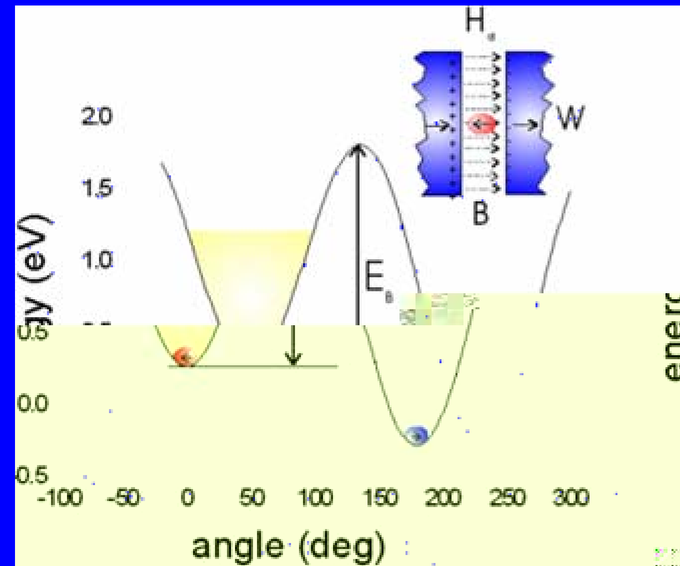

$$t = 10 \quad \text{year}$$

$$\frac{KV}{k_B T} > 40 \quad 60$$

E. A. Dobisz, et al., Proceedings of the IEEE 96,(2008), 1836

Importance of Magnetic anisotropy

•High frequency of magnetic materials

•For cubic symmetry

Natural Resonance frequency

$$f_r = \frac{\gamma K_u}{\pi M_s}$$

×

Peamibility of strong magnet

$$\bar{\mu} = \frac{M_s^2}{3\mu_0 K_u}$$

=

Limit of Snoek

$$f_r \cdot \bar{\mu} = \frac{\gamma M_s}{3\mu_0}$$

•For in-plane uniaxial anisotropy

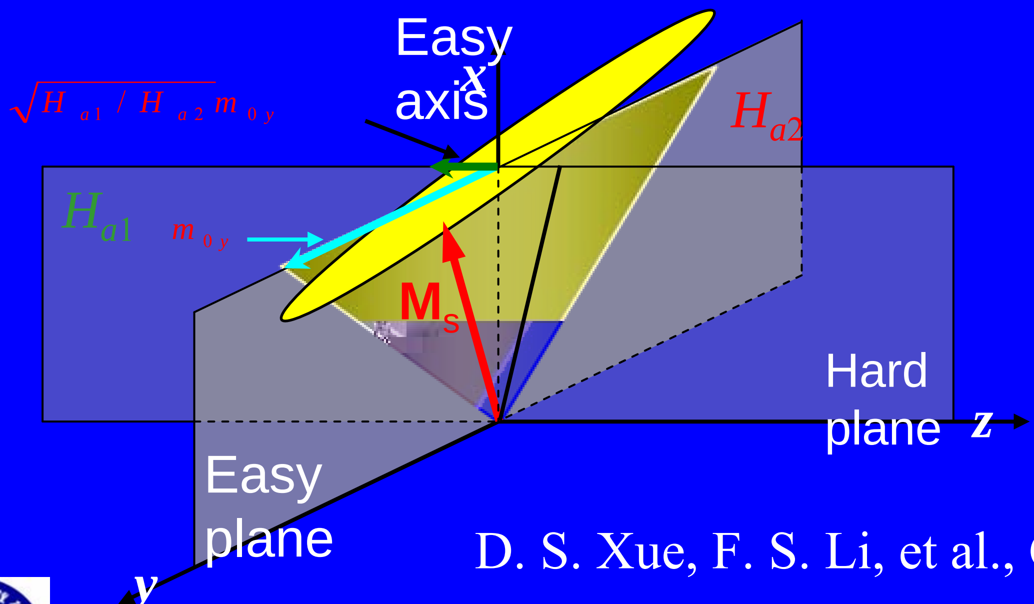

$$(\mu_s - 1) f_r = \frac{\gamma}{2\pi}\sqrt{\frac{H_{a1}}{H_{a2}}} M_s$$

D. S. Xue, F. S. Li, et al., Chin. Phys. Lett. **25**, 4120 (2008).

Magnetic Anisotropy

- **Magnetocrystalline anisotropy(MCA)**

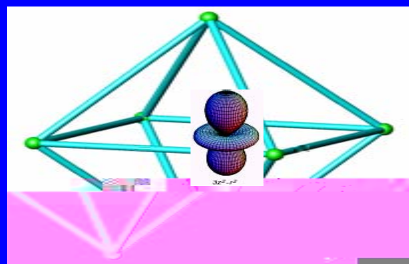
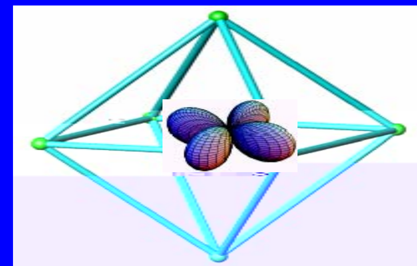
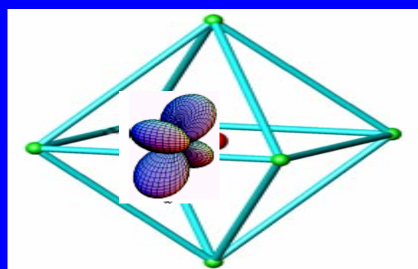
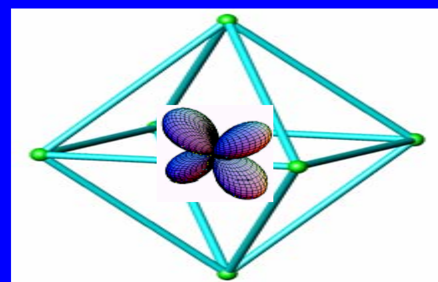
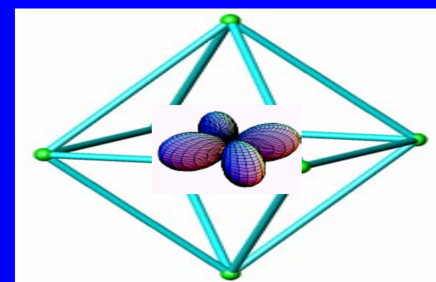

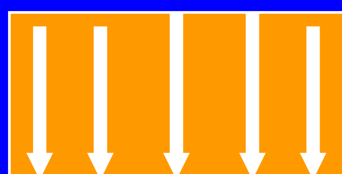

$$E_{LS} = \lambda \vec{L} \bullet \vec{S}$$

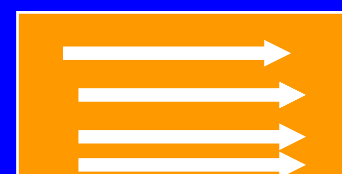

Single-Ion Model

LS

CEF → ***Orbital anisotropy*** → ***MCA***

Magnetic Anisotropy

Surface magnetic anisotropy

Fe/Cu(100) SRT=5ML

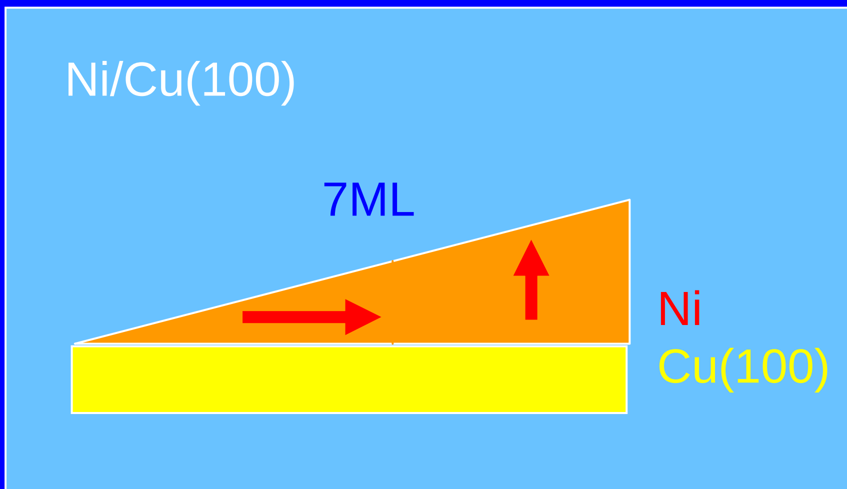

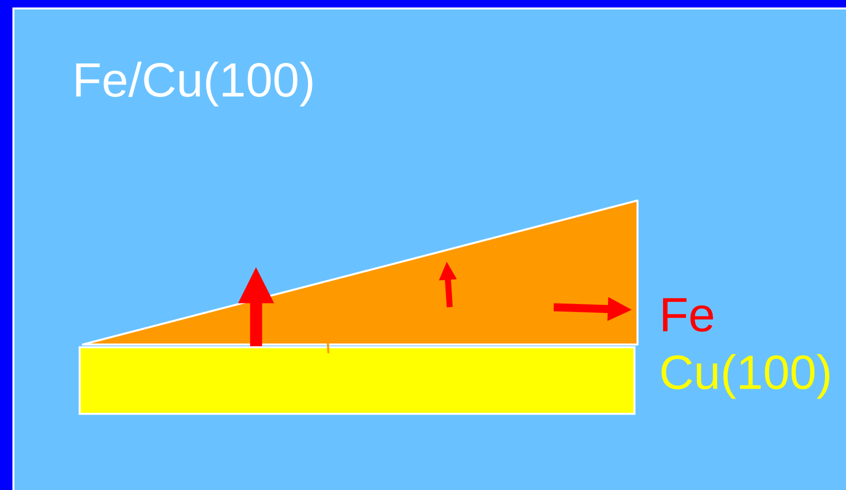

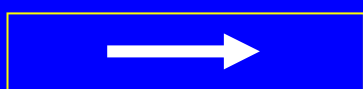

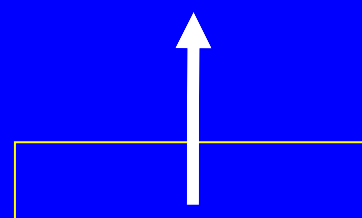

Ks < 0

Ks > 0

Perpendicular Magnetic Anisotropy Induced by Tetragonal Distortion of FeCo Alloy Films Grown on Pd(001)

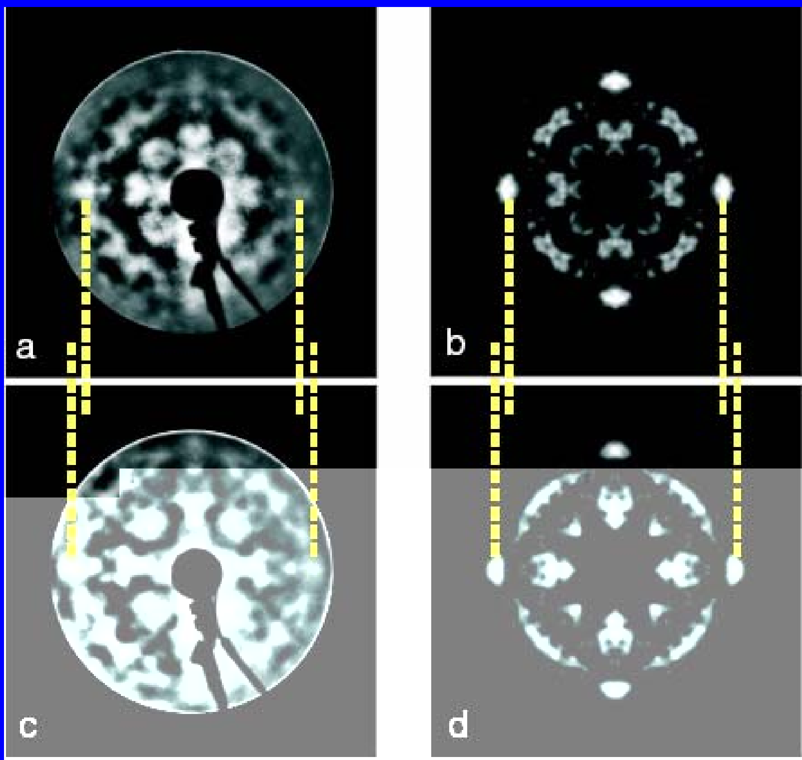

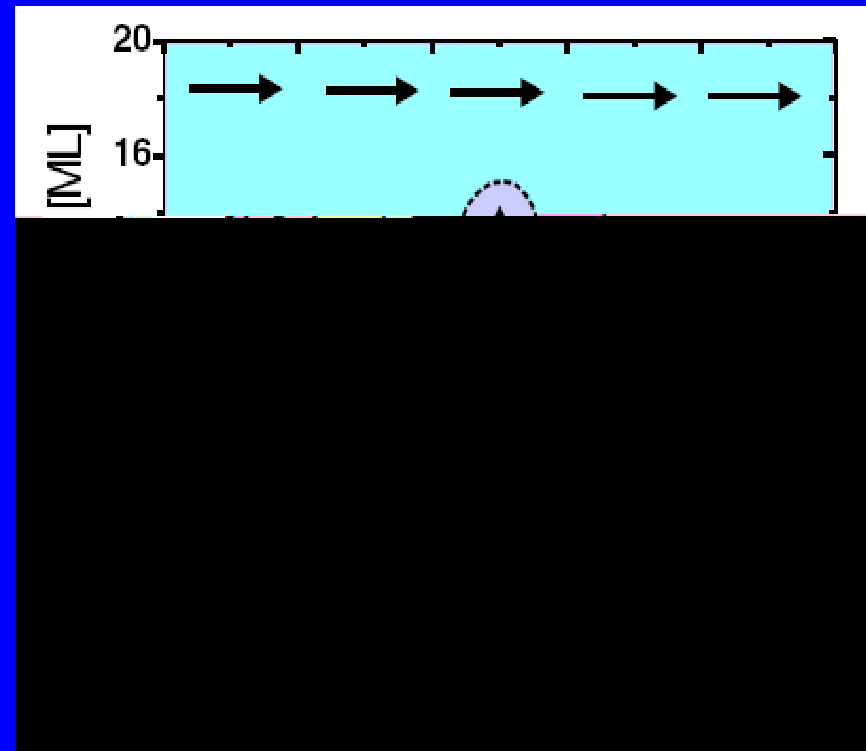

A.Winkelmann et al, PRL,96,257206(2006)

Strongly Enhanced Orbital Moment by Reduced Lattice Symmetry and varying Composition of Fe1-*x*Co*x* Alloy Films

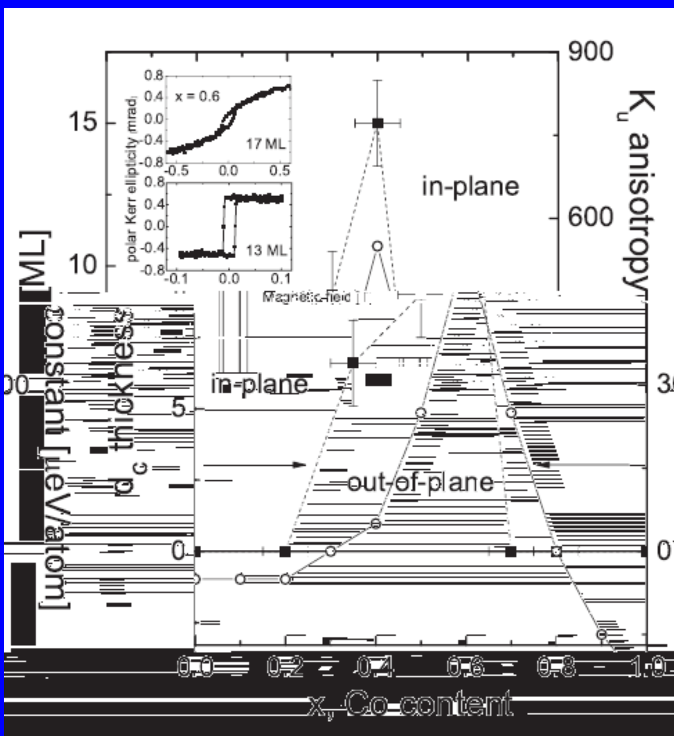

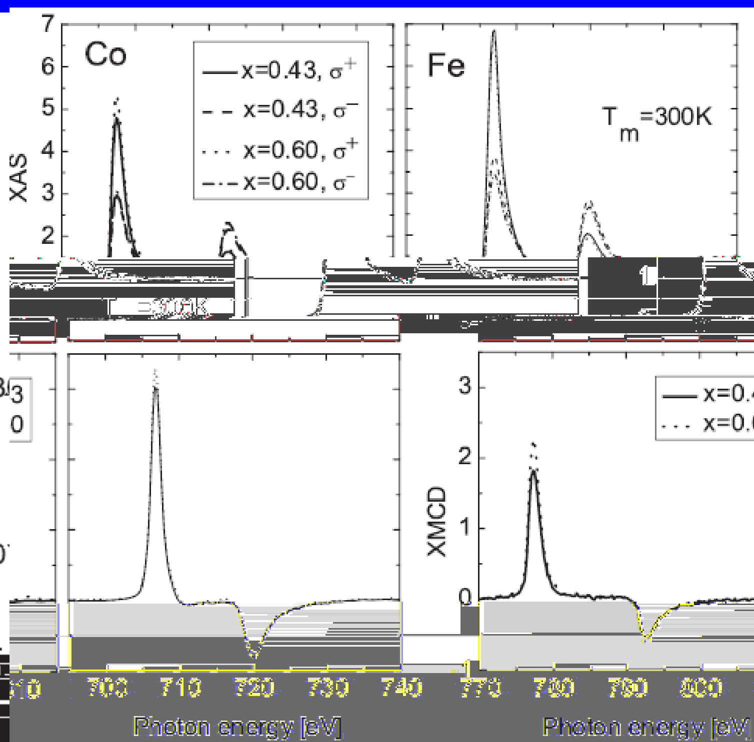

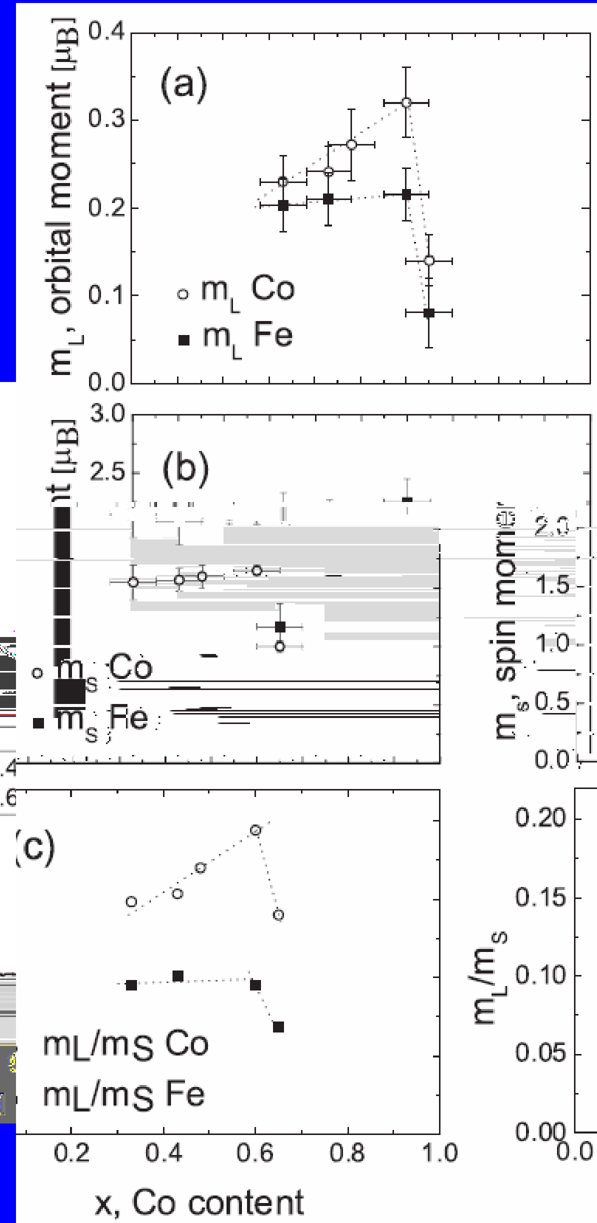

F. Yildiz et al, PRL,100,037205(2008)

Why chose Fe/Pb/Si(111)

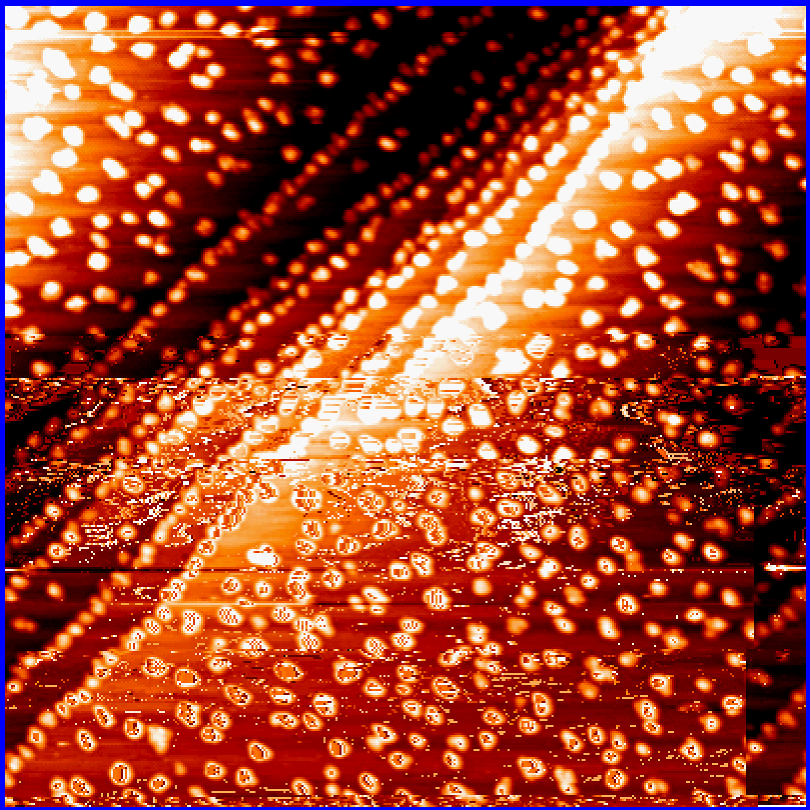

200nm

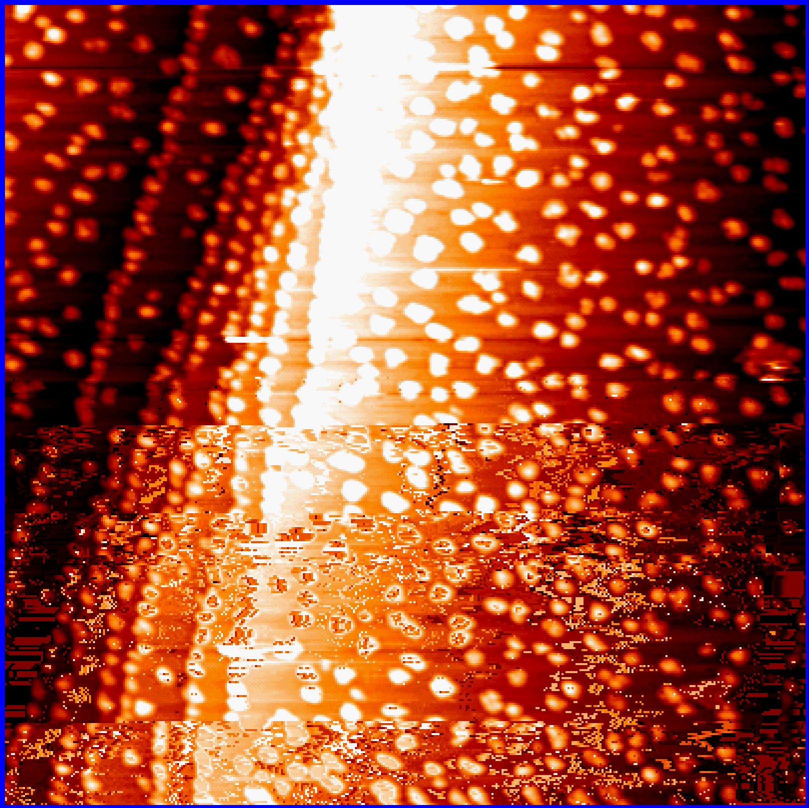

200nm

Growth at Low temperature for 30 seconds Co

Why chose Fe/Pb/Si(111)

1. Pb Si

2. Fe/Si FeSi
   Fe/Pb/Si

3. Fe $2.48 J/m^2$, Pb $0.5 J/m^2$
   Fe bcc 2.87A Fe(110) 2.49A
   Pb fcc 4.95A Pb(111) 2.8435A
   0D: "V W"
   1D: "Step-decoration"

Pb / Si(111)
0.1
500 × 500

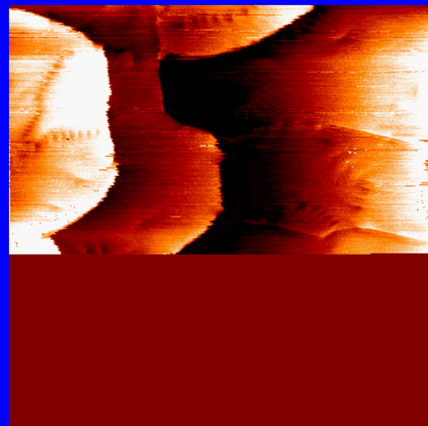

Pb / Si(111)
4
500 × 500

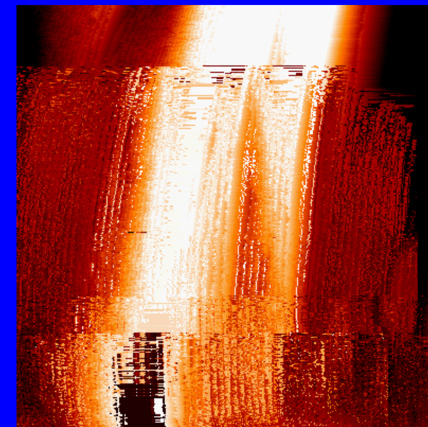

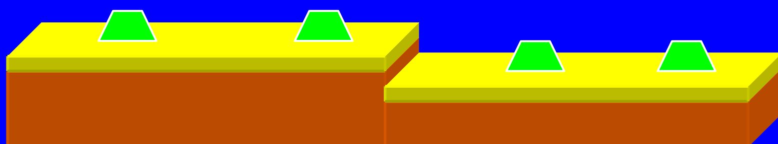

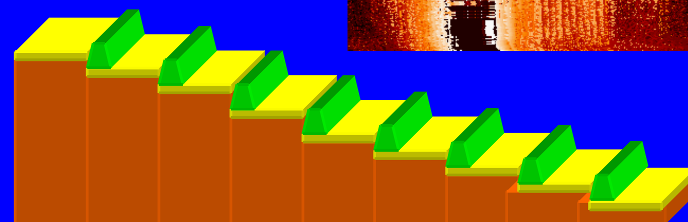

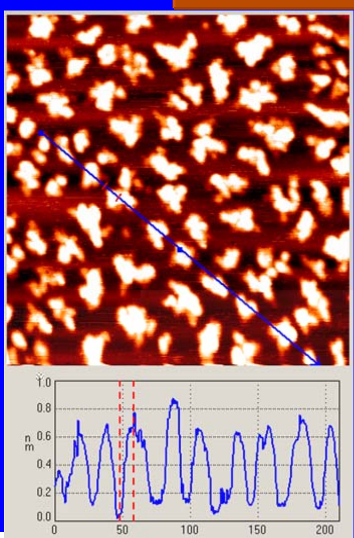

0.84ML

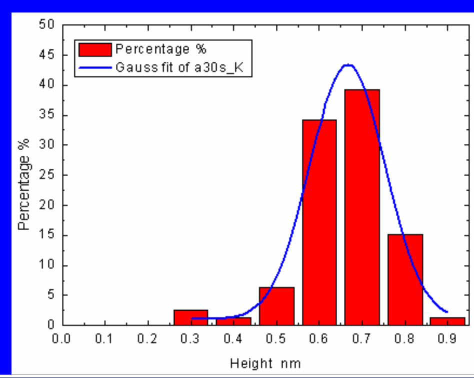

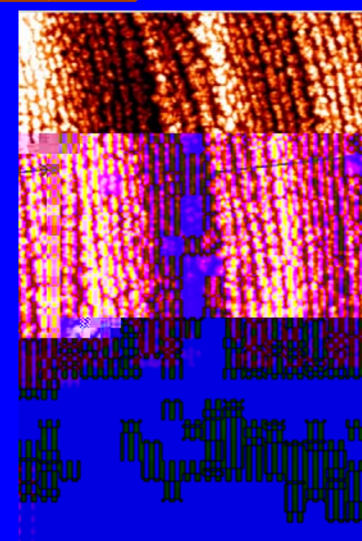

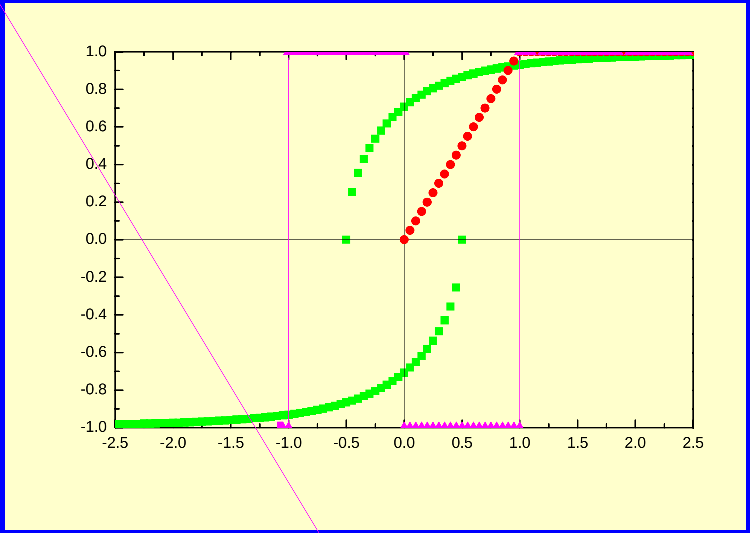
1.0
0.8
0.6
0.4
0.2
0.0
-0.2
-0.4
-0.6
-0.8
-1.0
-2.5 -2.0 -1.5 -1.0 -0.5 0.0 0.5 1.0 1.5 2.0 2.5

Pb

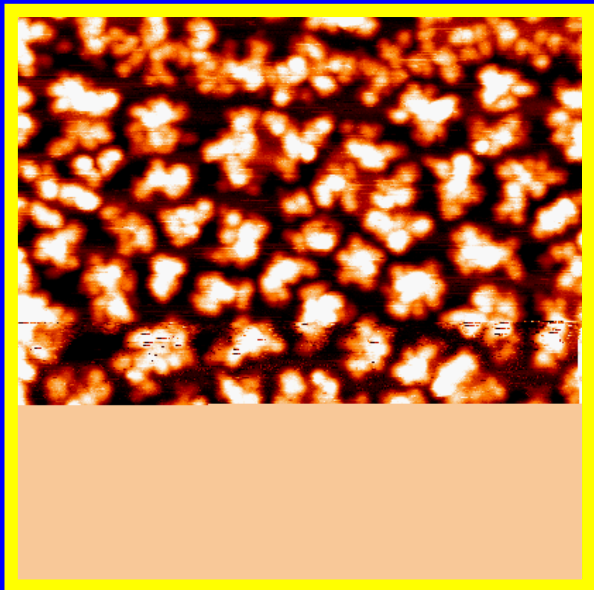

Fe

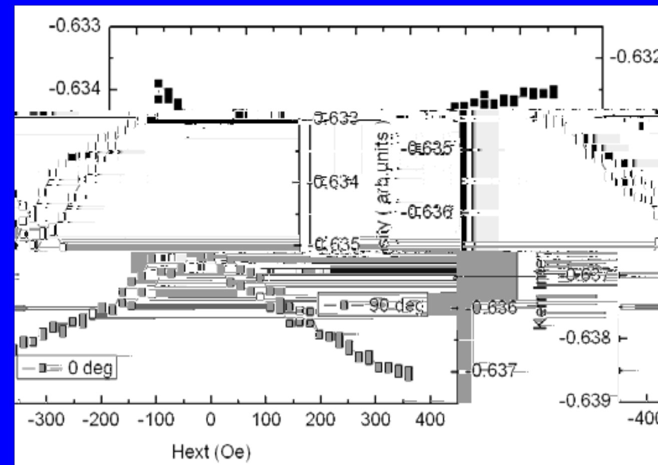

SMOKE 60

1.6 ML 300K

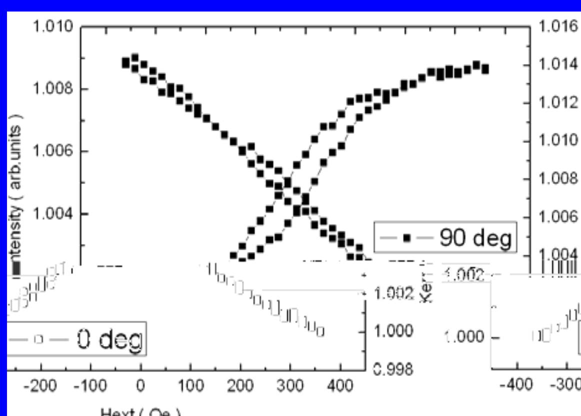

SMOKE 90

1.6 ML 300K

MBE-Step induced

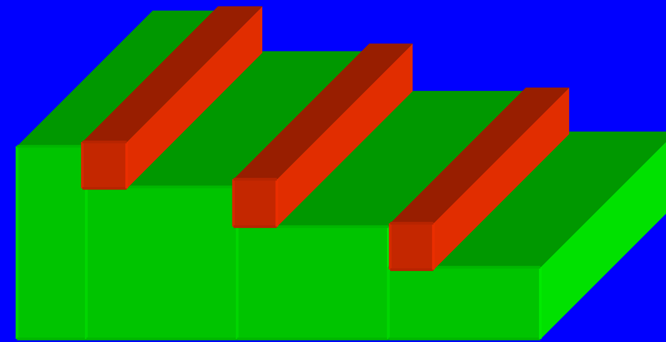

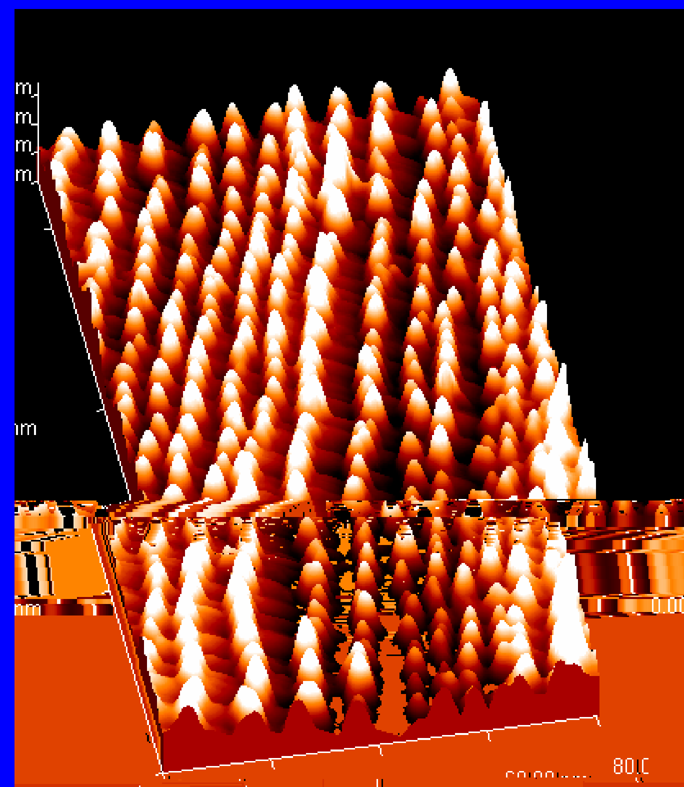

*300 nm*300 nm*

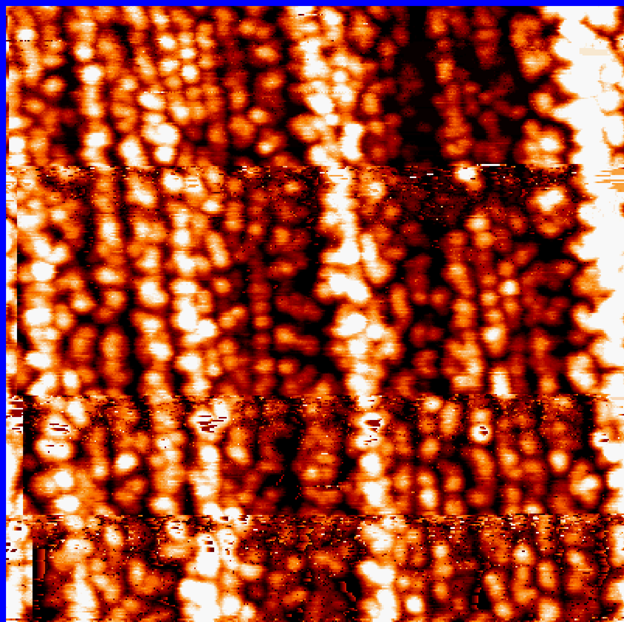

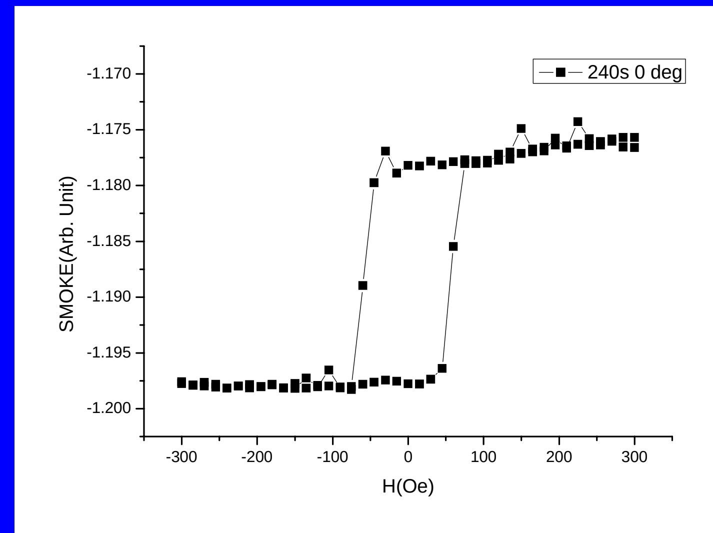
240s 0 deg
SMOKE(Arb. Unit)
H(Oe)
-1.170
-1.175
-1.180
-1.185
-1.190
-1.195
-1.200
-300
-200
-100
0
100
200
300

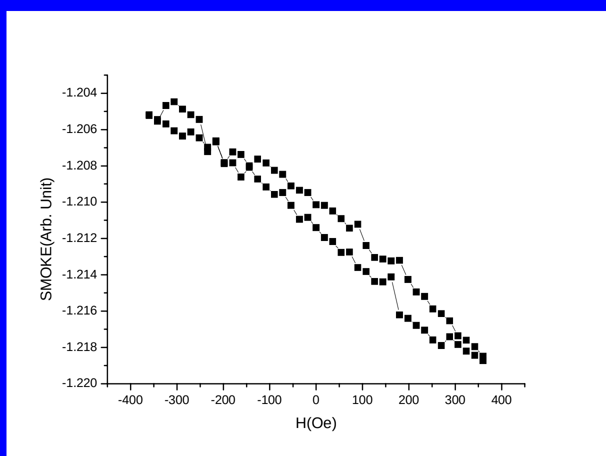
SMOKE(Arb. Unit)
H(Oe)
-1.204
-1.206
-1.208
-1.210
-1.212
-1.214
-1.216
-1.218
-1.220
-400
-300
-200
-100
0
100
200
300
400

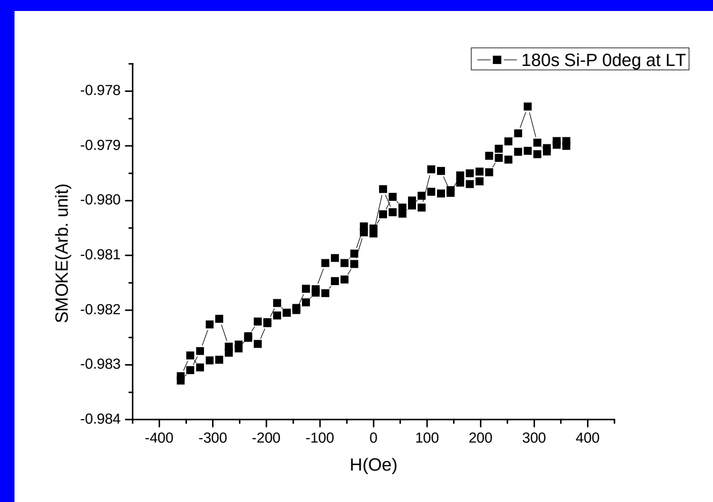
180s Si-P 0deg at LT
SMOKE(Arb. unit)
H(Oe)
-0.978
-0.979
-0.980
-0.981
-0.982
-0.983
-0.984
-400
-300
-200
-100
0
100
200
300
400

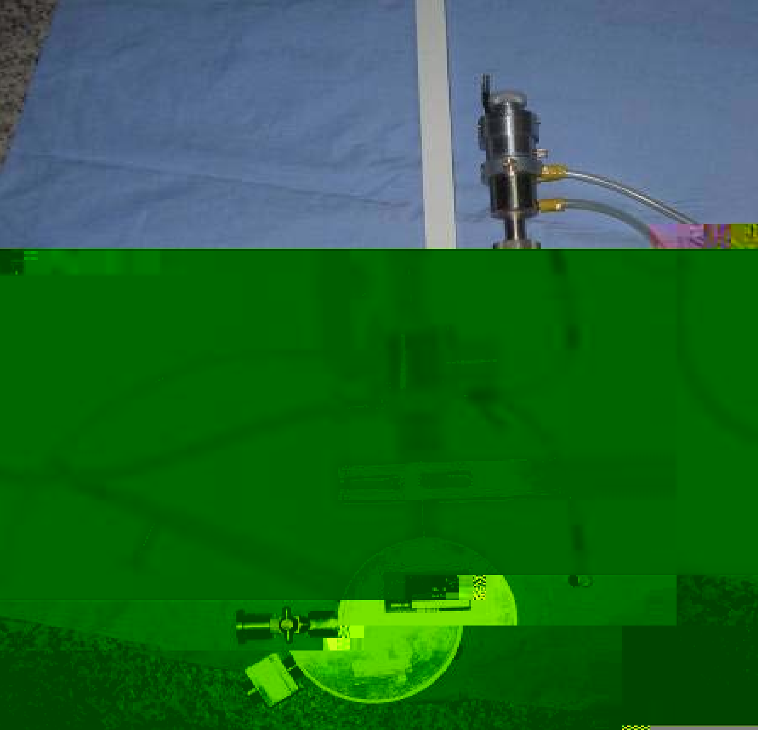

ESR)

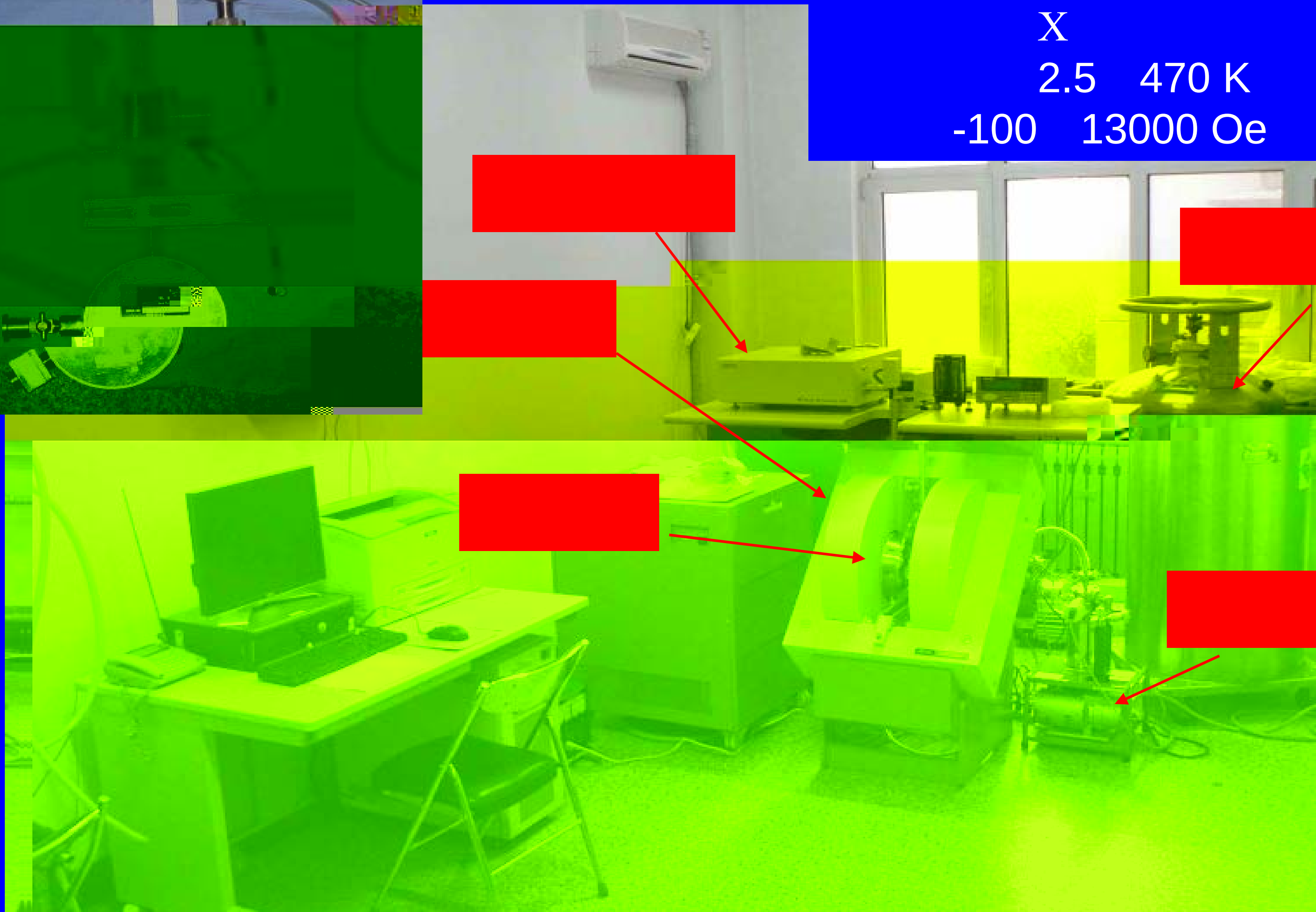

X

2.5 470 K

-100 13000 Oe

Short Time Scale

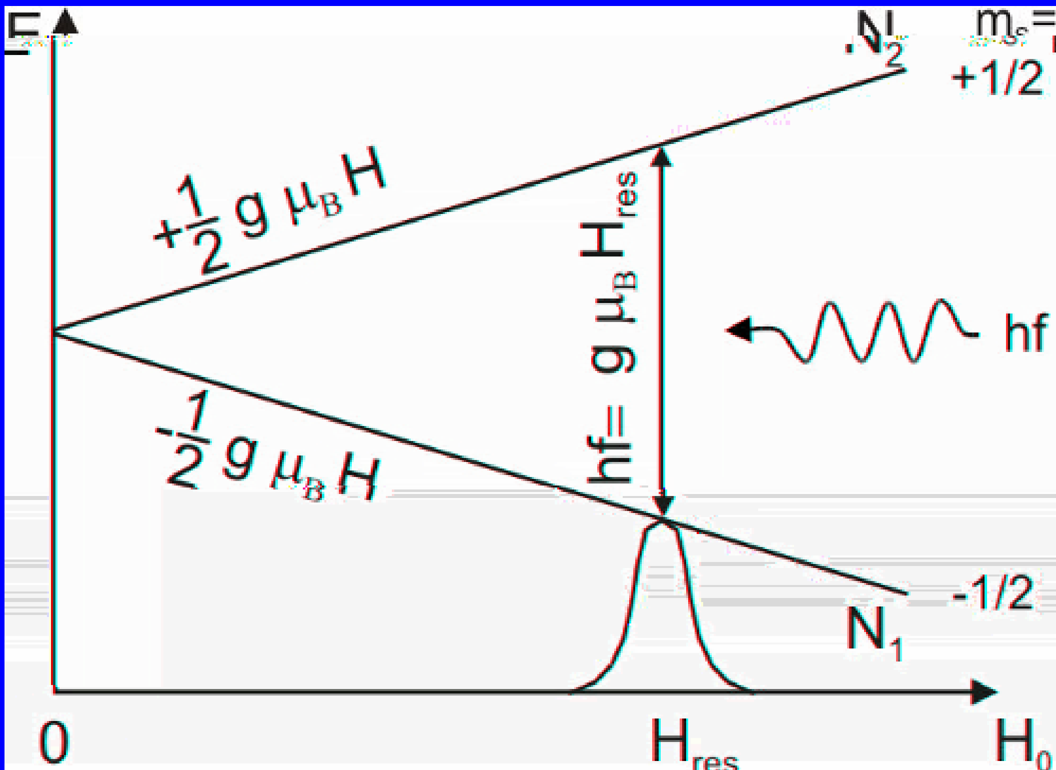

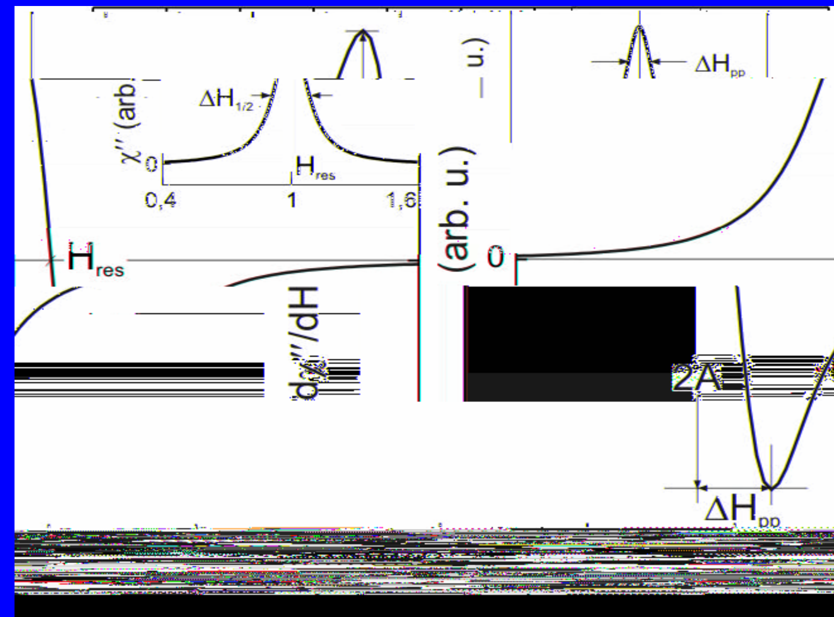

ΔH_{pp} - T_1

- T_2

g S L

I

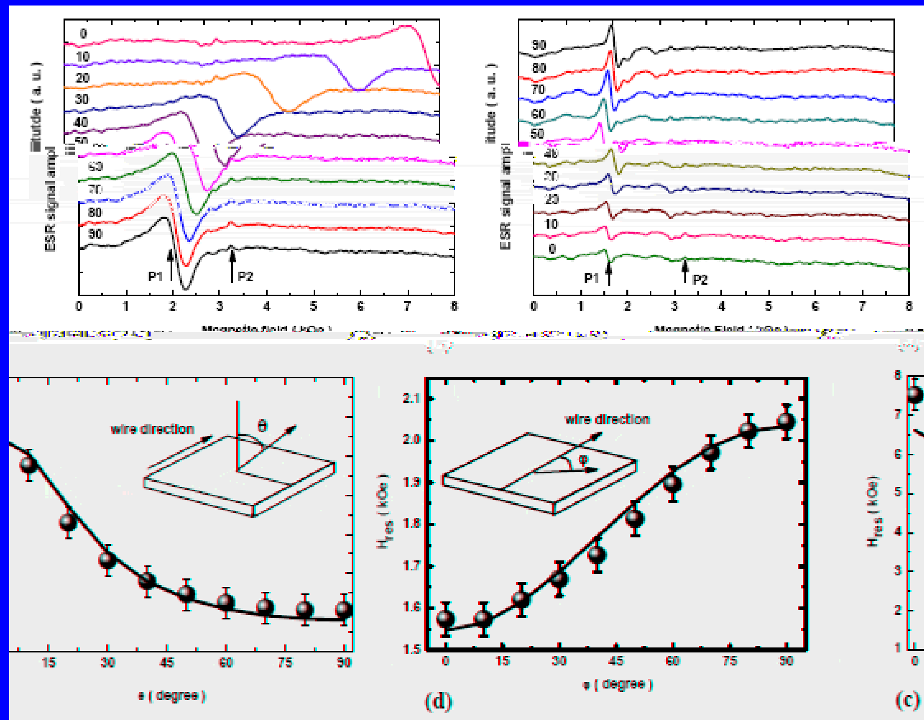

$$\left(\frac{\omega}{\gamma}\right)^2 = \left[H\cos(\varphi-\varphi_H) + 4\pi M_{eff} + \frac{2K_u}{M_S}\cos^2\varphi\right] \times \left[H\cos(\varphi-\varphi_H) + \frac{4K_u}{M_S}\cos 2\varphi\right].$$

Magnetic Anisotropy

Shape anisotropy –Dipolar Interaction

$$E_d = -\frac{1}{2} I_s H_d = \frac{I_s^2}{2\mu_0}\left(N_x \alpha_1^2 + N_y \alpha_2^2 + N_z \alpha_3^2\right)$$

$$E_d = \frac{\mu_0 M^2}{2}\cos^2\theta$$

$$E_d == \frac{\mu_0 M^2}{4}\sin^2\varphi$$

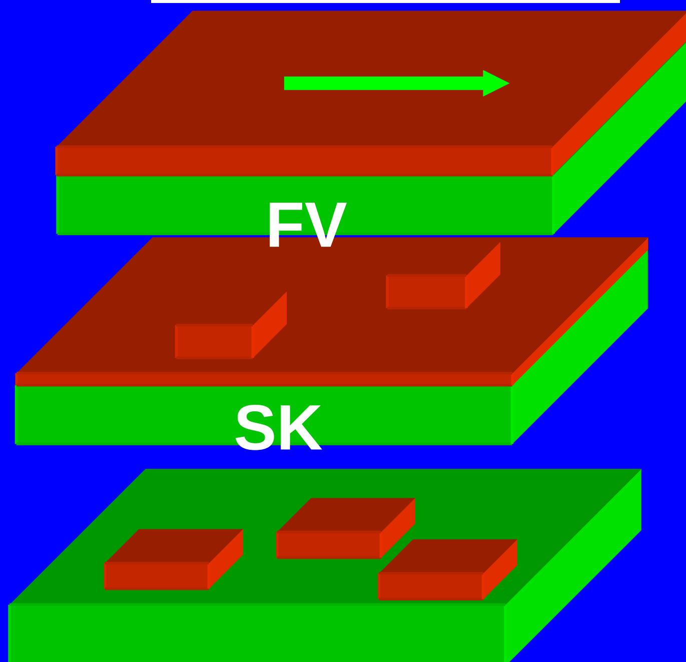

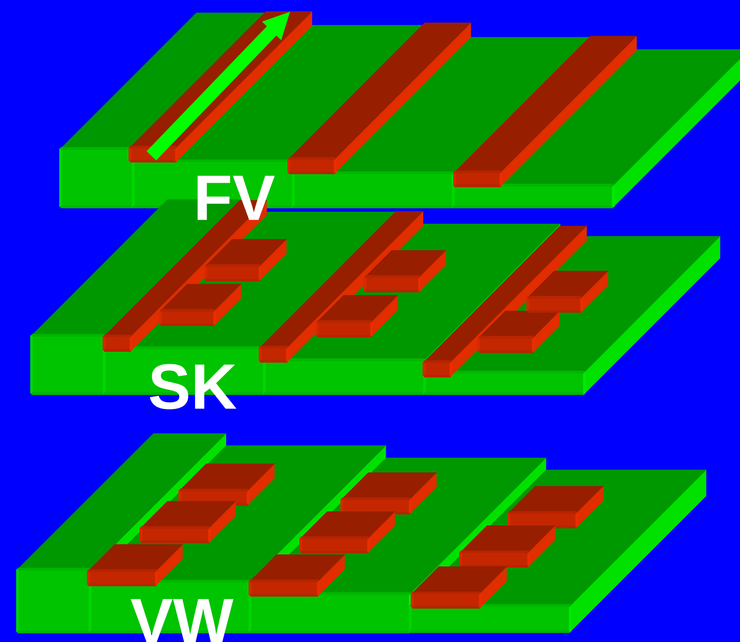

Magnetic Anisotropy

$$K^{\mathrm{eff}} = \frac{1}{d}\int_0^d \left(K^v + K^s\delta(z)\right)dz$$

$$K_{eff} = (K_V - K_d) + 2K_s/d$$

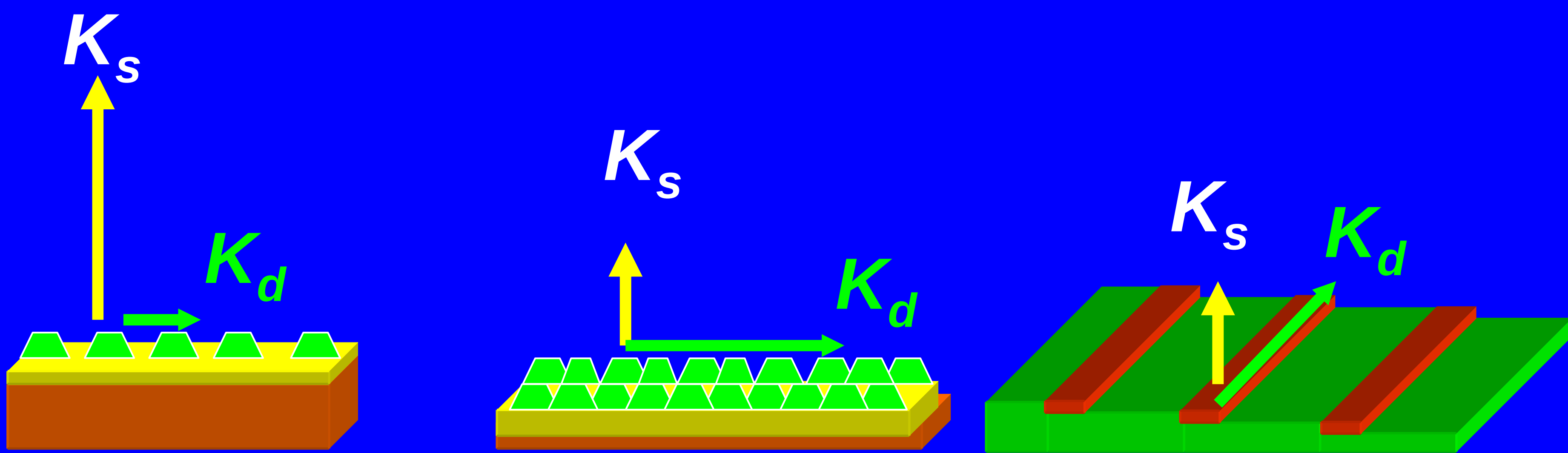

1.6 ML   5.0 ML   1.6 ML

- Fe
- 3.3 ML
  Fe SMOKE
- Si Fe

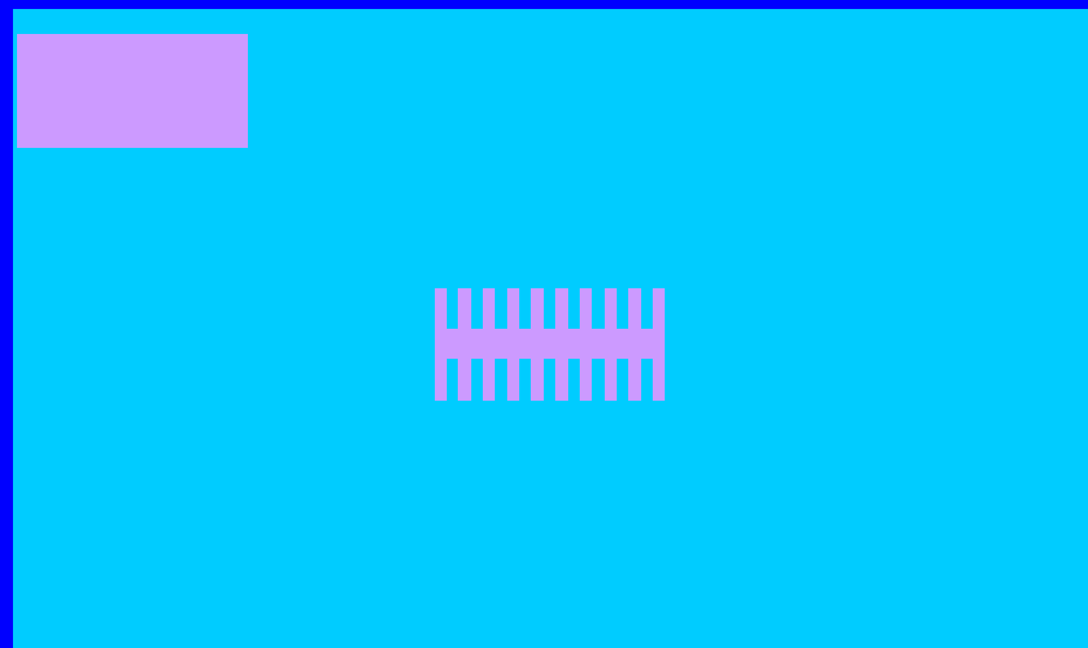

Fe3Pt nanowires

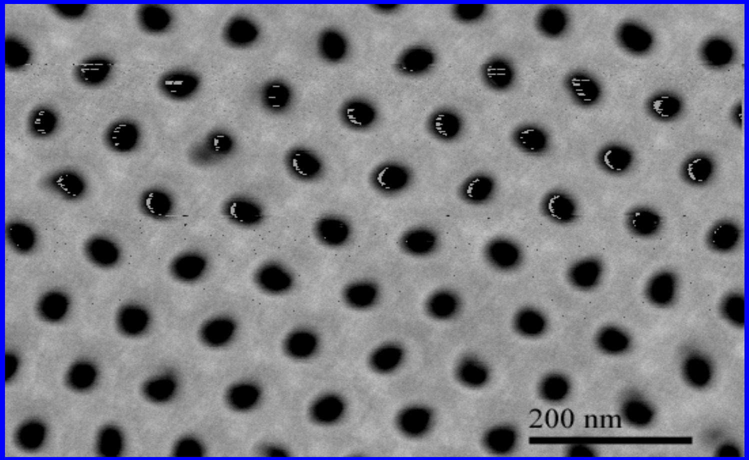

AAO template

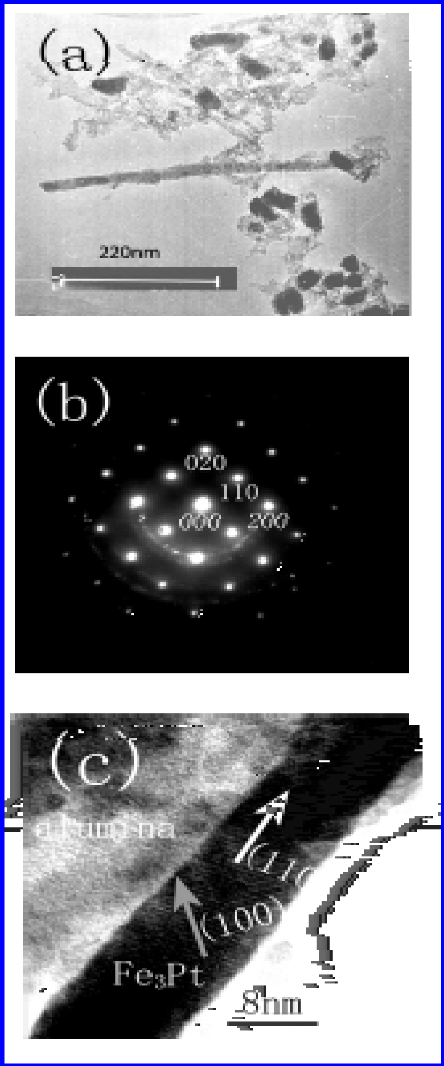

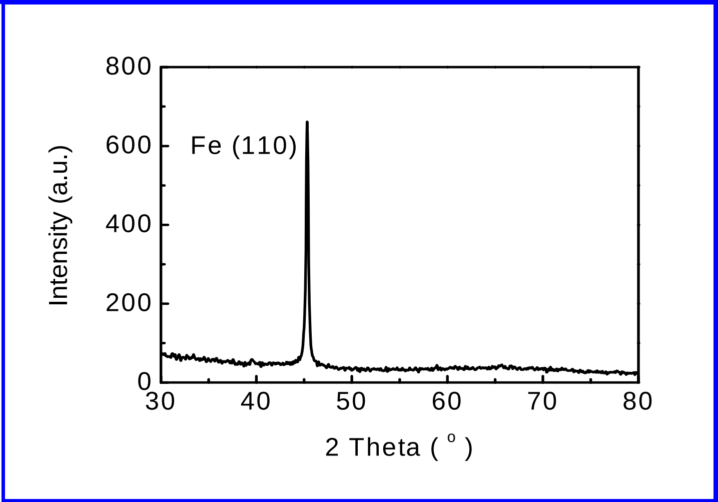

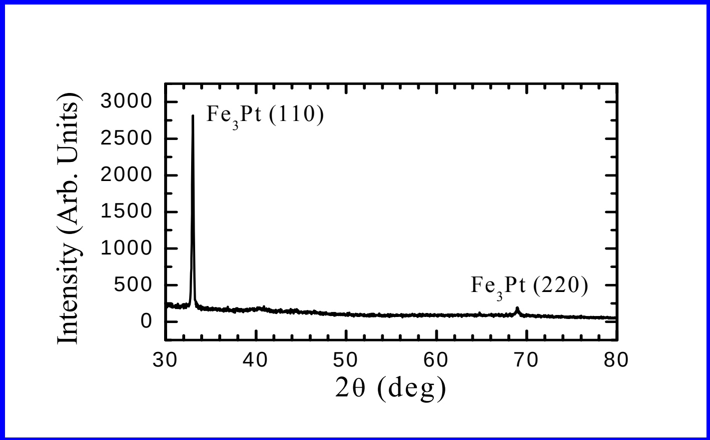

J.H. Gao, Appl. Phys. Lett. 86(2005)232506

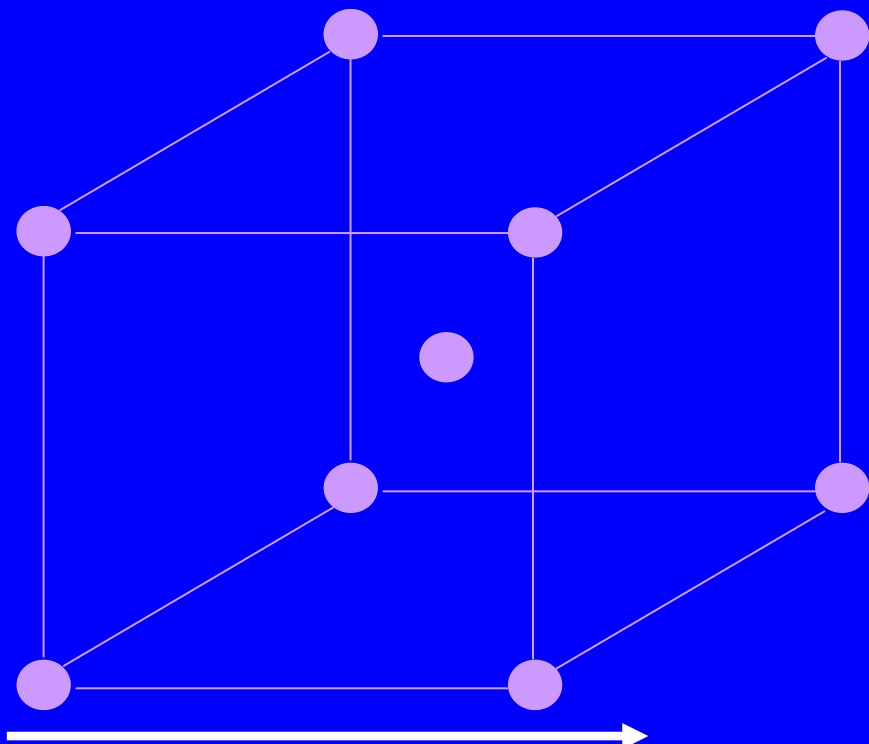

Low temperature and Superconducting Magnet for Mössbauer Spectrometer

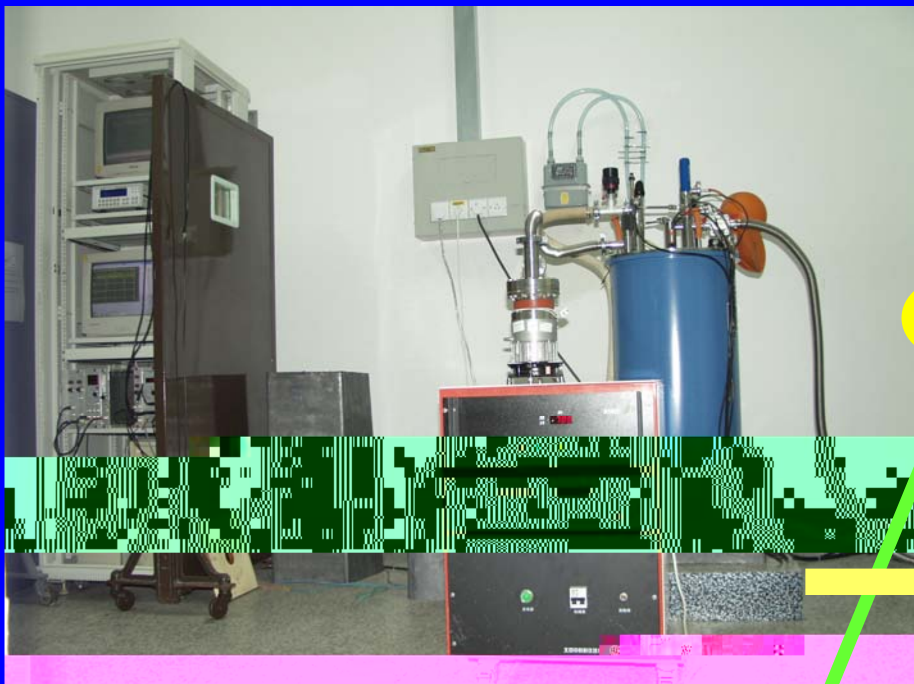

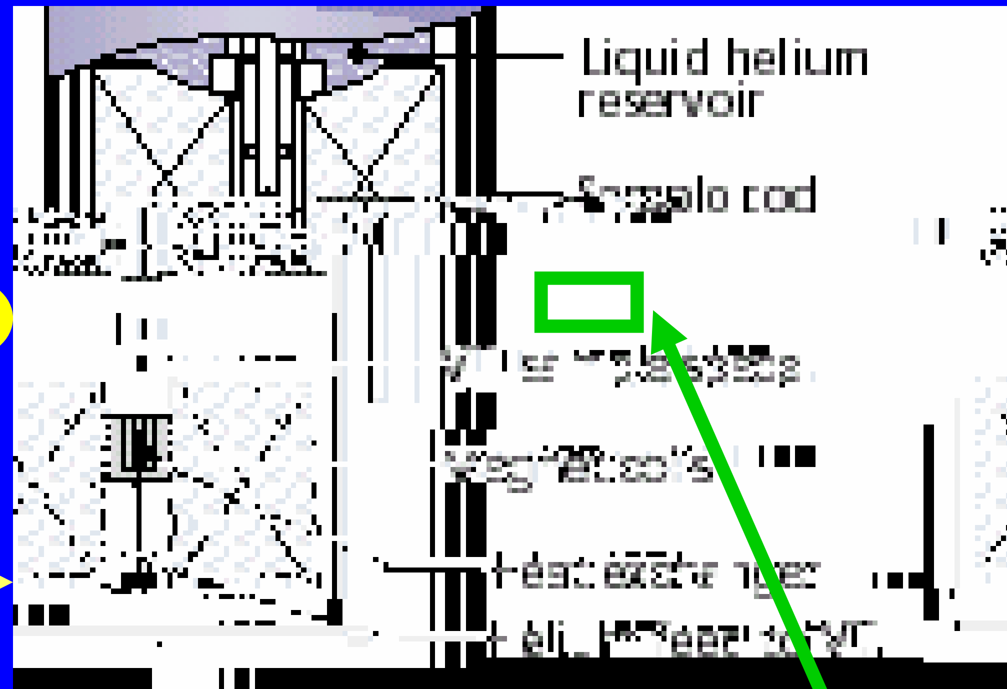

Source

Detector

Applications of In-field Mössbauer Spectroscopy

- Field-induced magnetic phase transition
- Magnetization processes of two phases individually from microscopic scale
- Magnetic anisotropy
- ……………….

γ-ray

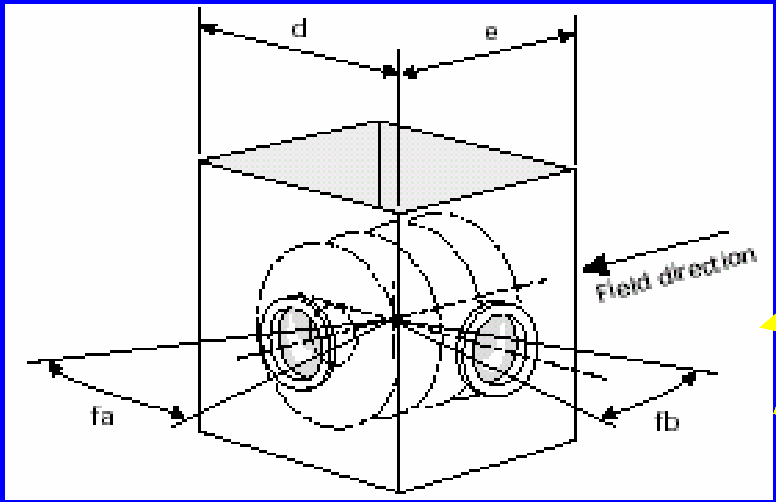

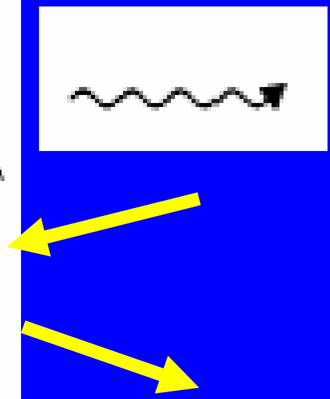

Magnetization processes

Intensities of the six lines

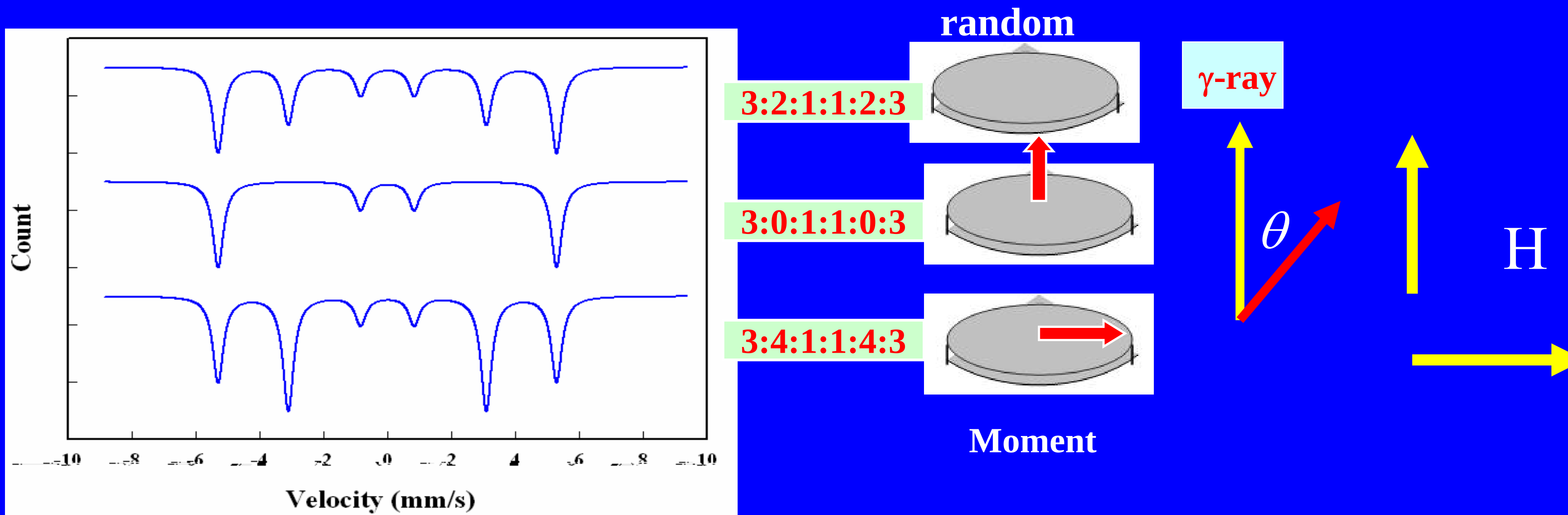

The intensity ratio among the six lines is $3:I_{2,5}:1:1:I_{2,5}:3$.

$$I_{2,5} = \frac{4\sin^2\theta}{1+\cos^2\theta}$$

θ *is the angle between Fe moment and* γ*-ray.*

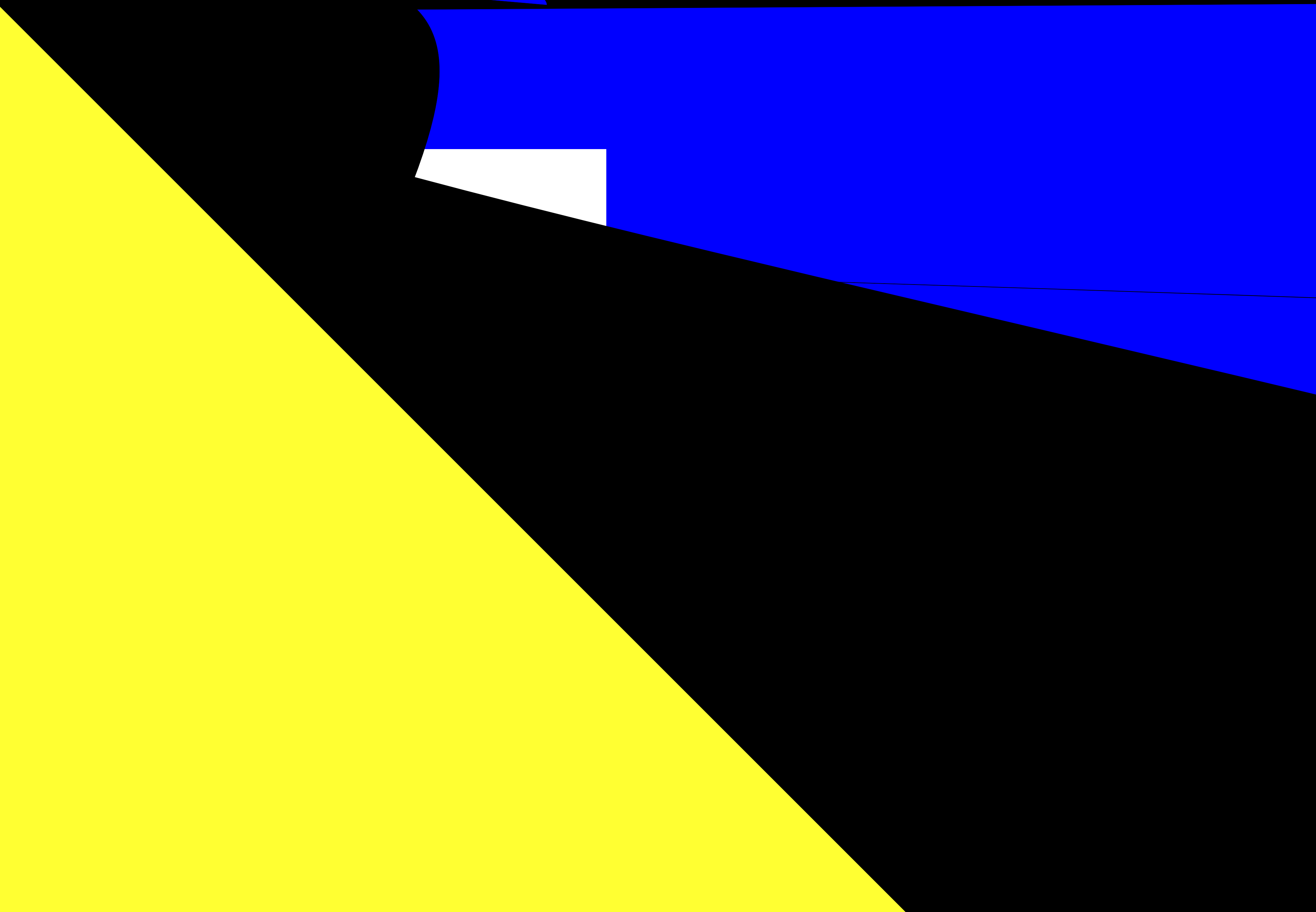

Magnetic shape anisotropy

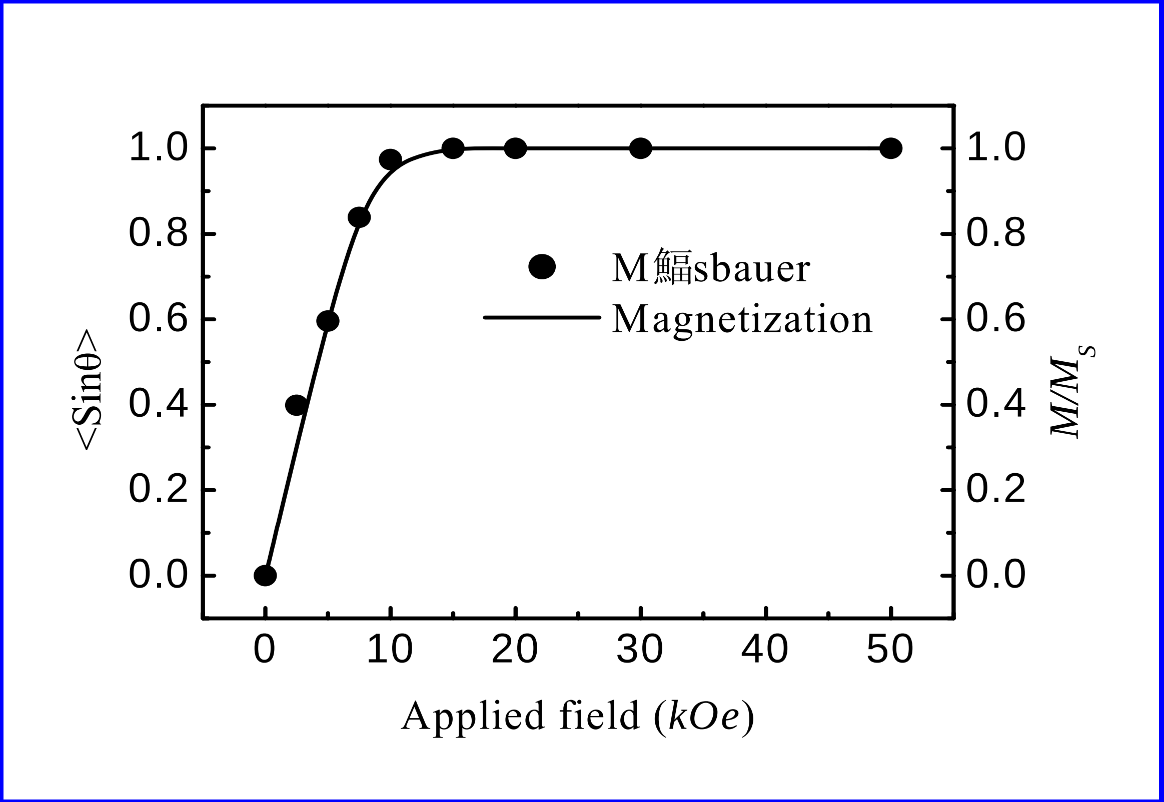

θ : *the angle between Fe moment and* γ *-ray,*

$\pi/2-\theta$: *the angle between Fe moment and applied field.*

$M/M_S = \langle \cos(\pi/2-\theta) \rangle = \langle \sin\theta \rangle$

Magnetic shape anisotropy

$$W = K \sin^2 \theta - \sum^{n} \mu_{Fe} H_{app} \cos\left(\frac{\pi}{2} - \theta\right)$$

$$K = \frac{M_S H_{app}}{2 \sin \theta}$$

$$0 < \theta < \pi/2$$

$$K \approx 7.3 \times 10^6 \,(ergs/cm^3)$$

$$K_1 \approx 5.21 \times 10^5 \,(ergs/cm^3)$$

$$K \approx 14\, K_1$$

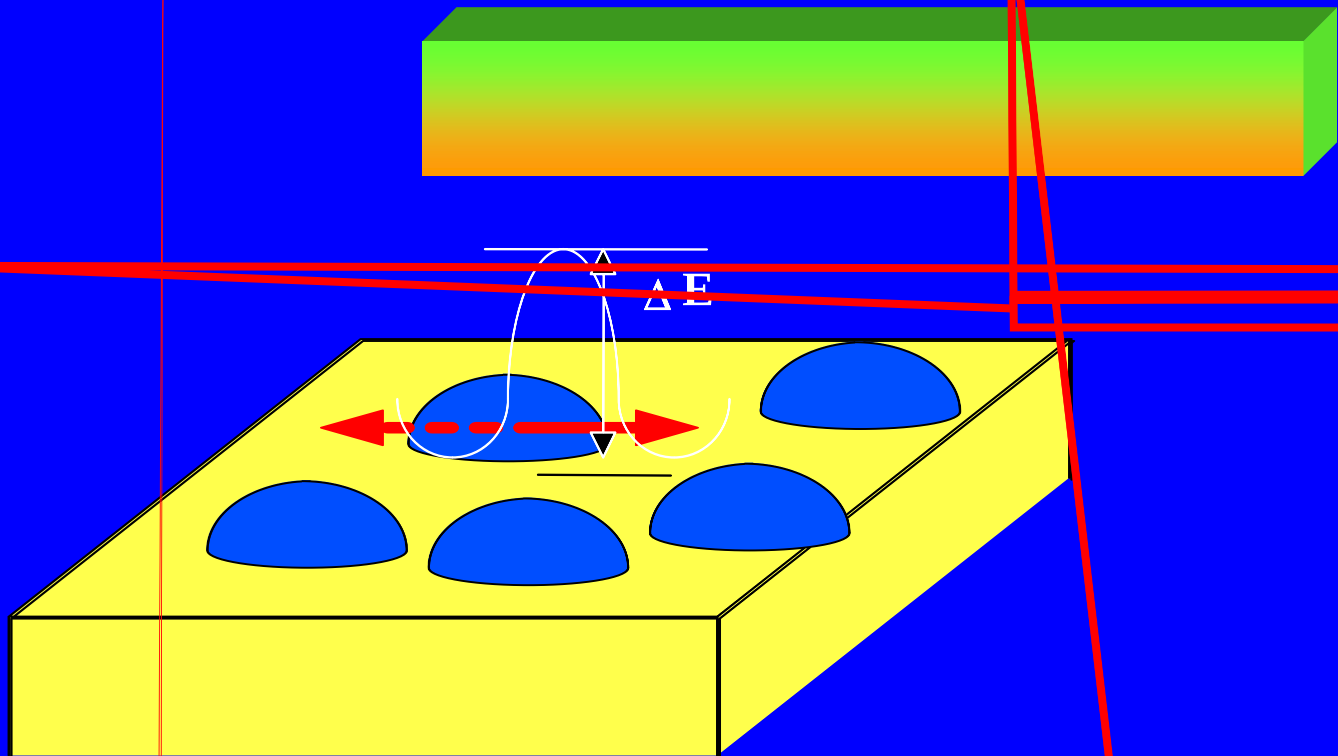
ΔE

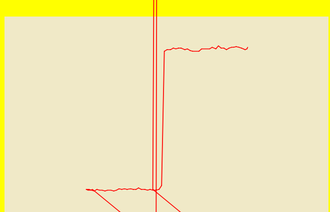

S.D. Bader
RMP (2006)

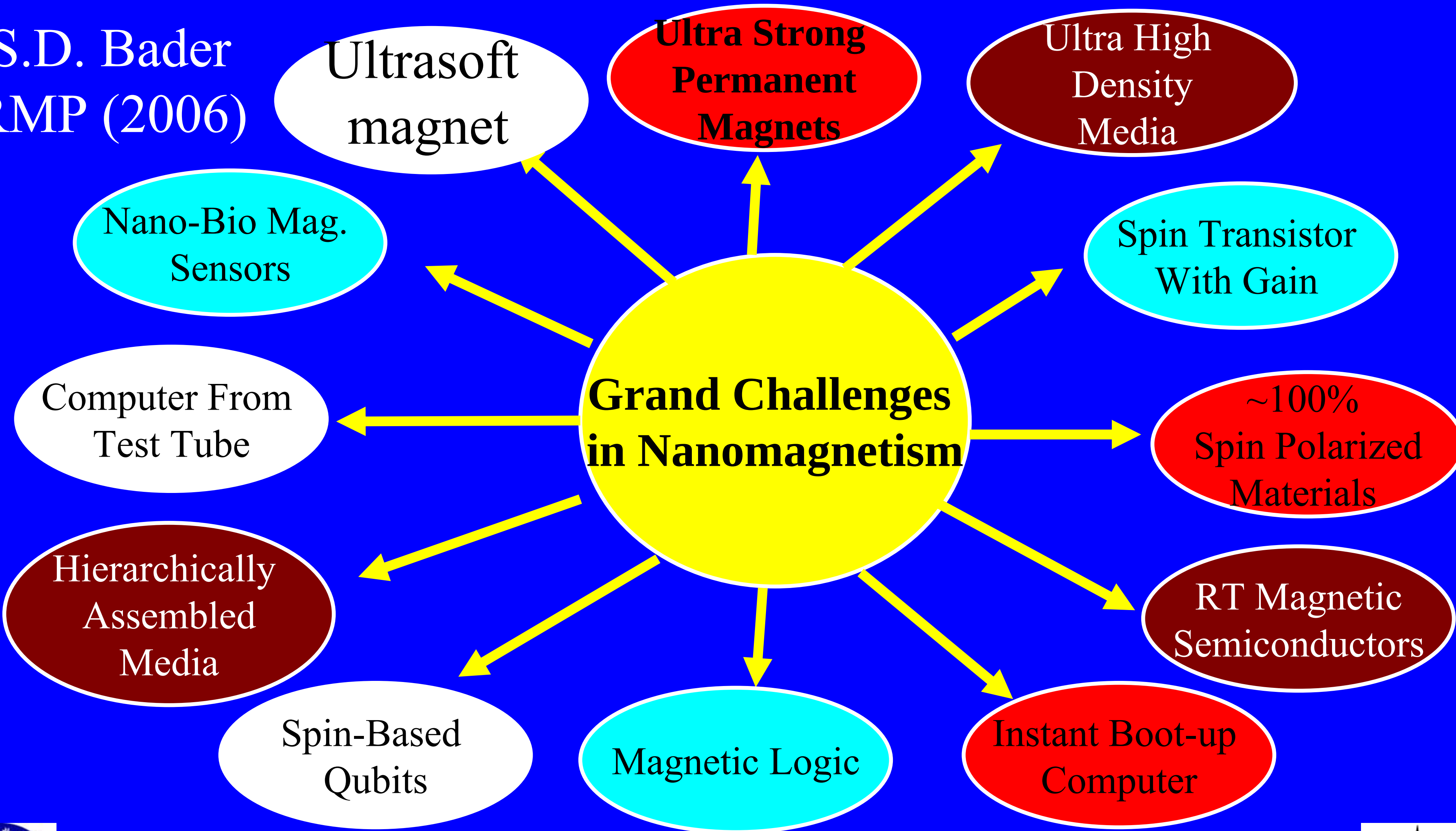

2001

40

- MOST
- NSFC
- CAS
- IOP